IAEA
International Atomic Energy Agency

INDC(NDS)-0624
Distr. AC/AD/G/IN/J/NM/RD/SC

INDC International Nuclear Data Committee

Summary Report of the Technical Meeting on

Primary Radiation Damage: from nuclear reaction to point defects

IAEA Headquarters, Vienna, Austria

1 – 4 October 2012

Prepared by

R. E. Stoller, Oak Ridge National Laboratory, Oak Ridge, USA

K. Nordlund, University of Helsinki, Helsinki, Finland

S.P. Simakov, Nuclear Data Section, IAEA, Vienna, Austria

November 2012

IAEA Nuclear Data Section
Vienna International Centre, P.O. Box 100, 1400 Vienna, Austria

Selected INDC documents may be downloaded in electronic form from
http://www-nds.iaea.org/reports-new/indc-reports/
or sent as an e-mail attachment. Requests for hardcopy or e-mail transmittal should be directed to services@iaeand.iaea.org or to:

Nuclear Data Section
International Atomic Energy Agency
Vienna International Centre
PO Box 100
1400 Vienna
Austria

Printed by the IAEA in Austria
November 2012

INDC(NDS)-0624

Distr. AC/AD/FE/G/IN/J/NM/RD/SC

Summary Report of the Technical Meeting on

Primary Radiation Damage: from nuclear reaction to point defects

IAEA Headquarters, Vienna, Austria

1 – 4 October 2012

Summary documentation prepared by

R. E. Stoller, Oak Ridge National Laboratory, Oak Ridge, USA

K. Nordlund, University of Helsinki, Helsinki, Finland

S. P. Simakov, Nuclear Data Section, IAEA, Vienna, Austria

Abstract

The Meeting was convened to bring together the experts from both the nuclear data and materials research communities because of their common objective of accurately characterizing irradiation environments and resulting material damage. The meeting demonstrated that significant uncertainties remain regarding both the status of nuclear data and the use of these data by the materials modeling community to determine the primary damage state obtained in irradiated materials. At the conclusion of the meeting, the participants agreed that there is clear motivation to initiate a CRP that engages participants from the nuclear data and materials research communities. The overall objective of this CRP would be to determine the best possible parameter (or a few parameters) for correlating damage from irradiation facilities with very different particle types and energy spectra, including fission and fusion reactors, charged particle accelerators, and spallation irradiation facilities. Regarding progress achieved during the last decade in the atomistic simulation of primary defects in crystalline materials, one of the essential and quantitative outcomes from the CRP is expected to be cross sections for point defects left after recoil cascade quenching.

November 2012

Table of Contents

Introduction

A Technical Meeting on "Primary Radiation Damage: from nuclear reaction to point defects" was held at IAEA Headquarters, Vienna, Austria from 1 to 4 October 2012. Fifteen experts J.-P. Crocombette, S. Dudarev, P. Griffin, T. Fukahori, A. Kahler, J. Kwon, A. Konobeev, F. Mota, K. Nordlund, V. Pechenkin, A. Ryazanov, D. Simeone, J.-C. Sublet, R.E. Stoller and R. Villa have attended this Meeting. A. Hogenbirk could not attend while excused. Mrs. T. Stahl and Z. Xiong Chong participated as observers. The IAEA was represented by R. Capote Noy, R. Forrest, V. Inozemtsev, N. Otuka, V. Semkova and S. Simakov.

The Meeting has the main goal to bring together the experts from the nuclear data and materials research communities and to discuss the issues of accurate characterization of irradiation environments and examine parameters predicting the resultant material damage.

This activity was recognised as important by the Advisory group on Long-term Needs for Nuclear Data Development during its Technical Meeting held 2 - 4 November 2011 in Vienna (see Report INDC(NDS)-0601 available on http://www-nds.iaea.org/publications/). The International Nuclear Data Committee at the 29th Meeting held 8-11 May 2012 in Vienna recommended to study the possibility to launch a new Coordinated Research Project (CRP). Moreover such CRP could be a logical extension of the work performed by the Expert Group on Primary Radiation Damage (PRD) of Working Party "Multi-scale Modelling of Fuels and Structural Materials for Nuclear Systems" at the OECD Nuclear Energy Agency (see summary by K. Nordlund).

The Meeting was opened by R. Forrest, Head of the Nuclear Data Section (NDS) of the Department of Nuclear Sciences and Applications of the IAEA by welcoming the participants and explaining the importance of this Technical Meeting for the work of NDS. The objective and goals of the Meeting were outlined by S. Simakov and V. Inozemtsev (Scientific Secretaries of the Meeting). Then the participants elected R.E. Stoller as the Chairman and K. Nordlund as the Rapporteur of the Meeting and approved Agenda (Appendix 1). The list of participants and their affiliations are summarised in Appendix 2.

During two and half days, participants gave presentations (the individual summaries are collected below) and had intensive discussions. The discussions resulted in the set of consolidated conclusions and recommendations which are collected in the next section.

The Nuclear Data Section acknowledged all participants for their cooperation and contributions to the Meeting.

Meeting summaries and recommendations

The IAEA Technical Meeting on Primary Radiation Damage: from Nuclear Reaction to Point Defects was convened on 1 October 2012 with participants from both the nuclear data and materials research communities because of their common objective of accurately characterizing irradiation environments. The mixing of these two groups enabled a healthy discussion of the technical issues involved and provided a unique opportunity for scientists from both disciplines to learn about the needs and interests of the other. It became clear that the nuclear data community would benefit from a better understanding of how the information they can provide is used in the materials community, and that the materials community needs a better understanding of the uncertainties in and range of validity for the nuclear data provided.

The meeting included presentations which demonstrated that significant uncertainties remain regarding both the development of nuclear data and the use of these data by the materials modeling community to determine the primary damage state obtained in irradiated materials. The longer-term damage evolution and accumulation was also discussed, and the group recognized that improved models for primary damage production must be suitable for inclusion in higher-level models (such as

kinetic models) capable of modeling the long-term evolution. Along with simple damage correlation, the impact of the primary damage source term in such models is a critical test of the validity of the primary damage terms.

Although the usefulness of the NRT-dpa for correlating many radiation damage phenomena was recognized, its limitations were also demonstrated. Examples were shown to indicate that other parameters could be used to better correlate certain kinds of data. For example, some material property changes are sensitive to the results of nuclear collisions, while others are more sensitive to the effects of ionization. The participants acknowledged that the development of specific damage models is best done within the materials community, based on information obtained from nuclear data researchers. For a given irradiation environment, this data needs to include the primary knock-on atom (PKA) spectrum, nuclear transmutation rates (particularly gas production), and partitioning of the PKA energy into nuclear and electronic stopping.

Even for materials in which the primary damage element is due to nuclear stopping, it was recognized that the current NRT-dpa could be augmented by the development of parameters which account for splitting of cascades in subcascades, athermal recombination within a collision cascade, in-cascade clustering of point defects, and atomic replacements that cause mixing of individual species. Although such information cannot be obtained from nuclear data, these four parameters can be obtained from binary collision and/or molecular dynamics simulations, using the PKA spectra calculated from the nuclear data.

For insulating materials, the problem is even more complicated. First, ionizing radiation alone can alter the atomic structure, leading to serious degradation of the physical properties. Second, in this case, primary defects also include electron-hole pair creation and trapping, which drastically alter their properties and therefore must be incorporated in a complete model. Examples were discussed where damage creation and accumulation is best represented as a function of ionizing flux and dose, using normally Gy/s and Gy, respectively. Therefore it is not possible to use a displacement-based parameter such as the NRT-dpa to correlate damage effects in this group of materials.

At the conclusion of the meeting, the participants agreed that there is clear motivation to initiate a CRP that engages participants from both the nuclear data and materials research communities. The overall objective of this CRP would be to determine the best possible parameter (or a few parameters) for correlating damage from irradiation facilities with very different particle types and energy spectra, including fission and fusion reactors, charged particle accelerators, and spallation irradiation facilities.

The scope of the proposed CRP comprises materials relevant to fission, fusion and spallation facilities and the nuclear data in the energy range relevant to their use. These materials include nuclear fuels, structural materials and special purpose materials such as W, SiC, and alumina.

Specific objectives of the proposed CRP include:

- Improve the communication and the interface (exchange of data and their uncertainties) between the nuclear data and materials communities.
- Assess the accuracy and completeness of current nuclear data, including the high-energy (>> 10 MeV) region which has not been subject to much attention until recently.
- Assess parameters derived from nuclear data such as energy partitioning, gas production, and PKA spectra as well as their uncertainties, taking into account input from the materials community on what kind of data is required.
- Develop material primary damage models that are more versatile than the NRT-dpa for both metallic and non-metallic materials and demonstrate their usefulness for both correlating data and use in predictive microstructural models to compare with experimental data.

The outcome will be a procedure for the calculation of new primary damage production parameters suitable for the radiation environments specified above.

The data on damage production in collision cascades will also be provided in tabulated form for the IAEA databases.

Participant summaries and recommendations

Meeting Objectives and relevant NDS databases

S.P. Simakov

Nuclear Data Section
International Atomic Energy Agency, Vienna
Austria

The Technical Meeting (TM) objectives were formulated through consultations with potential participants, communications with experts involved in the similar activities coordinated by IAEA and NEA and relying on information published in the literature. The information about this TM was made available on the dedicated web page http://www-nds.iaea.org/dpa/ well in advance.

Meeting Motivations

The displacement cross section is a reference measure used to characterize and compare the radiation damage induced by neutrons and charged particles in crystalline materials. To evaluate the number of displaced atoms Norget, Torrens and Robinson [1] proposed in 1975 a standard (the so-called NRT-dpa), which has been widely used from that time.

Nowadays this formulation is recognized as suffering from some limitations: it is not applicable for compound materials, does not account for the recombination of atoms during the cascade evolution, cannot be directly validated and has no uncertainties/covariancies as evaluated cross sections usually have now.

Upgrading of the dpa-standard means the inclusion of results of the Molecular Dynamics (MD), Binary Collision Approximation (BCA) or other simulations for primary radiation defects (PRD), i.e. Frankel pairs (FP) and Interstitial Clusters, which survive after relaxation of the Primary Knock-on Atom (PKA) cascade.

The essential advantages of the upgraded dpa-standard will be:

- non-dependence on the energy distribution of incident neutrons - this means more correct inter-comparison of radiation damage in the different facilities on the basis of the accumulated dpa-fluence;
- it also becomes more feasible for comparison of neutron and charged particles or ion induced damage;
- empirical validation against frozen defects at cryogenic temperature (NRT-dpa can never be observed);
- prediction of damage in polyatomic materials and alloys (NRT treats dpa in compounds by mathematical weighting of the separate elements).

Purpose of the Meeting

To find ways to overcome the drawbacks of the NRT standard and benefit from the recent developments in primary radiation damage simulations, the Technical Meeting has the objectives to discuss:

- revisiting the NRT standard with the purpose of improving it by the evaluation of uncertainties connected with recoil spectra and the energy partitioning model;
- proposal of a new upgraded standard that will capture the annealing of defects in the recoil cascade on the basis of MD, BCA and other models.

As an outcome of discussions the definition of objectives and participating organisations for a new Coordinated Research Project (CRP) on this topic are expected.

Specific issues to be addressed during the Meeting

Cross sections, evaluated data libraries and the NRT standard:

- PKA spectra - availability in libraries, methods of calculation, agreement and uncertainties,
- processing of cross section files to derive KERMA, damage energy and dpa,
- gas (helium, hydrogen) production cross sections,
- uncertainties/covariances for these quantities,
- others.

MD, BCA and other simulations of survived primary point defects in mono- and poly-atomic materials and thermal-spike-enhanced recombination:

- scope of materials - pure metals, Fe-xC, semiconductors (Si, Ge), insulators and ceramics (Al_2O_3, SiC ...),
- PKA energy range covered by different simulation methods,
- calculation outputs - survived Frankel Pairs (FP), simple interstitial clusters,
- dependence on temperature and material composition,
- incorporation of MD/BCA results in processing codes (NJOY) or storage in a separate cross section database,
- empirical validation,
- applications,
- others.

Illustrative examples

Fig. 1 shows the typical neutron spectra in the fast research reactor, first wall of power fusion plant and High Flux Test Module (HFTM) of IFMIF as well as spectra weighted recoil distributions in iron. The PKA spectra were obtained from the LA-150 evaluation [2] as a result of processing by the NJOY code [3]. The output of the GROUPR module was then processed by the additional subroutine to fold PKA matrices with the facility neutron spectra [4,5].

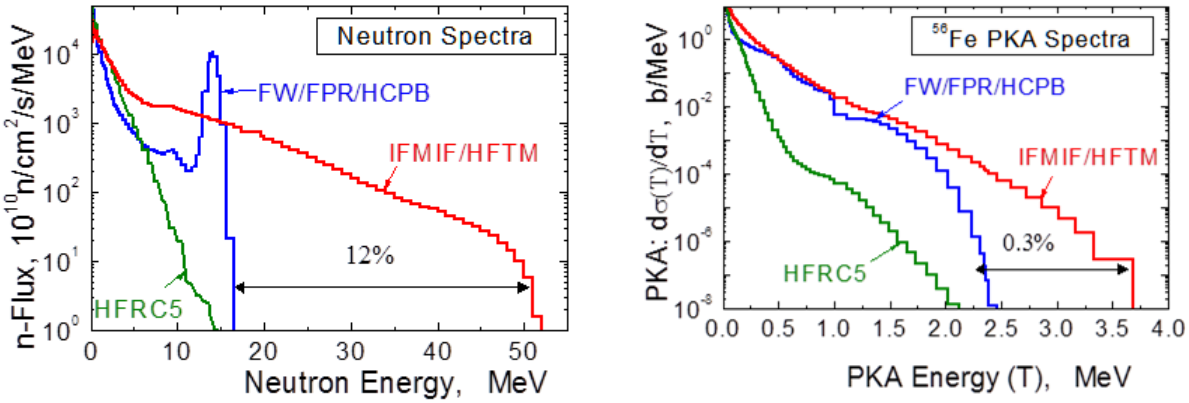

Fig. 1. Left: neutron spectra in the fast reactor, first wall of power fusion and HFTM of IFMIF. Right: recoil spectra in Fe weighted with these neutron spectra (percentage shows the fraction of neutrons or recoils in HFTM of IFMIF resulted from neutrons above fusion peak 15 MeV).

Fig. 2 shows surviving ratios, i.e. the number of Frankel pairs and interstitial clusters to the NRT dpa-standard, obtained from MD simulations [6,7] and extrapolated to the higher PKA energies based on the BCA calculation which uses MD results below 100 keV [9]. These surviving functions were incorporated in the HEATR module of NJOY (taking into account the difference of ion kinetic energies in nuclear data files and MD simulations) that eventually allowed computing of the damage energy and dpa-cross sections as demonstrated in Fig. 3 [4,5].

The Nuclear Data Section (NDS) currently stores and disseminates the damage cross section database DXS [9] (see http://www-nds.iaea.org/ndspub/download-endf/DXS/ and summary of A. Konobeyev). This includes dpa- (both NRT and survived Frankel pairs) and gas-production cross sections for several pure metals, Figs. 4 and 5.

NDS also hosts a set of damage cross sections as a part of the dosimetry file IRDF-2002 [11]. It is worthwhile to note that damage function for GaAs, Fig. 6, incorporates the empirical efficiency factor for better characterization of irradiated GaAs device performance (see [11] and P. Griffin' summary).

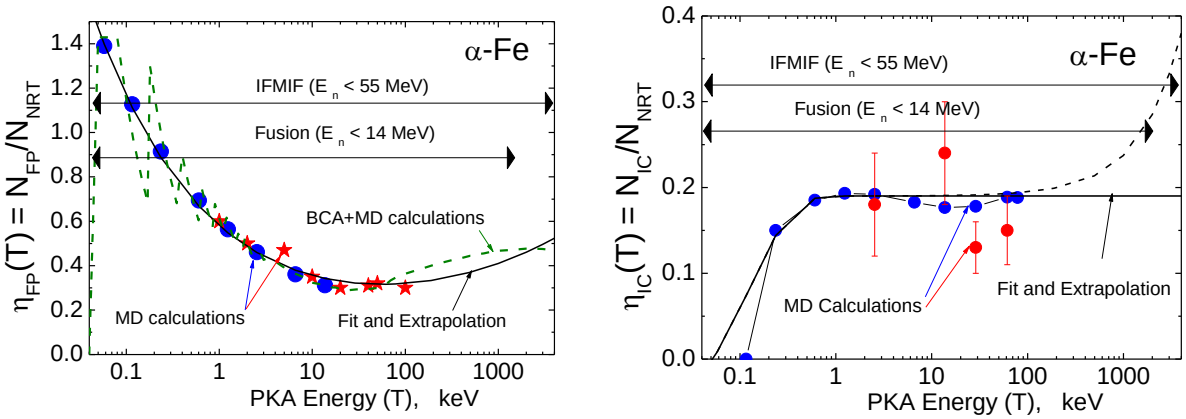

Fig. 2. Surviving ratios for Frankel pairs and interstitial clusters after cascade relaxation in α-Fe: symbols – results of MD simulations [6,7], curves – BCA+MD [9] or fit/extrapolation.

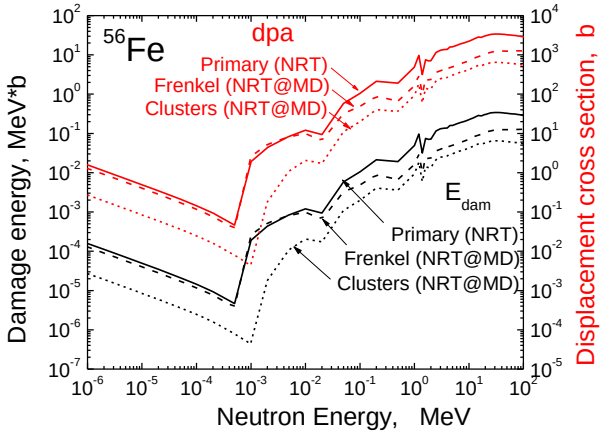

Fig. 3. Damage energy E_{dam} and dpa-cross sections for Frenkel pairs and interstitial clusters calculated for ^{56}Fe [4].

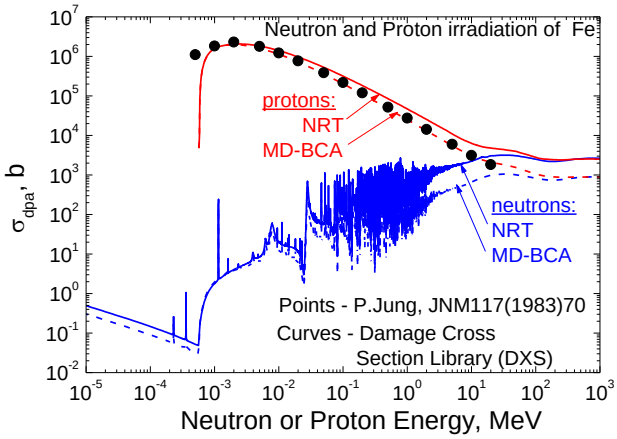

Fig. 4. Neutron and proton induced dpa-cross sections from the DXS library [9] (curves) and experimental data [10].

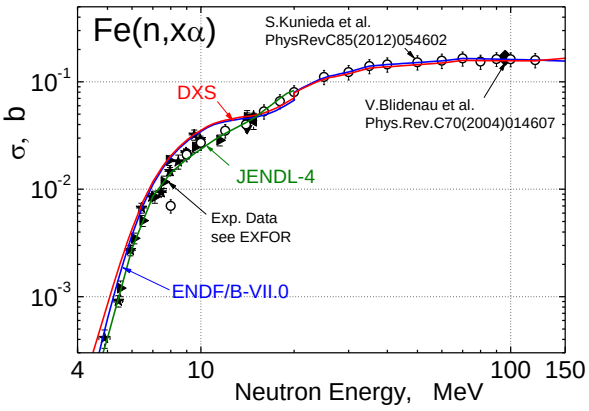

Fig. 5. Neutron induced He production cross section in Fe: evaluations (curves) and experimental data from EXFOR [12].

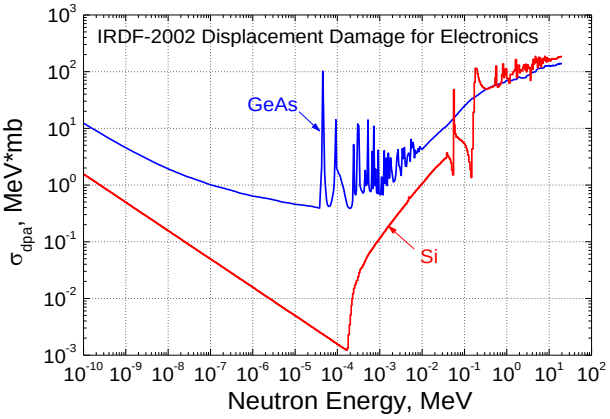

Fig. 6. Neutron damage energy for silicon and GaAs available in the IRDF-2002 file [11].

References

1. M.J. Norgett, M.T. Robinson, I.M. Torrens, A proposed method of calculating displacement dose rates, Nucl. Eng. Des. 33 (1975) 50.
2. M.B. Chadwick, P.G. Young, S. Chiba et al., Nucl. Sci. Eng. 131 (1999) 293.
3. R.E. MacFarlane, NJOY99.0: Code System for Producing Pointwise and Multigroup Neutron and Photon Cross Sections from ENDF/B Data, RSICC Code Package PSR-480.
4. S.P. Simakov, A.Yu. Konobeyev, U. Ficher, V. Heinzel, Comparative study of survived displacement damage defects in iron irradiated in IFMIF and fusion power reactors, JNM 386 (2009) 52.
5. S.P. Simakov, A.Yu. Konobeyev, U. Ficher, Assessment of survived radiation defects by a modified version of NJOY, Report JEFF-DOC-1223, NEA Data Bank, Nov. 2007.
6. R.E. Stoller and L.R. Greenwood, Subcascade formation in displacement cascade simulations: Implications for fusion reactor materials, JNM 271 (1999) 57.
7. D.J. Bacon, Yu.N. Osetsky, R. Stoller, R.E. Voskoboinikov, MD description of damage production in displacement cascades in copper and α-iron, JNM 323 (2003) 152.
8. C.H. Broeders, A.Yu. Konobeyev, JNM 328 (2004) 197.
9. A.Yu. Konobeyev, U. Fischer, L. Zanini, Advanced evaluations of displacement and gas production cross sections for chromium, iron, and nickel up to 3 GeV incident particle energy, Proc. of Int. Conf. on Accelerator Applications (AccApp-2011), April 2011, Knoxville, TN.
10. P. Jung, Atomic displacement functions of cubic metals, JNM 117 (1983) 70.
11. International Reactor Dosimetry File (IRFF-2002), Techn. Report Series No. 452, IAEA 2006, available on-line http://www-nds.iaea.org/irdf2002/.
12. N. Otuka, S. Dunaeva, E. Dupont, O. Schwerer, A. Blokhin, The Role of the Nuclear Reaction Data Centres in Experimental Nuclear Data Knowledge Sharing, Proc. Int. Conf. on Nuclear Data for Science and Technology (ND-2010), April 2010, Korea, p. 1292, on-line access: http://www-nds.iaea.org/exfor/exfor.htm.

Introduction: Issues Related to Dose Units and Damage Correlation

Roger E. Stoller

Materials Science and Technology Division
Oak Ridge National Laboratory, Oak Ridge, TN 37831-6138
USA

Objective

The objective of this presentation is provide a list of terms and their definitions that should be helpful in framing the discussion of dosimetry and damage correlation in irradiated materials. Some relevant work carried out over the last forty years is also summarized to provide an historical perspective on these issues.

Introduction

The two most common parameters used to characterize the cumulative exposure of a material to irradiation are the particle fluence and absorbed dose. The **particle fluence**, in units of $(\text{area})^{-1}$, depends only on the characteristics of irradiation source and can be quoted at a point or averaged over a surface or volume. Although it is often quoted as a free-field particle fluence, the actual fluence will be modified by particle absorption and scattering when a test object is in place – i.e. material perturbs local flux. The **absorbed dose**, in units of energy, depends on a variety of variables, including: particle fluence, particle type, particle energy spectrum, and the specific material being exposed. Thus, absorbed dose includes much more information about the irradiation environment, and it is material dependent.

In practice, both the particle fluence and absorbed dose are used as the independent variable in

attempts to correlate data, compare materials or irradiation environments, or extrapolate data to estimate the effects of a longer exposure. This use as a **damage correlation parameter** introduces a much broader range of influences than simply the material and the irradiation source. In general, the application of a damage correlation parameter will depend on: the particle fluence or absorbed dose, specific damage parameter being monitored (e.g. electrical resistivity, swelling, or embrittlement), the damage rate, previous damage, exposure conditions such as temperature and mechanical loads, and material composition (intentional alloy elements and impurities). The impact of correlated damage mechanisms such as transmutation production, notably helium and hydrogen, must also be considered.

Exposure to the sun provides a simple illustration of the difference between absorbed dose and damage. Any two individuals who spend the afternoon at the beach side-by-side in identical bathing suits will receive the same absorbed dose. However, the damage they accumulate (degree of sun burn) will vary depending on their previous recent exposure (how tan they are) and/or their genetic sensitivity to ultra-violet photons. It will not be possible to correlate the expected damage with only the time in the sun and the photon flux.

A Brief Anecdotal Description of NRT-dpa

By the mid-1970s, the need to obtain data on structural materials irradiated to the very high damage levels expected at the high lifetime fast neutron fluences of fast reactor core components led to increasing use of charged particle irradiation facilities to obtain comparable damage. Of course an ion fluence is not the same as a neutron fluence, and efforts were made to find a measure of dose that could be calculated in a similar fashion for these two very different irradiation conditions so that the data obtained from both could be correlated. Based on the early work of Kinchin and Pease [1], a group of international experts proposed a method for estimating the number of atom displacements from an atom recoiling from a collision with an energetic particle [2-4]. The fraction of the kinetic energy carried away by this primary recoil atom (PKA) that was deposited in elastic collisions with subsequent atoms was called the damage energy, and is therefore a measure of absorbed dose, specifically the energy per atom of kinetic energy absorbed by a material. The estimate of the number of displacements (Frenkel pair) this energy could create is given by the following expression:

$$\nu_{NRT} = \frac{0.8T_{\mathrm{d}}}{2E_{\mathrm{d}}} \quad , \quad (1)$$

where T_d is the damage energy, E_d is the minimum energy required on average to create a stable Frenkel pair, the factor of 0.8 was determined from binary collision models to account for realistic (i.e. not hard sphere) scattering. The damage energy in Eqn. (1) is obtained by the energy partitioning theory developed by Lindhard, et al. [5].

The number of displaced atoms predicted by Eqn. (1) became known as the NRT displacements based on the initials of the authors of Ref. [2], and the integral number of displacements normalized to the number of atoms is known as the NRT displacements per atom (dpa). The NRT-dpa was successfully applied to correlate date from many studies involving the direct comparison data from very different irradiation environments, e.g. reactor spectra with very different thermal-to-fast neutron flux ratios, and charged particle irradiation with neutron irradiation. Although it was never asserted that Eqn. (1) predicted the actual number of Frenkel pair created, it proved to be a powerful tool for data correlation for the materials for which it was originally developed, i.e. steels and other mid-atomic-weight metals. The use was broad enough that a dpa cross section was developed for iron under neutron irradiation [6] and recommended values for E_d have been compiled [7]. The dpa cross section for iron from ASTM E683 is shown in Fig. 1. The NRT-dpa remains the preferred correlation parameter for properties such as embrittlement of low alloy steels [8].

However, there a range of other materials and material properties for which atomic displacements are not the primary source of damage, notably the physical properties of covalent and ionic materials for which the ionizing dose is more important than the displacement dose. These materials are covered in another section of this report by Mota and Vila. Nevertheless, attempts are commonly made to use the NRT-dpa to correlate property changes in these materials. Such attempts often fail, leading to complaints that “dpa doesn’t work”. In addition, NRT-dpa cannot account for effects arising from

differences in damage rate or differences in the production of transmutation products such as helium. These failures to correlate specific data sets do not negate the value of the damage energy and NRT-dpa to account for differences in displacement dose among different environments; they simply illustrate that NRT-dpa cannot be used as a general radiation damage correlation parameter. Even though the displacement dose is accurate, not all phenomena are equally sensitive to this measure of dose, just as not all beach goers suffer equally from the same amount of sun.

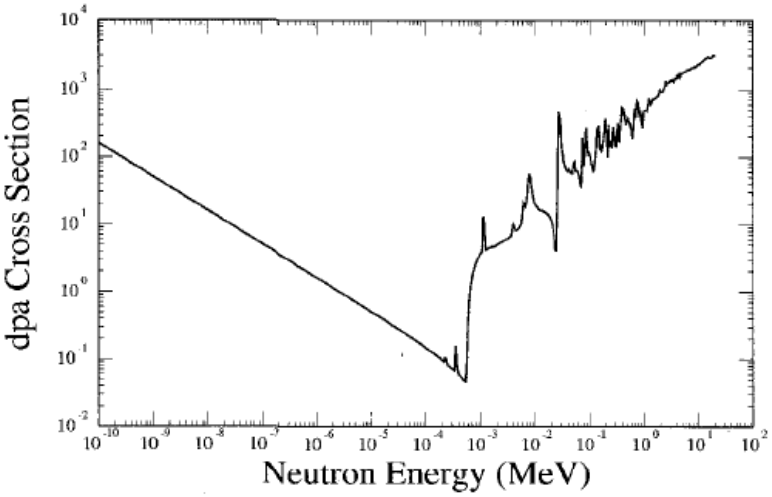

Fig. 1. ENDF/B-VI-based Iron Displacement Cross Section.

Direct Calculation of Atomic Displacements

Modern computing capabilities and improved interatomic potentials have enabled molecular dynamics (MD) simulations to characterize point defect formation in atomic displacement cascade simulations over a broad range of PKA energies. These simulations have demonstrated that many of the point defects produced are found in small interstitial and vacancy clusters. This in-cascade clustering is another example of a phenomenon related to the displacement dose, but which cannot be predicted by the damage energy per se. Fig. 2 provides a summary of a large MD cascade database with for cascade energies up to 200 keV at temperatures of 100, 600, and 900K [9]. Because these simulations did not incorporate electronic stopping, these cascade energies approximately correspond the damage energy in Eqn. (1) and thus to PKAs of higher energy. For example, cascades of 10 and 200 keV would be generated by PKA with energies of 13.7 and 425 keV, respectively. A 425 keV PKA energy is the average iron recoil energy from a collision with a 12.3 MeV neutron.

The total number of point defects produced is shown in Fig. 2(a), the number of interstitials in clusters in 2(b), and the number of interstitials in large clusters containing ten or more interstitials is shown in 2(c). In all three cases, the numbers have been divided by the number of NRT displacements (Eqn. (1)). Note that the number stable displacements in the MD simulations is about 30% of the NRT above about 20 keV. The saturation of this fractional value has been shown to arise from the breakup of a single cascade into multiple subcascades at the higher energies [10]. The error bars shown in the figure are the standard error of the mean, and the statistical scatter increases for the clustering parameters compared to total defect production. The temperature dependence of large cluster formation, Fig. 2(c) is also stronger than for the other two parameters.

With the energy dependence information in Fig. 2, it has been possible to obtain average damage production values for a range of neutron energy spectra by weighting the MD-derived quantities with the PKA spectrum. The results of this exercise are shown in Fig. 3 for the same three parameters plotted in Fig. 2 [11]. The values in Fig. 3 can be thought of as effective, spectrum-averaged primary damage cross sections for the range of irradiation environments included: ITER is a DT fusion first wall spectrum, in the water-cooled HFIR, PTP and RB are the target and removable beryllium

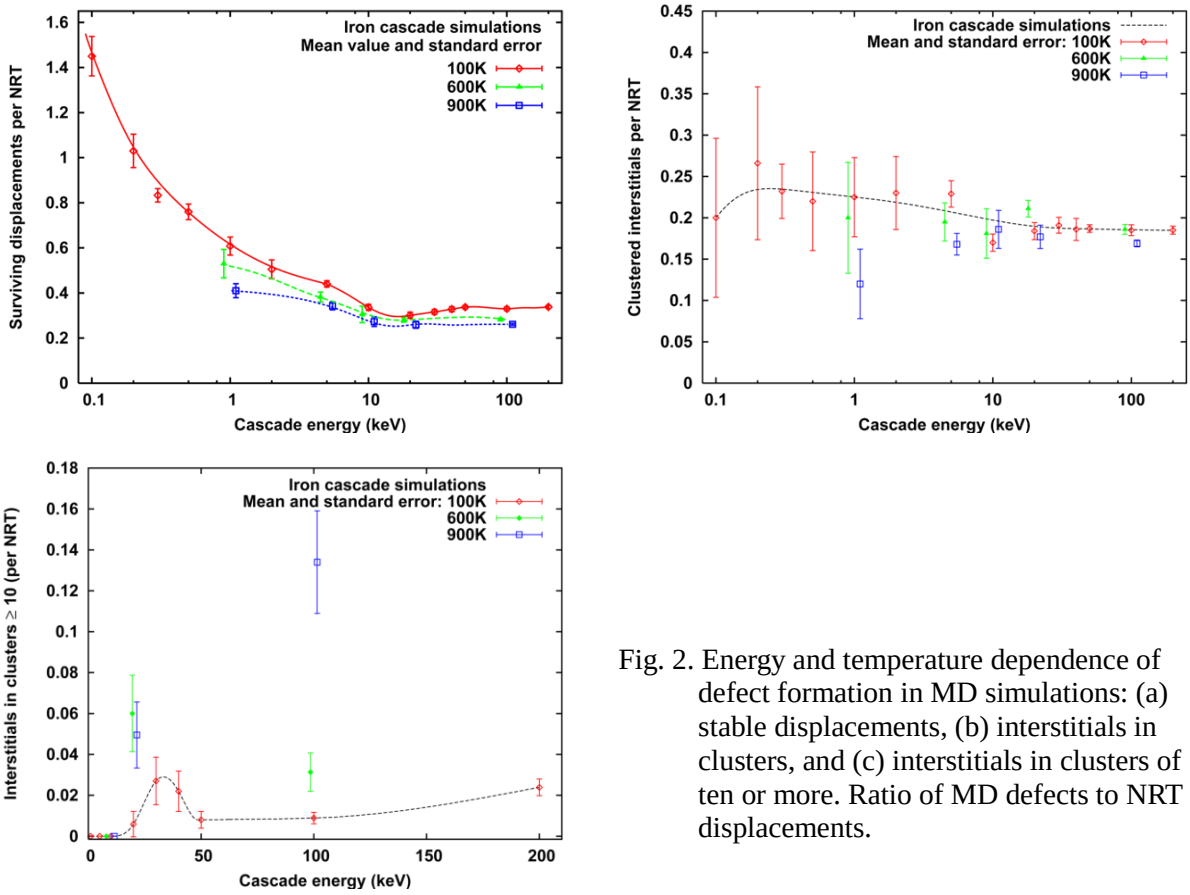

Fig. 2. Energy and temperature dependence of defect formation in MD simulations: (a) stable displacements, (b) interstitials in clusters, and (c) interstitials in clusters of ten or more. Ratio of MD defects to NRT displacements.

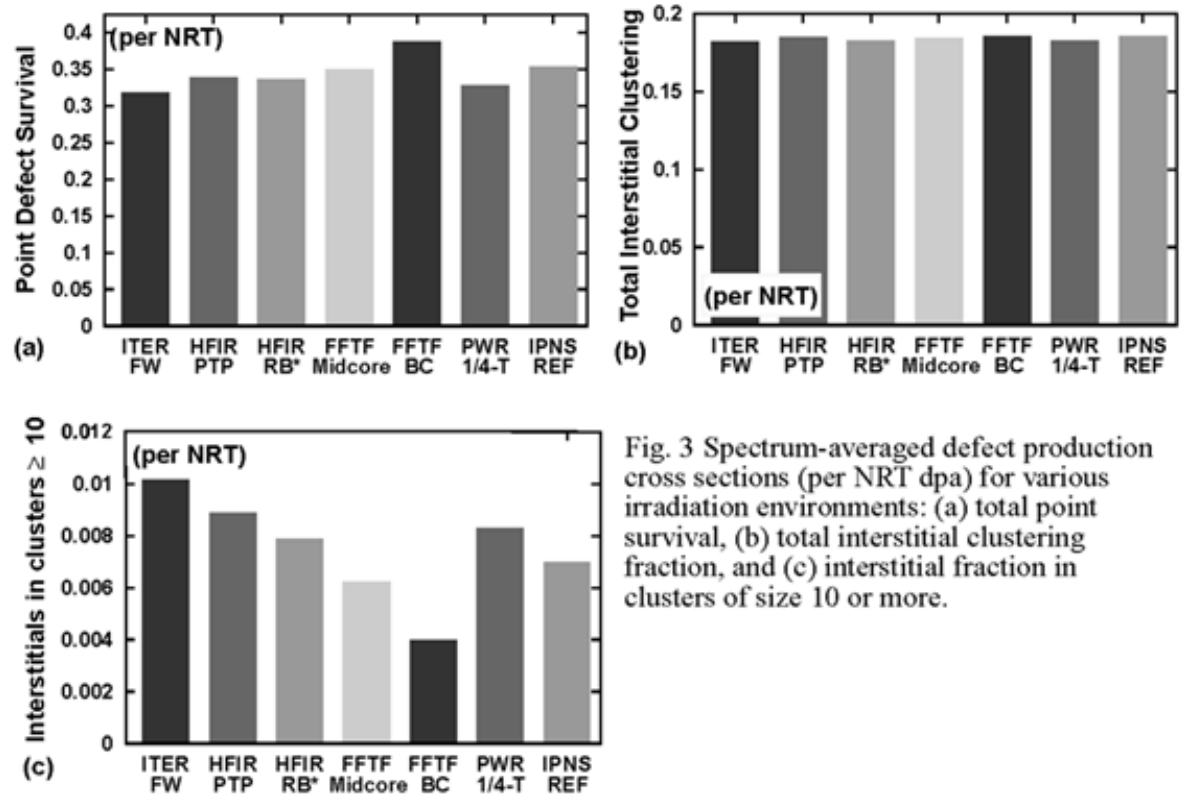

Fig. 3 Spectrum-averaged defect production cross sections (per NRT dpa) for various irradiation environments: (a) total point survival, (b) total interstitial clustering fraction, and (c) interstitial fraction in clusters of size 10 or more.

irradiation positions, in the sodium cooled FFTF, the mid-core and below-core positions are used, PWR denote the ¼-T position in a light water reactor pressure vessel, and IPNS is 400 MeV spallation neutron source. These results demonstrate how atomistic simulations can be used to obtain damage correlation parameters based on the NRT damage energy (displacement dose). Moreover, the information they contain is suitable for use in kinetic models that are used to simulation damage accumulation over long times [11-13].

Damage Function Analysis

For historical reasons, it is also useful to briefly discuss an attempt from the early 1970s to develop neutron-energy-specific damage cross sections which were called damage functions [14-17]. Damage function analysis slightly predated the development of the NRT dpa. Rather than being an attempt to develop a cross environment dose unit, the objective was to provide effective cross sections to permit comparisons of specific property changes obtained from different irradiation environments. These damage functions were developed in a similar way to other cross sections; simplistically:

1) an attempt is made to determine which part of neutron energy spectrum is responsible for the specific radiation effect of interest, such as hardening or embrittlement,
2) multiple irradiations are carried out in different environments, and the specimens are tested, and
3) the data are used in unfolding schemes to obtain the damage function.

The complexity of this approach to obtaining very specific damage correlation parameters can be illustrated by reference to Eqn. (2) in which it is clear that the damage function G_P is analogous to a cross section for the property P (e.g. change in yield strength) with $\phi(E,t)$ the neutron flux and $f(t)$ the incremental fluence [14].

$$P(\tau, T, F, \alpha_i) = \int_t \int_E G_P(T, t, E, f(t), \alpha_i)\varphi(E, t)\, dE\, dt \qquad (2)$$

where τ is the total irradiation time, T is the temperature, $F=f(\tau)$ is the total fluence, and the α_i are metallurgical variables such as composition or thermo-mechanical treatment. Along with the difficulty of actually carrying out enough irradiation experiments with sufficient sensitivity to the neutron spectrum and the measured properties, there are too many variables to make this approach practicable in general.

Representative damage functions are shown in Fig. 4 for the Charpy shift of an A302-B reactor pressure vessel steel (a) [15], and for the change in total elongation in 20% cold-worked AISI-316 stainless steel irradiated in the EBR-II (b) and in both the HFIR and EBR-II (c) [17]. Note how similar the A302-B damage function is to the dpa cross section in Fig. 1. This is consistent with the observation that such embrittlement correlates well with NRT-dpa [8]. The tensile elongation damage function for irradiation in EBR-II in Fig. 4(b) is also similar to the NRT-dpa cross section, but the energy dependence is significantly altered when the HFIR data is included in Fig. 4(c). This difference was attributed to the higher production of helium by nuclear transmutation in the HFIR, and improved correlation of the data between these two reactors was obtained with a correlation parameter that included both He and dpa [17]. The reason for presenting the damage function results here is to illustrate the inherent complexity on obtaining an adequate data correlation parameter for a single mechanical property, for a single material, in a limited range of irradiation conditions (note that Fig. 4(a) is limited to temperatures of 288 to 307°C).

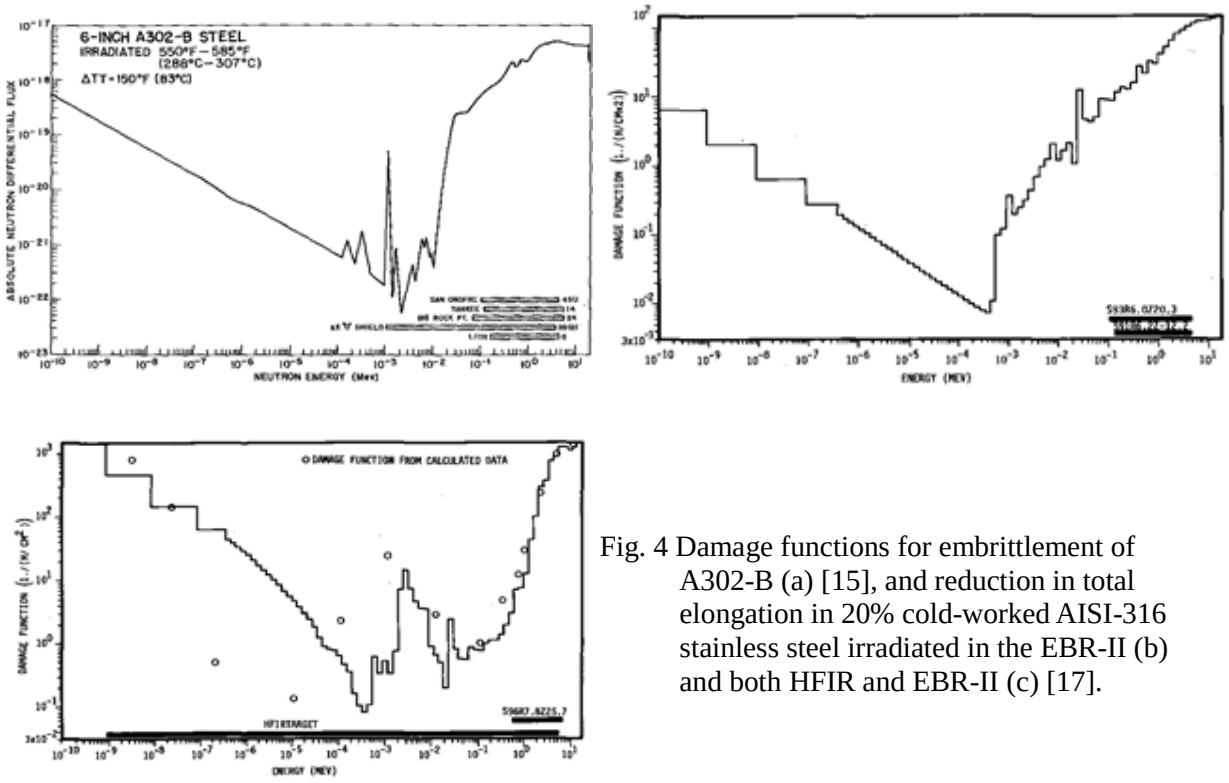

Fig. 4 Damage functions for embrittlement of A302-B (a) [15], and reduction in total elongation in 20% cold-worked AISI-316 stainless steel irradiated in the EBR-II (b) and both HFIR and EBR-II (c) [17].

Summary

The observable effects of irradiation on material properties are complex and each such property changed depends sensitively on a range of irradiation and material parameters. This works against development of a universal exposure parameter. The irradiation dose to the material (both ionizing and displacement dose) can be calculated with good accuracy as long as the relevant reaction cross sections are known and implemented in the codes used. This suggests that a focus on dose calculations is warranted.

When assessing damage correlation parameters, it is important to determine the appropriate dose parameter first. Then a clear distinction between damage formation and damage accumulation needs to be kept in mind. The dose unit is most helpful for estimating the primary damage generation, e.g. how damage energy is used to estimate atomic displacements. However, damage accumulation requires longer times and involves kinetic and thermodynamic processes that cannot be accounted for in a dose or primary damage unit. The adequacy of the primary damage formulations can be assessed through their use in mean field reaction rate theory or kinetic Monte Carlo microstructural evolution models to predict damage accumulation. The results of these models can be directly compared with experimental observations.

References

1. G.H. Kinchin and R.S. Pease, Reports on Progress in Physics 18 (1955) 1-51.
2. M.J. Norgett, M.T. Robinson, and I.M. Torrens, Nucl. Engr. and Des. 33 (1975) 50-54.
3. M.T. Robinson and O.S. Oen, J. Nucl. Mater. 110 (1982) 147-149.
4. M.T. Robinson, J. Nucl. Mater. 216 (1994) 1-28.
5. J. Lindhard, V. Nielson, M. Scharff and P. V. Thomsen, Kgl. Dan. Vidensk. Selsk. Mat.-Fys. Meld. 33 (1963) 1-42.
6. ASTM E693, ASTM International, West Conshohocken, PA.
7. ASTM E521 ASTM International, West Conshohocken, PA.
8. R. E. Stoller and G. R. Odette, J. Nucl. Mater.186 (1992) 203-205.
9. R. E. Stoller, "Primary Radiation Damage Formation", in Comprehensive Nuclear Materials,

R. J. M. Konings, T. R. Allen, R. E. Stoller, and S. Yamanaka, Editors, Elsevier Ltd., Amsterdam, 2012, pp. 293-332.
10. R. E. Stoller and L. R. Greenwood, J. Nucl. Mater.271 & 272 (1999) 57-62.
11. R. E. Stoller and L. R. Greenwood, “From Molecular Dynamics to Kinetic Rate Theory: A Simple Example of Multiscale Modeling”, Multiscale Modeling of Materials, Vol. 538, V. V. Butalov, T. Diaz de la Rubia, P. Phillips, E. Kaxiras, and N. Ghoniem, Editors, Materials Research Society, Pittsburgh, PA, 1999, pp. 203-209..
12. S. I. Golubov, A. V. Barashev, and R. E. Stoller, "Radiation Damage Theory," in Comprehensive Nuclear Materials, R. J. M. Konings, T. R. Allen, R. E. Stoller, and S. Yamanaka, Editors, Elsevier Ltd., Amsterdam, 2012, pp. 357-391.
13. R. E. Stoller, S. I. Golubov, C. Domain, and C. S. Becquart, J. Nucl. Mater.382 (2008) 77-90.
14. Gold, R., Lippincott, E. P., McElroy, W. N., and Simons, R. L., "Radiation Damage Function Analysis”, Effects of Radiation on Structural Materials. ASTM STP 683, J. A. Sprague and D. Kramer, Eds., ASTM International, West Conshohocken, PA, 1979, pp. 380-401.
15. Serpan, C.Z., Jr., "Damage-Function Analysis of Neutron-Induced Embrittlement in A302-B Steel at 550 F (288 C)", Effects of Radiation on Substructure and Mechanical Properties of Metals and Alloys”, ASTM STP 529, ASTM International, West Conshohocken, PA, 1973, pp. 92-106 .
16. Yoshikawa, H. H., "Materials Performance Prediction from Irradiation Test Data”, Effects of Radiation on Substructure and Mechanical Properties of Metals and Alloys. ASTM STP 529, ASTM International, West Conshohocken, PA, 1973, pp. 337-348.
17. Simons, R. L., "Neutron Energy Dependent Damage Functions for Tensile Properties of 20 Percent Cold-Worked Type 316 Stainless Steel", Irradiation Effects on the Microstructure and Properties of Metals, ASTM STP 611, ASTM International, West Conshohocken, PA, 1976, pp. 181-192.

Modified NRT equations for damage and mixing developed by the OECD NEA primary damage group

Kai Nordlund

University of Helsinki
Finland

1. Background

This report summarizes the work done recently at the OECD Nuclear Energy Agency working group on primary damage.

Particles with kinetic energies clearly above conventional thermal energies, i.e. with E_{kin} > 1 eV, exist in nature due to cosmic radiation and radiation decay, but are nowadays produced in a wide range of man-made devices for basic research and practical applications. For instance, the great accelerators at CERN and other particle physics laboratories in the world attempt to unravel the fundamental nature of the universe, and numerous smaller devices are widely used for equally exciting research in physics, chemistry, medicine and nanoscience [JAPreview09]. On the application side, ion implantation is one of the key technologies in silicon chip manufacturing, and electron accelerators are one of the key ways to treat cancer. All of these activities make it interesting and important to understand what the fundamental effects of high-energy particles on matter are.

One of the main consequences of the interaction of high energy particles (photons, neutrons, ions or electrons) with materials is the formation of lattice defects resulting from the energy transfer towards the atoms (other consequences include production of non-damage-producing phonons, excitons and plasmons, secondary electrons and photons, and heating of the material). Indeed, this consequence is the main reason why radiation has both detrimental and beneficial effects on materials. The damage can take many forms: in a crystal it is easy to understand that an atom can be kicked out from its initial lattice site, leaving an empty site (a vacancy) behind and creating an atom at an interstitial site in front.

But it is important to realize the crystal defects formed can also be much more complicated: they can for instance be defect clusters [Par00], amorphous zones [Rua84], dislocation loops [Eyr73] or three-dimensional defects [Sil59b, Kit85]. On surfaces the damage can also take the form of adatoms [Has04], craters [Gha94, Bir99] and ripples [Erl99], and in amorphous materials over- or undercoordinated atoms [Laa99I] or empty regions [Roo92]. Photon irradiation creates damage largely by electronic excitation processes causing bond breaking [Ref], although very high-energy gamma photons can also produce damage by atomic recoil processes [Ram94].

The damage production mechanisms can in most cases be well divided into two categories by time scale. The **primary damage** is formed immediately of the particle impact by atomic collision processes and strong material heating caused by them far from thermodynamic equilibrium. Numerous computer simulation and experimental studies have shown that the time scale for the ballistic atom collision processes is of the order of 100 fs, and the time scale for subsequent thermalization of the collisions $1 - 10$ ps [Dia87, Stu99]. After this athermal (in the sense that equilibrium thermally activated processes are not significant) stage, long-time scale (nanoseconds to years) damage evolution caused by thermally activated processes can occur.

The displacements-per-atom concept was introduced from the original ideas of production of primary point defects in materials. The idea is that the energetic particle travels mostly straight in a material, but occasionally collides strongly in a binary collision and imparts energy to a lattice atom.

As an aside, we note that for neutrons and electrons this is a very good approximation due to their very small collision cross sections, while for ions and atomic recoils it is questionable: in many cases these can collide with several nearest-neighbour atoms in sequence, making the process inherently many-body rather than binary in nature. The multiple simultaneous collisions can be described as a "displacement spike" or "heat spike". This concept was already proposed in the 1950's [Bri54, Koe56] and is by now well established [Bac94, Ave98].

For a binary collision, it is intuitively clear that of the energy imparted to a lattice atom is less than the cohesive energy of an atom in the lattice, it will not leave its lattice site, and no defect will be produced. On the other hand, if the energy given to the atom is orders of magnitude higher than the cohesive energy, the atom can be expected to become a recoil that travels itself in the lattice and produces more defects. Such considerations lead Kinchin and Pease to formulate the Kinchin-Pease equation, which states that the number of defects produced is [Kin55]:

$$N_d(T_d) = \begin{bmatrix} 0 & , & T_d < E_d \\ 1 & , & E_d < T_d < 2E_d \\ \dfrac{T_d}{2E_d} & , & 2E_d < T_d < \infty \end{bmatrix}$$

Here the quantity T_d stands for the energy available for damage production. For a single neutron or ion it is equal to the nuclear deposited energy $F_{D,n}$ = the total particle energy minus the energy that is lost to electronic stopping power. In the field of radiation safety, we note that the nuclear deposited energy is known as "non-ionizing energy loss", NIEL, and the electronic deposited energy as "Linear energy transfer", LET, although depending on precise definition these quantities may not be exactly equal.

We note that for many ions one can also give $F_{D,n}$ as the total nuclear deposited energy per volume or depth. In this case, $F_{D,n}$ contains also the energy deposited to sub-threshold atomic recoils, and it is not exactly correct to insert $F_{D,n}$ into the last line of equation 1, as then also the energy given to subthreshold recoils becomes calculated into the damage production. In practice, the fraction of energy deposited to subthreshold recoils is often quite small and this distinction can be ignored.

The only parameter in equation (1) is the **threshold displacement energy** E_d. This parameter can be expected to be higher than the cohesive energy (which are of the order of 5 eV/atom in typical hard solids [Kittel]), and will be discussed in the next subsection.

Later on, equation (1) was specified by Norgett, Robinson and Torrens based on binary collision approximation (BCA) computer simulations to take into account the possibility of ballistic processes recombining the defect as it was produced [NRT]. This lead to the modified Kinchin-Pease equation, nowadays most often known as the NRT equation, that gives the number of defects produced as:

$$N_d(T_d) = \begin{bmatrix} 0 & , & T_d < E_d \\ 1 & , & E_d < T_d < 2E_d / 0.8 \\ \dfrac{0.8T_d}{2E_d} & , & 2E_d / 0.8 < T_d < \infty \end{bmatrix}$$

where the new factor 0.8 come from the BCA simulations.

This basic equation can be used to calculate the number of "defect-producing" or displaced atoms in any material for which E_d is known and the damage energy T_d can be calculated. For instance, neutron transport codes such as SPECTR and NJOY can calculate the energy given by neutrons to lattice atoms, and tables of nuclear deposited energy can then tell for each atom energy the value of T_d. This way, one can calculate the number of atoms displaced according to the Kinchin-Pease or NRT models in a given volume of material. Furthermore, if this quantity is normalized by the number of atoms in the same volume, one obtains the **displacements-per-atom (dpa)** unitless quantity,

$$\text{dpa} = \text{displacements per atom} = \frac{\text{Number of displaced atoms in volume from NRT equation}}{\text{Number of materials atoms in same volume}},$$

which in this simplified model gives the defect concentration c of primary damage vacancies and interstitials in the material. Assuming there are no surfaces or defect sinks in the system, naturally the concentrations for vacancies, interstitials and Frenkel pairs (FP's) are equal: $c_v = c_i = c_{FP}$.

The dpa concept and KP/NRT equations are widely used in estimating the amounts of radiation damage in materials. The main reason is of course simplicity: doing the calculation is very easy. Similarly, the "dpa" concept is appealing in that it is easy to understand, and gives (if calculated correctly) a good idea of what fraction of atoms are displaced during an irradiation process. For instance, a total radiation dose of, say, 10 kJ/cm^3 does not tell a non-expert anything about how many defects such a dosage can be expected to cause, whereas a value of, say, 0.01 dpa would tell any physicists that one atom in a hundred has been displaced (and hence likely to be a defect).

Another major advantage of the dpa concept is that it can be used for scaling radiation doses or fluences between different kinds of irradiations. Since it included implicitly the value of the nuclear deposited energy, which can be reliably calculated, it can be used to estimate how much damage different irradiations cause. For instance, if damage has been produced in a material by, say, 50 keV Ne ions, and one later on wants to switch to using, say, Ar ions, a dpa calculation can tell what energy for the Ar ions can be expected to produce about the same damage as the 50 keV Ne irradiation did. If the damage later on turns out not to follow the dpa scaling, this indicates nonlinear behavior in the damage production [Kuc01b, Kar09].

The problems in using the dpa standard arise from that the name "displacements-per-atom" makes it very tempting to interpret that dpa = defect concentration. Indeed, within the original Kinchin-Pease and NRT definitions and the approximations and assumptions built into them, it is fully valid to do so. However, in many cases current knowledge shows that many of these approximations and assumptions are very problematic, and lead to major (even more than an order of magnitude) errors in equating the dpa value with the number of defects.

2. Athermal Recombination-Corrected dpa (arc-dpa)

It is well established that the damage in elemental metals is much smaller than the value predicted by the NRT equation that forms the basis for standard dpa calculations. Numerous experimental and simulation studies have shown that in most metals studied, the damage level for low-energy recoils is fairly close to the NRT value, but on increasing nuclear damage energy, the relative damage efficiency

$$\xi(E) = \frac{N_{True-number-of-FP's}}{N_{NRT-prediction}}$$

decreases from $\xi \approx 1$ near the threshold to a value that saturates around roughly 0.2-0.4 [Ave98], see Figs. 1 and 2. Note that in this discussion, E signifies specifically the nuclear deposited (damage) energy by a single recoil $F_{D,n}$. Part of the total recoil energy E_{rec} also goes into electronic deposited energy $F_{D,e}$ and for very high (MeV or more) some may also go into nuclear reactions $F_{D,nr}$ such that $E_{rec} = F_{D,n} + F_{D,e} + F_{D,nr}$.

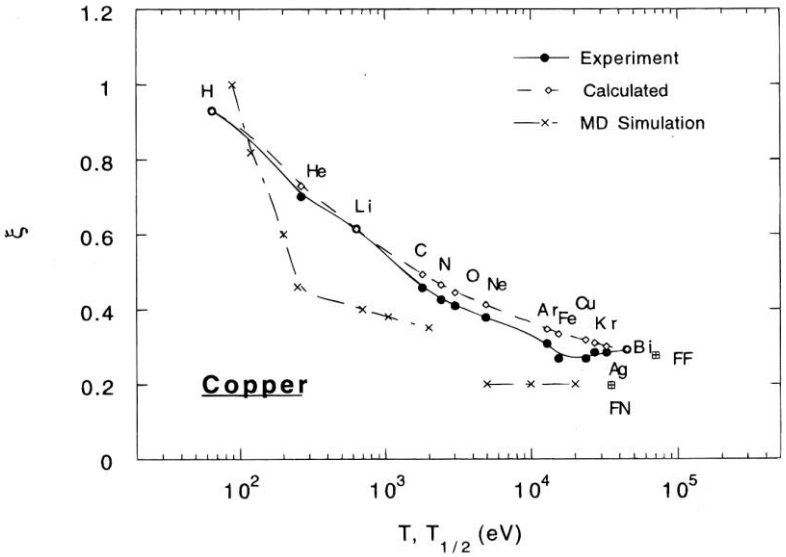

Fig. 1. Experimental and simulation evidence that the ratio ξ between real damage and that predicted by the Kinchin-Pease equation is much below 1 in Cu. The MD simulation is the raw MD data for a fixed energy T, and the "Calculated" curve is a calculation from the MD results for the ions used in the experiments, plotted as a function of the weighted average recoil energy $T_{1/2}$. Plot from Ref. [Ave98].

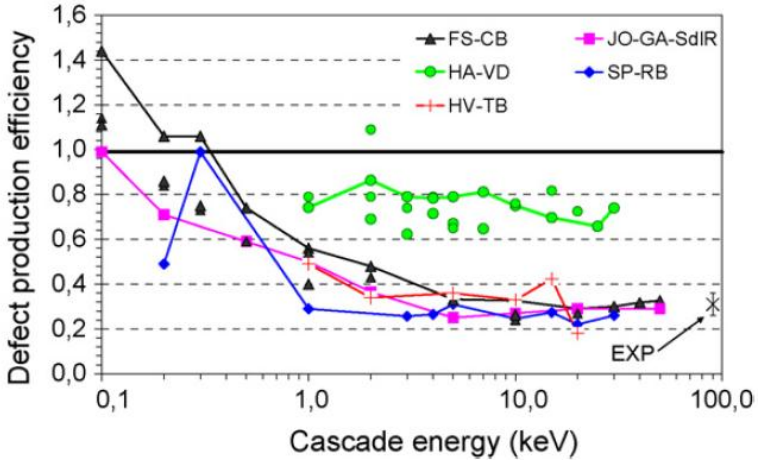

Fig. 2. Simulation evidence that the ratio ξ between real damage and that predicted by the Kinchin-Pease equation is much below 1 in Cu. Plot from Ref. [Mal06].

At intermediate energies, several groups have found that the data increases following a power law E^x where the exponent gets a value of about 0.8, see Fig. 2.KN.1. On the other hand, it is clear from binary collision approximation simulations that at very high energies (of the order of 10-100 keV depending on material) the cascades split into separated subcascades. Hence the scaling with energy must eventually turn to be linear with damage energy.

Within the OECD NEA working group, we developed a new damage function formalism. The new form is

$$N_d(E) = \begin{bmatrix} 0 & E < E_d \\ 1 & E_d < E < 2E_d/0.8 \\ \frac{0.8E}{2E_d}\xi(E) & 2E_d/0.8 < E < \infty \end{bmatrix}$$

with the efficiency function $\xi(E)$ given by

$$\xi(E) = \frac{1-c}{(2E_d/0.8)^b}E^b + c$$

Figure 3 illustrates that this damage function fits very well the data for fraction of surviving defects in Fe. Considering that there is fairly large variation between data obtained with different potentials, it does not make sense to aim for a better fit until the data itself becomes more reliable.

The parameter values E_d, b and c can be obtained from MD simulations, as experimental data obtained systematically as a function of energy is available only in Cu (Figure 3.). Naturally the fits can be redone when improved MD or experimental data becomes available.

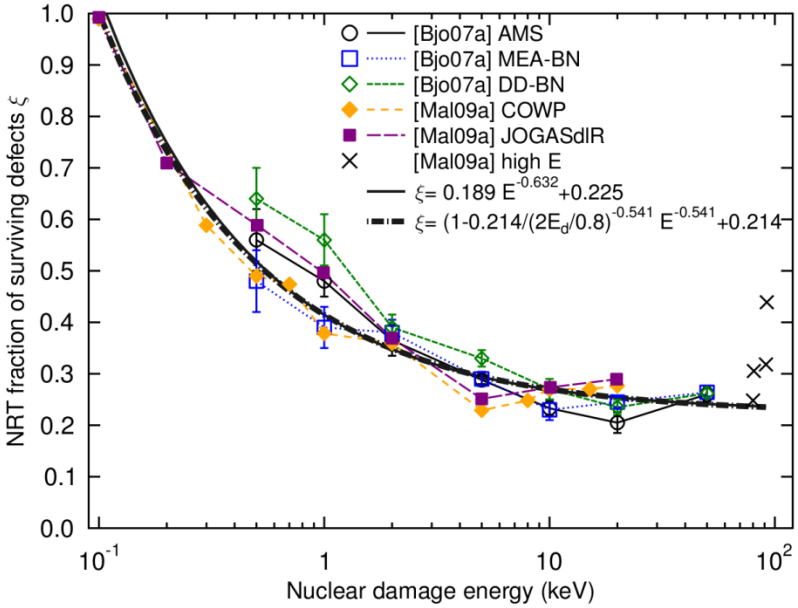

Fig. 3. Fit of the new damage function ξ(E) to data in Fe for the arc-dpa. The data sets and their notation are from Refs. [Bjo07a, Mal09a].

3. Athermal mixing-corrected dpa or replacements-per-atom (rpa)

As part of the OECD NEA work group activity, we also developed an alternative dpa function to describe the athermal mixing in cascades. The correction function, which based on discussions at the IAEA meeting will be named "replacements-per-atom" or rpa, has the form

$$\xi_{\mathrm{mix}}(E) = \left(\frac{b^c}{(2E_d/0.8)^c} + 1 \right) \frac{E^c}{b^c + E^c}$$

This correction fraction is in dense metals >> 1, because atom motion in heat spikes is enhanced beyond a binary collision picture.

4. Conclusions

I presented a summary of the work in the OECD NEA primary damage working group, which lead to two modified dpa functions, one for defect production in terms of Frenkel pairs, another one for ion beam mixing.

I emphasized that this correction function is largely relevant and needed only for irradiation effects in metals in the nuclear collisions regime. It does not in any way account for ionization or the complex forms of damage often observed in semiconductors and ionic materials

References

[Ave78] R.S. Averback, R. Benedek, and K.L. Merkle. Ion-irradiation studies of the damage function of copper and silver. Phys. Rev. B, 18(8):4158, 1978.

[Mau76] F. Maury, M. Biget, P. Vajda, A. Lucasson, and P. Lucasson. Anisotropy of defect creation in electron-irradiated iron crystals. Phys. Rev. B, 14(12):5303, 1976.

[And79] H.H. Andersen. The depth resolution of sputter profiling, Appl. Phys., 18:131, 1979.

[ASTMFe] ASTM Standard E693-94. Standard practice for characterising neutron exposure in iron and low alloy steels in terms of displacements per atom (dpa), 1994.

[Ave98] R. S. Averback and T. Diaz de la Rubia. Displacement damage in irradiated metals and semiconductors. In H. Ehrenfest and F. Spaepen, editors, Solid State Physics, volume 51, pages 281-402. Academic Press, New York, 1998.

[Bac94] David J. Bacon and Tomas Diaz de la Rubia. Molecular dynamics computer simulations of displacement cascades in metals. J. Nucl. Mat., 216:275--290, 1994.

[Bau69] W. Bauer, A. I. Anderman, and A. Sosin. Atomic displacement process in gold. Phys. Rev. A, 185(3):870, 1969.

[Bjo07a] C. Björkas and K. Nordlund, Comparative study of cascade damage in Fe simulated with recent potentials, Nucl. Instr. Meth. Phys. Res. B, 259:853, 2007.

[Cat94] M.-J. Caturla, T. Diaz de la Rubia, and G.H. Gilmer. Point defect production, geometry and stability in silicon: a molecular dynamics simulation study. Mat. Res. Soc. Symp. Proc., 316:141, 1994.

[Jun81] P. Jung. Average atomic-displacement energies of cubic metals. Phys. Rev. B, 23(2):664, 1981.

[Kin55] G. H. Kinchin and R. S. Pease, Rep. Prog. Phys. 18, 1 (1955)

[Kin82] W. E. King, R. Benedek, K. L. Merkle, and M. Meshii. Re-examination of the threshold energy surface in copper. In Jin-Ichi Takamura, editor, Point Defects and Defect Interactions in Metals, page 789. North Holland, Amsterdam, 1982.

[Lom67] J. N. Lomer and M. Pepper. Anisotropy of defect production in electron irradiated iron. Phil. Mag., 16:119, 1967.

[Luc62] P. G. Lucasson and R. M. Walker. Production and recovery of electron-induced radiation damage in a number of metals. Phys. Rev., 127:485, 1962.

[Luc75] P. Lucasson, The production of frenkel defects in metals. In M. T. Robinson and F. N. Young Jr., editors, Fundamental Aspects of Radiation Damage in Metals, pages 42--65, Springfield, 1975. ORNL.

[Mal02] L. Malerba and J. M. Perlado. Basic mechanisms of atomic displacement production in cubic silicon carbide: A molecular dynamics study. Phys. Rev. B, 65:045202, 2002.

[Mal06] L. Malerba, J. Nucl. Mater. 351 (2006) 28.

[Mal09a] L. Malerba, M. C. Marinica, N. Anento, C. Björkas, H. Nguyen, C. Domain, F. Djurabekova, P. Olsson, K. Nordlund, A. Serra, D. Terentyev, F. Willaime, and C.S. Becquart, Comparison of empirical interatomic potentials for iron applied to radiation damage studies, J. Nucl. Mater., 406:19-38, 2010.
[Mau75] F. Maury, P. Vajda, M. Biget, A. Lucasson, and P. Lucasson. Anisotropy of the displacement energy in single crystals of molybdenum. Radiation Effects, 25:175-185, 1975.
[Mil94] LeAnn A. Miller, David K. Brice, Anil K. Prinja, and S. Thomas Picraux. Anisotropic displacement threshold energies in silicon by molecular dynamics simulations. Mat. Res. Soc. Symp. Proc., 209:171, 1991.
[NRT] M. J. Norgett, M. T. Robinson, and Ian M. Torrens. A proposed method of calculating displacement dose rates, Nucl. Engr. and Design, 33(1):50-54, 1975.
[Smi01] Brian W. Smith and David E. Luzzi. Electron irradiation effects in single wall carbon nanotubes. J. Appl. Phys., 90(7):3509, 2001.
[Urb82] K. Urban, B. Saile, N. Yoshida, and W. Zag. The temperature dependence of the displacement threshold energy in f.c.c. and b.c.c. metals. In Jin-Ichi Takamura, editor, Point Defects and Defect Interactions in Metals, page 783. North Holland, Amsterdam, 1982.
[Vaj77] P. Vajda. Anisotropy of electron radiation damage in metal crystals. Rev. Mod. Phys., 49:481, 1977.
[Veh68] W. E. Vehse, W. A. Sibley, F. J. Keller, and Y. Chen. Radiation damage in zno single crystals. Phys. Rev., 167(3):828, 1968.
[Vit77] N. A. Vitovskii, D. Mustafakulov, and A. P. Chekmareva. Threshold energy for the displacement of atoms in semiconductors. Sov. Phys. Semicond., 11(9):1024-1028, 1977.
[Win98] W. Windl, T. J. Lenosky, J. D. Kress, and A. F. Voter. First-principles investigation of radiation induced defects in Si and SiC. Nucl. Instr. and Meth. B, 141:61-65, 1998.

What we can improve in the calculation of displacement cross-sections

A.Yu. Konobeyev, U. Fischer

Karlsruhe Institute of Technology, Karlsruhe
Germany

The goal of the report is to discuss briefly ways of the improvement of displacement cross-section calculations including the calculation of the number of stable defects produced in irradiated materials, recoil energy distributions, and various aspects of the nuclear data processing.

1. NRT model: applications, the relative success and problems

The NRT model [1,2] is widely used for the estimation of the number of defects produced in materials under irradiation. The implementation of the model in many codes used extensively, like NJOY, MCNPX, LAHET, and SPECTER reflects its popularity. According to the model the number of stable defects produced in materials by the ion with the kinetic energy T_{PKA} is equal to

$$N_{NRT}(T_{PKA}) = (0.8/2E_d)\, T_{dam}(T_{PKA}), \qquad (1)$$

where T_{dam} is the "damage energy" equal to the energy transferred to lattice atoms reduced by the losses for electronic stopping of atoms in displacement cascade, E_d is the effective threshold displacement energy derived from electron irradiation experiments. On the practice, a more general formula of Robinson [2] is used for calculations, for example in NJOY [3], as one presented in the work of Norgett, Robinson, and Torrens [1].

The success and the wide application of the NRT model can be attributed to its simplicity as to the relative low influence of irradiation conditions on realistic numbers of defects produced in materials referred to ones calculated with NRT in a number of important applications [4-6].

The efficiency of defects production in irradiated materials is used as a measure of deviations of the number of defects obtained experimentally or theoretically to the number of defects predicted by the NRT model:

$$\xi(T_{PKA}) = N_D(T_{PKA}) / N_{NRT}(T_{PKA}) , \qquad (2)$$

where N_D is the number of stable displacements measured or calculated using theoretical models.

"Internal" limitations of the model. The usage of the NRT model is limited at least by two conditions [1]: i) atomic and mass numbers of PKA (Z_1,A_1) are to be close to ones of a target $Z_1 \approx Z_2$, $A_1 \approx A_2$, ii) the PKA energy is to be less than the maximal energy T_{max} [MeV] < 0.025 $Z_1^{4/3}A_1$. The influence of the limitations on calculated displacement cross-sections were considered in details in Ref. [7].

Comparison with measured data. Model predictions differ appreciable from available experimental data corresponding to different types of irradiation: i) with neutrons in reactors, ii) with neutrons from d+Be reaction initiated by deuterons with energies 30 and 40 MeV (see Ref. [5]), iii) with protons at primary energy 1.1 and 1.94 GeV [8], and iv) with high energy heavy ions [9].

Comparison with MD simulations. The simulations using the method of molecular dynamics show the marked deviation of obtained $\xi(T_{PKA})$ from $\xi = 1$ predicted by the NRT model.

The use of the model faces problems, which cannot be apparently solved by a simple redefinition of E_d values in Eq. (1).

2. Use of BCA model

The potential of the model for reliable predictions of the number of stable defects produced under irradiation seems rather limited. Usually, BCA calculations with commonly adopted E_d values [3,5] overestimates results of NRT calculations as well in cases were NRT predictions seems higher than results of MD simulations and measured data (Slide[1] 11).

An attempt to reproduce results of MD calculations with the BCA model at relative low ion energies by the appropriate choice of the value of effective threshold energy leads to markedly unphysical E_d values and gives quite different results by applying different codes, SRIM [10] and IOTA [11].

More advanced calculations [5] performed with the MARLOWE code [12] using the same interatomic potentials, which were applied in MD simulations, shows a noticeable difference in the number of created defects calculated with BCA and MD at ion energies, where parameters of the BCA model were not special fitted to get an agreement with the numbers of defects predicted by the MD method (Slide 13).

3. MD simulation and "constant efficiency" approximation

An additional test of N_D values calculated using the MD method can be the comparison with the data extracted from experimental damage rates for materials irradiated with neutrons in reactors and from the d+Be reaction. Such data were compiled in Ref. [5]. With rather rare exceptions [13,14], such comparison was made with certain reservations, usually ignored, perhaps because of expected difficulties associated with nuclear data processing.

The comparison shows the perfect agreement of averaged ξ value obtained using results of MD simulations performed by Stoller for iron [15] $<\xi> = 0.32 \pm 0.1$ and one derived from experimental data [5] 0.32 ± 0.05, the good agreement between $<\xi>$ from MD calculations of Caturla and co-authors [16] for copper 0.27 ± 0.03 and the experimental value 0.31 ± 0.03, and rather underestimated $<\xi>$ value from MD calculations for tungsten comparing with measured data [5] (Slide 15).

[1] Slides of the presentation "What we can improve in the calculation of displacement cross-sections" of A.Yu. Konobeyev and U. Fischer on the Technical Meeting on Primary Radiation Damage, October 1-4, 2012, Vienna, available on: http://www-nds.iaea.org/dpa/

The difference of the temperature of measurements, 4-5 K and ones adopted in MD simulations, T = 10-900 K, makes to attract attention. The agreement of simulations and experiments in this case can be attributed to the important role of the temperature increase during the displacement cascade and the weak influence of equilibrium temperature on results.

To use MD results in some way outside of the range of relatively low energies adopted in the modelling, the obtained values are extrapolated sometimes to higher energies using the "constant efficiency" approximation (see, for example, Ref. [17]). In this case the ξ value corresponding to the maximal energy available in MD calculations is used at any high energy of ions (Slide 16).

Despite the attractive simplicity of the approximation it faces a number of problems: i) calculated displacement cross-sections (σ_d) at high projectile energies are appreciably lower as measured data [16,17] and σ_d values obtained using combined BCA-MD approach (Sect. 4), ii) experimental data [9] show marked deviations from the constant ξ assumption (Slide 18). The "constant efficiency" approximation seems questionable, while more advanced calculations are required to estimate the number of defects produced in materials during the irradiation (see below).

4. Combined BCA-MD simulations

Combined BCA-MD simulation seems a rather consistent approach to the evaluation of the number of defects produced in materials under the irradiation with intermediate and high energy ions [11, 17-20].

In such modelling, for an energetic ion moving in the material the simulation of atomic collisions is performed using the BCA model up to a certain "critical" energy of the ion (T_{crit}). Below this energy the BCA calculation is stopped and the number of defects is evaluated according to the result of MD simulations. Such procedure is performed for all PKA produced in the atomic collision cascade. The value of the "critical" energy is taken as large as possible to minimize the effect of the overlapping of cascade branches before the MD simulation starts. Usually T_{crit} corresponds to the T_{dam} energy equal to 30-60 keV.

The BCA-part of simulations discussed below has been performed using the IOTA code developed in KIT, Karlsruhe (Slide 20) and described in details in Ref. [11]. The last improvements of the code were made in 2011.

The results of BCA-MD simulations are in a quite good agreement with experimental data [5,8,9,21] (Figs. 1, 2). The typical difference between displacement cross-sections (σ_d) for incident neutrons calculated using the NRT model and the BCA-MD approach is shown in Slide 27. The example of calculations for iron carbide is shown in Slide 28.

The results of BCA-MD calculations can be parameterized in the form of $\xi(T_{PKA})$ and implemented in the NJOY code concerning the calculations with the DF routine [3] responsible for the NRT model. Before applying such approach for the processing of nuclear data getting σ_d values several questions need to be clarified: i) the influence of the temperature on the evaluated number of defects produced in materials, ii) the modelling using the kinetic Monte Carlo method (kMC), and iii) the uncertainty of predicted results.

The kinetic Monte Carlo method predicts the reduction of the number of stable displacements obtained with MD to 70% for iron at T=300-600 K [22]. The reduction can be taken into account in the data processing getting σ_d values for iron using NJOY and other codes.

Results of kMC modelling [22] can be used to improve additionally the T-dependence of survived defects for iron. The problem remains open for other materials.

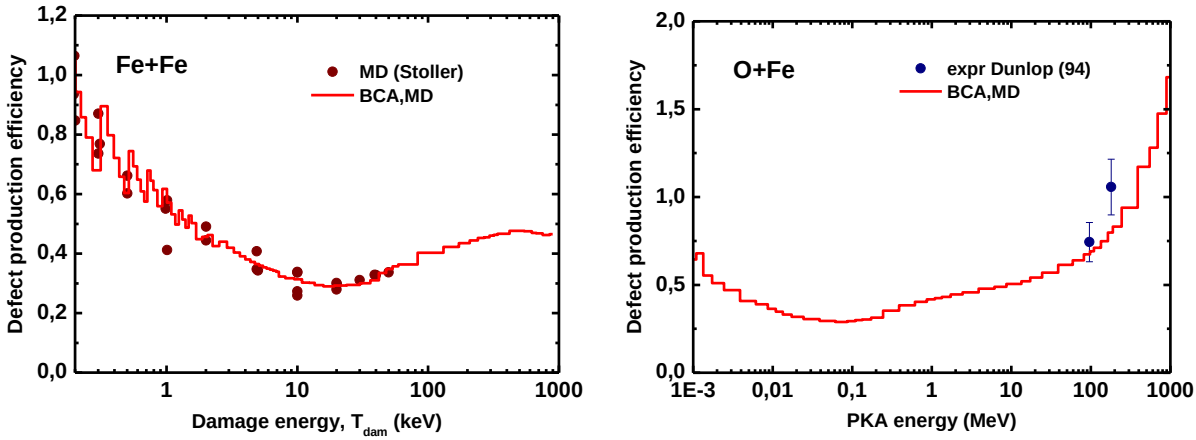

Fig. 1. Efficiency of the defect production ξ for the Fe + Fe and O + Fe irradiation obtained using the combined BCA-MD method, results of the MD simulation [15], and measured data [9].

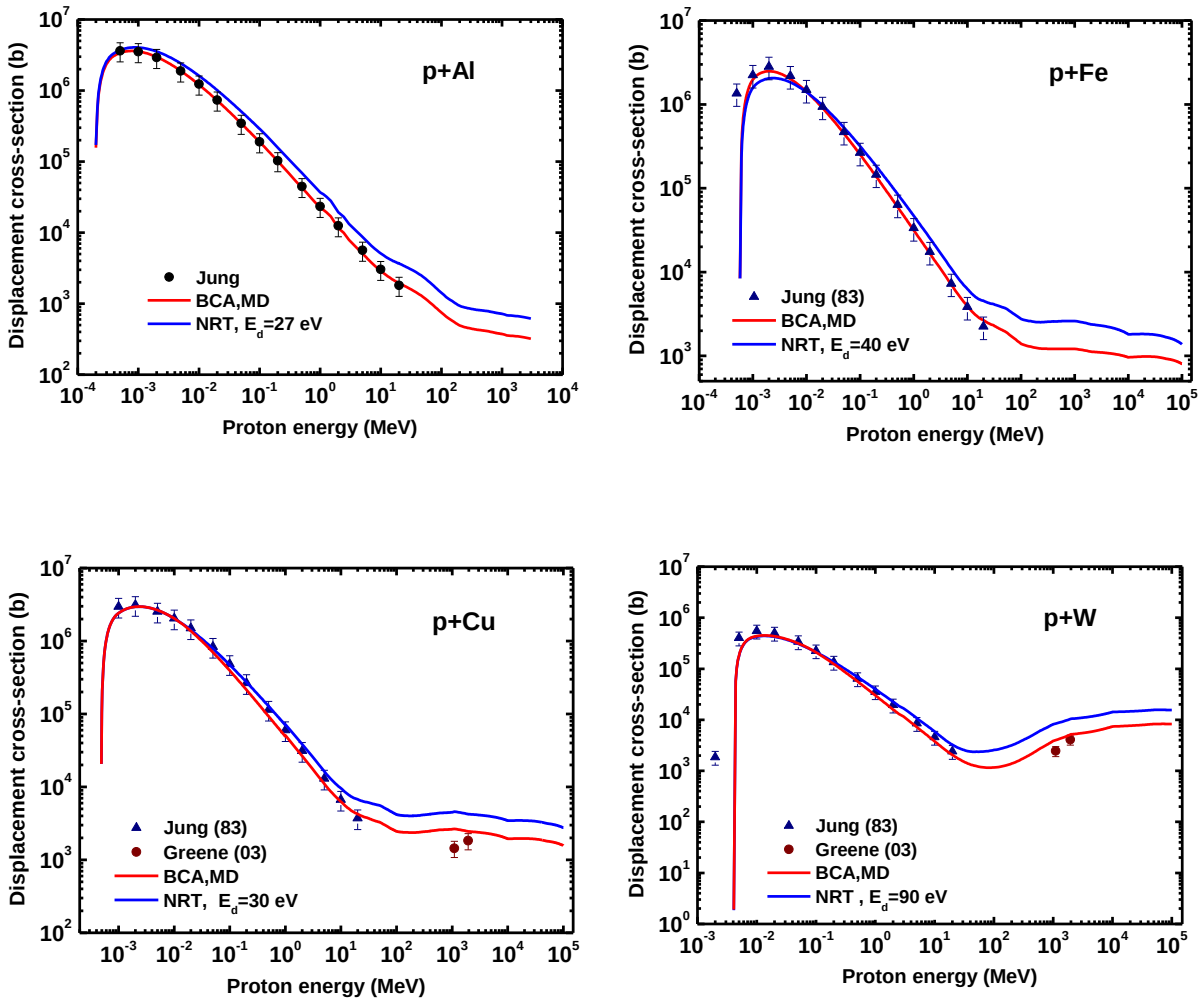

Fig.2 Displacement cross-sections calculated using BCA-MD approach and NRT model. Measured data are taken from Refs. [8,21].

The uncertainty of MD predictions resulting from the use of different interatomic potentials was discussed recently in a number of works (see e.g. [13, 14, 23, 24]. This uncertainty can be reduced after the comparison of <ξ> values obtained using results of MD simulations and <ξ> values derived from experimental damage rates for materials under neutron irradiations compiled in Ref. [5].

Other factors resulting to the scatter of calculated displacement cross-sections were discussed in Ref. [25].

5. Proposed improvements in the evaluation of the number of defects produced in materials

Improvements concern the application of combined BCA-MD method for calculations and the use of experimental data and systematics for additional correction of results of simulations.

Materials can be divided into three groups according to completeness of information required for the evaluation of the number of defects produced under the irradiation. Accordingly, evaluation approaches are varied.

I. Results of MD simulations and <ξ> values derived from experimental damage rates in various units are available (Fe, Al, Ti, V, Ni, Cu, Zr, and W). The calculation of the number of stable defects is performed using the BCA-MD approach up to hundreds of keV of PKA kinetic energy. The subsequent correction is performed using results of kMC, at least for iron, and the averaged values of defect generation efficiency <ξ> derived from experimental data [5]. Some compounds, Fe_3C, Fe_xCr_y, Ni_3Al, WC can also be attributed to this group, at least, as concerns BCA-MD calculations.

II. MD simulations were not performed, while the experimental values of <ξ> are available (Mg, Co, Nb, Mo, Ta, and some others). The typical energy dependence of defect production efficiency derived from MD calculations (Slide 10) is parameterized, for example in the form $\xi(T_{PKA},C_{\xi,exp})$ (Slide 38, see also Ref. [18]). Parameter values are estimated using averaged <ξ> values extracted from experimental data [5].

III. MD simulations were not performed and experimental values <ξ> are absent. Parameters for $\xi(T_{PKA},C_{\xi,exp})$ are evaluated using <ξ> values obtained for the considered type of materials (Table 4 from Ref. [5]).

6. Proposed improvements in processing of nuclear data using NJOY concerning displacement cross-sections

Total displacement cross-sections. Two different approaches can be considered as alternative to the current processing of nuclear data using the NJOY code concerning σ_d calculations.

Explicit form of the data presentation. Taking into account that MD and BCA-MD simulations are performed outside of the NJOY code, it seems reasonable to record obtained displacement cross-sections in ENDF files using a special MT-number [26]. It can be one of the currently unassigned numbers, for example MT=901 to record the total displacement cross-section. The covariance information, if available, is written in MF=33, MT=901.

The other way to deal with new displacement cross-sections is the modification of the DF-routine of NJOY responsible for NRT calculations, as described below. It makes the data processing consistent, while it brings more uncertainties to final data.

$\xi(T_{PKA})$ or $N_D(T_{PKA})$ in the parametric form. Calculations involving the NRT model with the NJOY routine DF can be supplemented by the calculation of the defect production efficiency $\xi(T_{PKA})$ or the number of created defects $N_D(T_{PKA})$ obtained in the parameterized form. Global parameters (Section 5, III.) and specific values derived from MD, BCA-MD simulations can be built in NJOY, as currently it is made, for example, for E_d values. Parameters can also be entered in the code through the input file for the HEATR module similar to E_d values.

Elastic displacement cross-sections for incident charged particles. Currently, such calculations are ignored, despite the important contribution of elastic displacement cross-section σ_{del} in the total displacement cross-section (Slide 41). As in the case with total σ_d, elastic displacement cross-sections can be presented in the explicit form or calculated by NJOY.

In the first case, the special section, for example, MT=902, can be reserved for the recording of σ_{del} values obtained by an evaluator.

Built-in calculations of σ_{del} using NJOY lack an advantage of the data preparation outside of NJOY and recording them in evaluated data files. The main problem of the built-in approach involving for example the model from Ref. [27] is the proper calculation of the σ_{del} considering the interference between screened Coulomb and nuclear scattering.

Displacement cross-sections for compounds. Proposed improvements concern the calculation of displacement cross-sections using advanced methods (Sect. 3, 4) and the NRT model. At present, the data processing for compounds implies the use of the weighted sum of compound components relating to the damage production in each component separately without the consideration of the defect creation in a "common" media.

Different currently unassigned MT-sections can be reserved for the proper recording of displacement cross-sections for various compounds. For example, in the evaluated neutron data file for iron the MT number X_1 (=901) can be kept for n+Fe+Fe displacement cross-sections, MT=X_2 for n+Fe+Fe_3C displacement cross-sections, MT=X_3 for commonly used stainless-steel of the first type (1), X_4 for other stainless steel (2) etc. The data corresponding to other components of considered compounds, for example, for carbon should be presented in appropriate data files.

The other way is the preparation of special data files with displacement cross-sections for compounds.

7. Conclusion

A number of improvements in the calculation of the number of defects in irradiated materials and displacement cross-sections is proposed. The gain in the consistency of the nuclear data processing as the better agreement of calculations and measurement comparing with existing approaches is expected.

References

[1] M.J. Norgett, M.T. Robinson, I.M. Torrens, A proposed method of calculating displacement dose rates, *Nucl. Eng. Des.* 33 (1975) 50.

[2] M.T. Robinson, Basic physics of radiation damage production, *J. Nucl. Mater.* 216 (1994) 1, and references on older works of M.T.Robinson therein.

[3] NJOY 99, Nuclear Data Processing System, http://t2.lanl.gov/codes/njoy99/index.html

[4] R.E. Stoller, L.R. Greenwood, Subcascade formation in displacement cascade simulations: Implications for fusion reactor materials, *J. Nucl. Mater.* 271–272 (1999) 57.

[5] C.H.M. Broeders, A.Yu. Konobeyev, Defect production efficiency in metals under neutron irradiation, *J. Nucl. Mater.* 328 (2004) 197.

[6] S.P. Simakov, A.Yu. Konobeyev, U. Fischer, V. Heinzel, Comparative study of survived displacement damage defects in iron irradiated in IFMIF and fusion power reactors, *J. Nucl. Mater.* 386–388 (2009) 52.

[7] A.Yu. Konobeyev, Yu.V. Konobeev, Yu.A. Korovin, Nuclear data to study damage in materials under irradiation by nucleons with energies up to 25 GeV, *J. Nucl. Sci. Technol.* Suppl. 2, (2002) 1236.

[8] G.A. Greene, C.L. Snead Jr., C.C. Finfrock, A.L. Hanson, M.R. James, W.F. Sommer, E.J. Pitcher, L.S. Waters, Direct measurements of displacement cross sections in copper and tungsten under irradiation by 1.1-GeV and 1.94-GeV Protons at 4.7 K, Proc. Sixth International Meeting on Nuclear Applications of Accelerator Technology (AccApp'03), San Diego, June 1-5, 2003, p. 881.

[9] A. Dunlop, D. Lesueur, P. Legrand, H. Dammak, J. Dural, Effects induced by high electronic excitations in pure metals: a detailed study in iron, *Nucl. Instr.Meth. Phys. Res.* B90 (1994) 330.
[10] J.F. Ziegler, Particle interactions with matter, http://www.srim.org/.
[11] C.H.M. Broeders, A.Yu. Konobeyev, K. Voukelatou, IOTA - a code to study ion transport and radiation damage in composite materials, FZKA 6984 (2004), http://bibliothek.fzk.de/zb/berichte/FZKA6984.pdf.
[12] M.T. Robinson, MARLOWE: Computer Simulation of Atomic Collisions in Crystalline Solids (Version 15b), RSICC Code Package PSR-137.
[13] L. Malerba, Molecular dynamics simulation of displacement cascades in α-Fe: A critical review, *J. Nucl. Mater.* 351 (2006) 28.
[14] M. Victoria, S. Dudarev, J.L. Boutard, E.Diegele, R. Lässer, A. Almazouzi, M.J. Caturla, C.C. Fu, J. Källne, L. Malerba, K. Nordlund, M. Perlado, M. Rieth, M. Samaras, R. Schaeublin, B.N. Singh, F. Willaime, Modelling irradiation effects in fusion materials, *Fus. Eng. Des.* 82 (2007) 2413.
[15] R.E. Stoller, The role of cascade energy and temperature in primary defect formation in iron, *J. Nucl. Mater.* 276 (2000) 22.
[16] M.J. Caturla, T. D. de la Rubia, M. Victoria, R.K. Corzine, M.R. James, G.A. Greene, Multiscale modelling of radiation damage: applications to damage production by GeV proton irradiation of Cu and W, and pulsed irradiation effects in Cu and Fe, *J. Nucl. Mater.* 296 (2001) 90.
[17] A.Yu. Konobeyev, C.H.M. Broeders, U. Fischer, Improved displacement cross sections for structural materials irradiated with intermediate and high energy protons, Proc. 8th International Topical Meeting on the Nuclear Applications of Accelerator Technology (AccApp'07), July 30 - August 2, 2007, Pocatello, Idaho, USA, p. 241.
[18] C.H.M. Broeders, A.Yu. Konobeyev, Displacement cross-sections for tantalum and tungsten irradiated with protons at energies up to 1 GeV, *J. Nucl. Mater.* 336 (2005) 201.
[19] C.H.M. Broeders, A.Yu. Konobeyev, C. Villagrasa, Neutron displacement cross-sections for tantalum and tungsten at energies up to 1 GeV, *J. Nucl. Mater.* 342 (2005) 68.
[20] A.Yu. Konobeyev, U. Fischer, L. Zanini, Advanced evaluations of displacement and gas production cross sections for chromium, iron, and nickel up to 3 GeV incident particle energy, Tenth International Topical Meeting on Nuclear Applications of Accelerators (AccApp'11), Knoxville, TN April 3-7, 2011.
[21] P. Jung, Atomic displacement functions of cubic metals, *J. Nucl. Mater.* 117(1983) 70.
[22] T. Suzudo, S.I. Golubov, R.E. Stoller, M. Yamaguchi, T. Tsuru, H. Kaburaki, Annealing simulation of cascade damage in α-Fe – damage energy and temperature dependence analyses, *J. Nucl. Mater.* 423 (2012) 40.
[23] K. Vörtler, C. Björkas, D. Terentyev, L. Malerba, K. Nordlund, The effect of Cr concentration on radiation damage in Fe–Cr alloys, *J. Nucl. Mater.* 382 (2008) 24.
[24] C. Björkas, K. Nordlund, L. Malerba, D. Terentyev, P. Olsson, Simulation of displacement cascades in $Fe_{90}Cr_{10}$ using a two band model potential, *J. Nucl. Mater.* 372 (2008) 312.
[25] A.Yu. Konobeyev, U. Fischer, Uncertainty in displacement cross-section calculations at intermediate and high proton energies, Proc. 4th Workshop Neutron Measurements, Evaluations and Applications. Nuclear Data Needs for Generation-IV and Accelerator Driven Systems (NEMEA-4), October 16 - 18, 2007, Prague, Czech Republic, p. 51.
[26] ENDF-6 Formats Manual Document ENDF-102, Report BNL-90365-2009, Rev. July 2010
[27] K.B. Winterbon, P. Sigmund, J.B.K. Sanders, Spatial distribution of energy deposited by atomic particles in elastic collisions, *K. Dan. Vidensk. Selsk. Mat. Fys. Medd.* 37 (1970) 14.

A Calculation Method of PKA, KERMA and DPA from Evaluated Nuclear Data with an Effective Single-particle Emission Approximation (ESPEA) and Introduction of Event Generator Mode in PHITS Code

Tokio Fukahori, Yosuke Iwamoto

Japan Atomic Energy Agency
Tokai-mura, Naka-gun, Ibaraki-ken, 319-1195
Japan

1. Introduction

The JENDL PKA/KERMA File is prepared from the evaluated nuclear data file, for radiation damage calculations used to support programs such as the International Fusion Material Irradiation Facility (IFMIF) [1]. The file contains primary knock-on atom (PKA) spectra, KERMA factors and displacement per atom (DPA) cross sections in the energy range between 10^{-5} eV and 50 MeV. Table 1 shows physical quantities included in PKA/KERMA File as well as MF number defined in the ENDF-6 format. The processing code system, ESPERANT, was developed to calculate quantities of PKA, KERMA and DPA from evaluated nuclear data for medium and heavy elements by using an effective single particle emission approximation (ESPEA). The PKA/KERMA File will contain the data for 78 isotopes of 29 elements in the energy region up to 50 MeV. A trial task of ESPERANT, which is file production of PKA spectra for 69 nuclides from ^{19}F to ^{209}Bi in the energy region up to 20 MeV for fusion application from the JENDL Fusion File [2] in order to supply the PKA data to the FENDL project [3], was presented at the Ninth International Symposium on Reactor Dosimetry. The JENDL PKA/KERMA File has been enlarged up to 50 MeV based on JENDL High Energy File for IFMIF [4] by means of the same methods as the trial work below 20 MeV. In this report, the ESPEA reliability is checked in the higher energy region.

Table 1 Physical Quantities Included in the PKA/KERMA File (En=10^{-5} eV - 50 MeV)

MF	Quantities
3	Cross sections and KERMA factor
4	Angular distributions for discrete levels
6	Double-differential light particles and PKA cross sections
63	DPA cross sections
66	Damage energy spectra

2. A Calculation Method of PKA, KERMA and DPA from Evaluated Nuclear Data

2.1 Effective Single Particle Emission Approximation (ESPEA)

It is often impossible to calculate PKA spectra exactly for reactions emitting two or more particles from an evaluated nuclear data file, which usually has no separated spectrum of each reaction step and channel above threshold energy of multi-particle emission reaction. The effective single particle emission approximation (ESPEA) has been developed for these cases with the assumption that the particles are emitted from sequential reactions, which cannot emit the particles simultaneously, and only the first emitted particle contributes to determination of energy and angular distributions of PKA. Basic notations are shown in Fig. 1, where superscripts of C and L mean center-of-mass (CMS) and laboratory (LAB) systems, subscripts of p, 1, t, 2 and G show incident and emitted particles, target and residual nucleus, and CMS-point, and symbols of E, V, m and θ are energy, velocity, mass and emitted angle ($\mu = \cos\theta$).

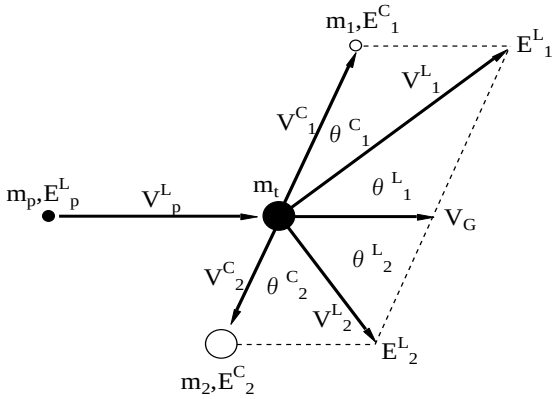

Fig. 1. Kinematics for PKA Calculation.

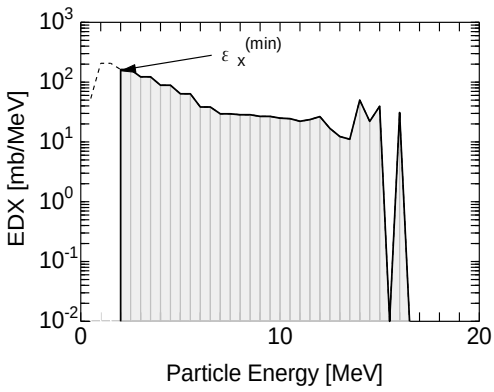

Fig. 2. Schematic diagram of $\varepsilon_x^{(min)}$ determination.

Double-differential cross section (DDX) of emitted particle in CMS, $DDX_1^C(E_p^L, E_1^C, \mu_1^C)$, is assumed to be given in evaluated nuclear data files. PKA spectrum in CMS, $DDX_2^C(E_p^L, E_2^C, \mu_2^C)$, is directly calculated by using energy and momentum conservation laws. That for particle emission reaction is written

$$DDX_2^C(E_p^L, E_2^C, \mu_2^C) = \frac{m_2}{m_1} DDX_1^C(E_p^L, E_1^C, \mu_1^C) \tag{1}$$

$$E_2^C = \frac{m_1}{m_2} E_1^C, \quad \mu_2^C = -\mu_1^C \tag{2}$$

and that for γ-ray emission reaction is

$$DDX_2^C(E_p^L, E_2^C, \mu_2^C) = \frac{m_2 c^2}{E_\gamma} DDX_\gamma(E_p^L, E_\gamma, \mu_\gamma) \tag{3}$$

$$E_2^C = \frac{E_\gamma^2}{2m_2 c^2}, \quad \mu_2^C = -\mu_\gamma \tag{4}$$

where c is light speed. In order to apply ESPEA, the sum of particle production cross sections (MT = 201, 203-207 in ENDF-6 format, similar as following) must be equal to the total reaction cross section. Hence some re-normalization is necessary to maintain a number of recoil nuclei. A normalization factor, R, for ESPEA is given as follows.

$$R = \frac{\sigma_R}{\sum_x \int_{\varepsilon_x^{(\min)}} d\varepsilon_x \int d\mu_x \sigma_x(E_p^L, \varepsilon_x, \mu_x)} \tag{5}$$

where σ_R and σ_x indicate cross sections of total reaction and each particle emission channel, and $\varepsilon_x^{(min)}$ is the lower limit of the energy for spectrum considered. It means the first emitted particles are distributed in a higher energy region in the emitted spectra. A schematic diagram is shown in Fig. 2. The lower energy limit, $\varepsilon_x^{(min)}$, is determined from the following equation of average energy for light particle emitted from the reaction ***x***.

$$\int_{\varepsilon_x^{(\min)}} \varepsilon_x f_x(\varepsilon_x) d\varepsilon_x = \left[\frac{m_t}{m_p + m_t} E_p^L + Q_x\right] \Big/ \left[1 + \left(\frac{m_{1x}}{m_{2x}}\right)^2\right] \tag{6}$$

$$\int_0^\infty f_x(\varepsilon_x) d\varepsilon_x = 1 \tag{7}$$

where Qx is Q-value of reaction x, and fx the normalized DDX_1^C of reaction ***x***.

DDX of PKA in LAB, $DDX_D^L(E_D^L,E_2^L,\mu_2^L)$, is obtained after conversion from CMS to LAB, then the damage energy spectra, σ_D, can be given by

$$\sigma_D(E_p^L,E_2^L,\mu_2^L)=E_D(E_2^L)\cdot DDX_2^L(E_p^L,E_2^L,\mu_2^L) \quad (8)$$

where E_D is given by Lindhard-Robinson model [7] with unit of E_2^L in eV as following.

$$E_D(E_2^L)=\frac{E_2^L}{1+k\cdot g(\varepsilon)} \quad (9)$$

$$k=0.13372\cdot Z^{2/3}/A^{1/2} \quad (10)$$

$$g(\varepsilon)=3.48008\varepsilon^{1/6}+0.40244\varepsilon^{3/4}+\varepsilon \quad (11)$$

$$\varepsilon=E_2^L/86.931Z^{7/3} \quad (12)$$

The DPA Cross Section, σ_{DPA}, can be obtained by using the damage energy spectra,

$$\sigma_{DPA}(E_p^L)=\iint \nu(E_2^L)\sigma_D(E_p^L,E_2^L,\mu_2^L)dE_2^L d\mu_2^L \quad (13)$$

$$\nu(E_2^L)=\frac{\kappa}{2\varepsilon_d}E_D(E_2^L), \quad \kappa=0.8 \quad (14)$$

where ε_d is the threshold energy for knock-on atom displaced from lattice point, and its amount strongly depends on materials. The kerma factor for ***x***-reaction, $KERMA_x(E_p^L)$, is also calculated by using double differential PKA spectrum as following.

$$KERMA_x(E_p^L)=\iint (E_{1x}^L+E_{2x}^L)DDX_{2x}^L(E_p^L,E_{2x}^L,\mu_{2x}^L)dE_{2x}^L d\mu_{2x}^L \quad (15)$$

For neutron and photon emission reactions, the term of E_{1x} is eliminated.

2.2 Test Calculations

The test calculation has been done by processing from the JENDL Fusion File [2] below 20 MeV. Considered reactions are elastic (MT=2) and discrete inelastic scattering (MT = 51-90), continuum neutron emission reaction (MT = 201), and charged particle emission reactions (MT = 203-207).

The processed PKA spectra were compared with those calculated with the Monte-Carlo exciton model code, MCEXCITON [6]. For example, PKA spectra for ^{27}Al and ^{56}Fe at incident neutron energies of 10 and 20 MeV are shown in Figs. 3 and 4. The results are in good agreement with each other, considering the large secondary particle energy meshes of the processed one. In Fig. 3(a), the PKA spectra given by Doran [7] at incident energies of 9 and 11 MeV are also indicated. Doran processed the PKA spectra from ENDF/B-IV [8] by assuming evaluation spectra for charged particles, since ENDF/B-IV does not have charged particle spectrum. However, the results of his processing are similar to the present results.

The DPA cross sections for ^{27}Al and ^{56}Fe are also compared with calculations by RADHEAT-V4 [9] and Doran [7] as a function of incident neutron energy in Fig. 5. Results of ESPERANT are in good agreement with other calculations. The KERMA factors for ^{27}Al and ^{56}Fe are compared with Howerton's calculation [10] in Fig. 6. The displacement energies for ^{27}Al and ^{56}Fe were selected here as 10 and 30 eV, respectively. Howerton's results have a resonance-like structure. Results of ESPERANT show the averaged kerma factor, since they have full resonance structure.

Trial calculations for neutron incident energy from 20 to 50 MeV also have been done with a preliminary version of JENDL High Energy File for IFMIF. The calculated PKA spectra are shown in Fig. 7. It seems that the processed PKA spectra have reasonable shapes and distributions. It is

concluded that ESPEA can be applied at least below 50 MeV. More benchmark tests might be necessary to estimate accuracy of the data in the JENDL PKA/KERMA File at this energy region.

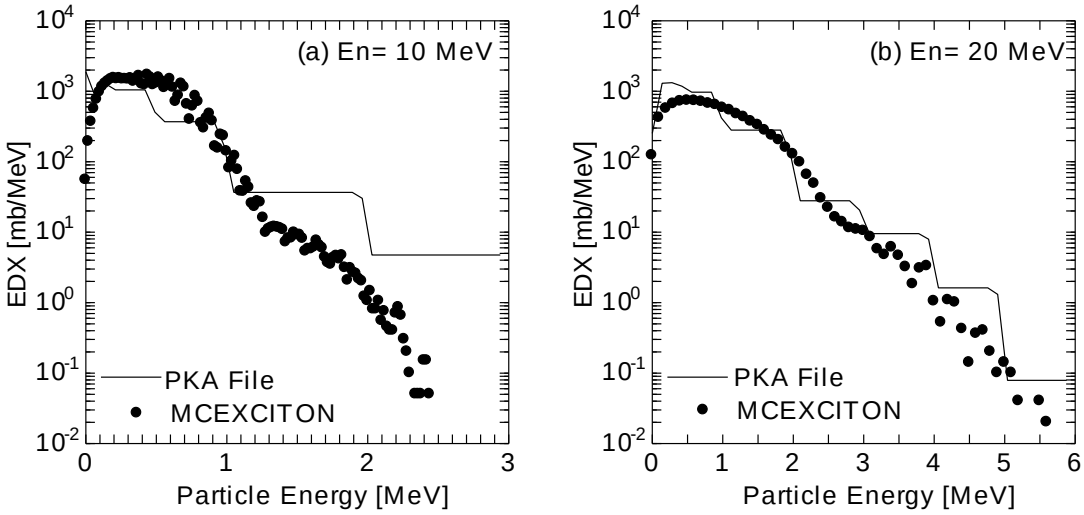

Fig. 3. ^{27}Al PKA spectra compared with calculations by MCEXCITON [6] at (a) E_n = 10 MeV and (b) E_n = 20 MeV.

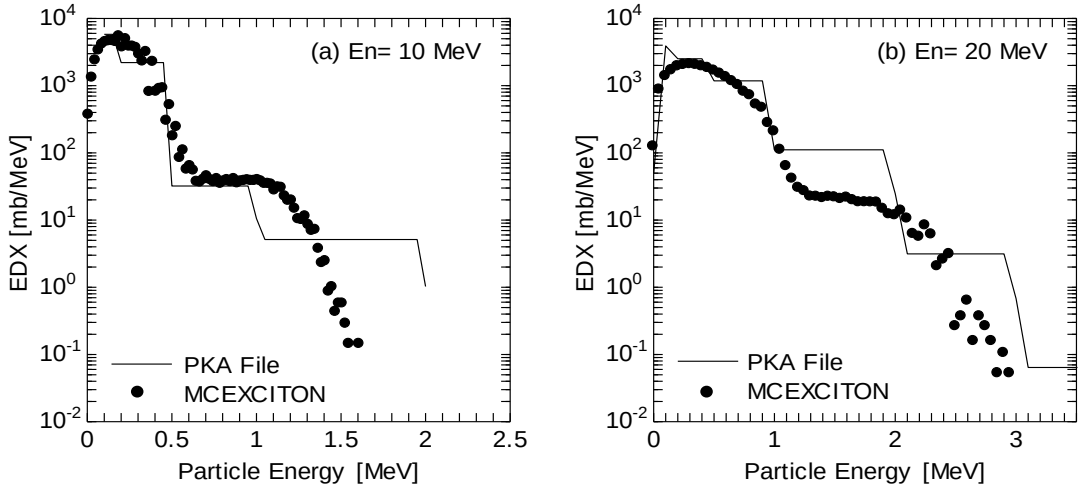

Fig. 4. ^{56}Fe PKA spectra compared with calculations by MCEXCITON [6] at (a) E_n = 10 MeV and (b) E_n = 20 MeV.

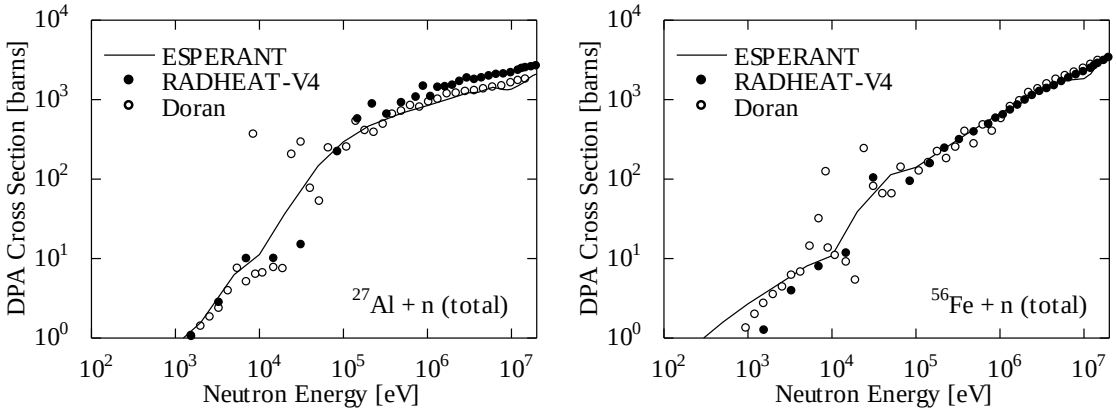

Fig. 5. ^{27}Al and ^{56}Fe DPA cross sections compared with calculations by RADHEAT-V4 [9] and Doran [7].

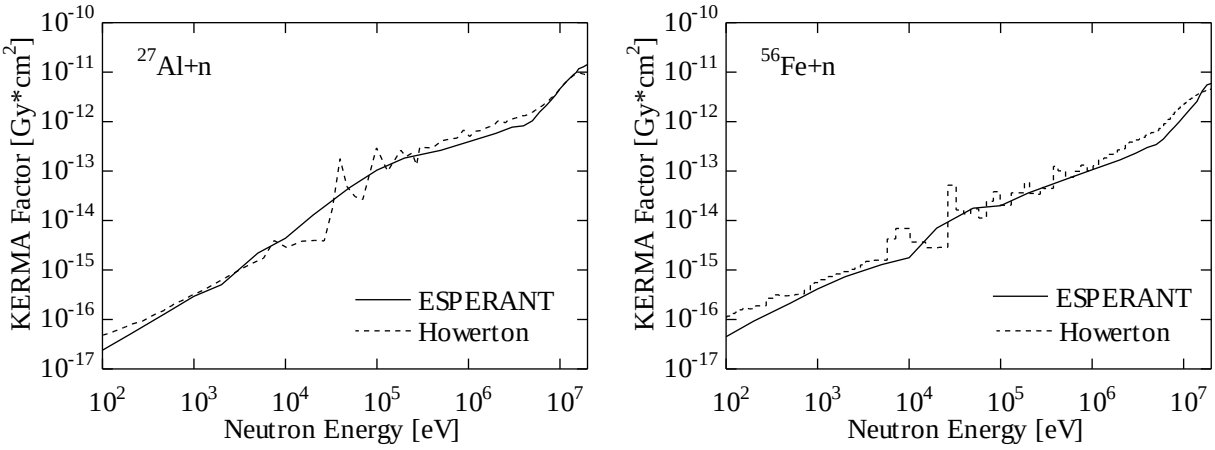

Fig. 6. ^{27}Al and ^{56}Fe KERMA factors compared with calculations by Howerton [10].

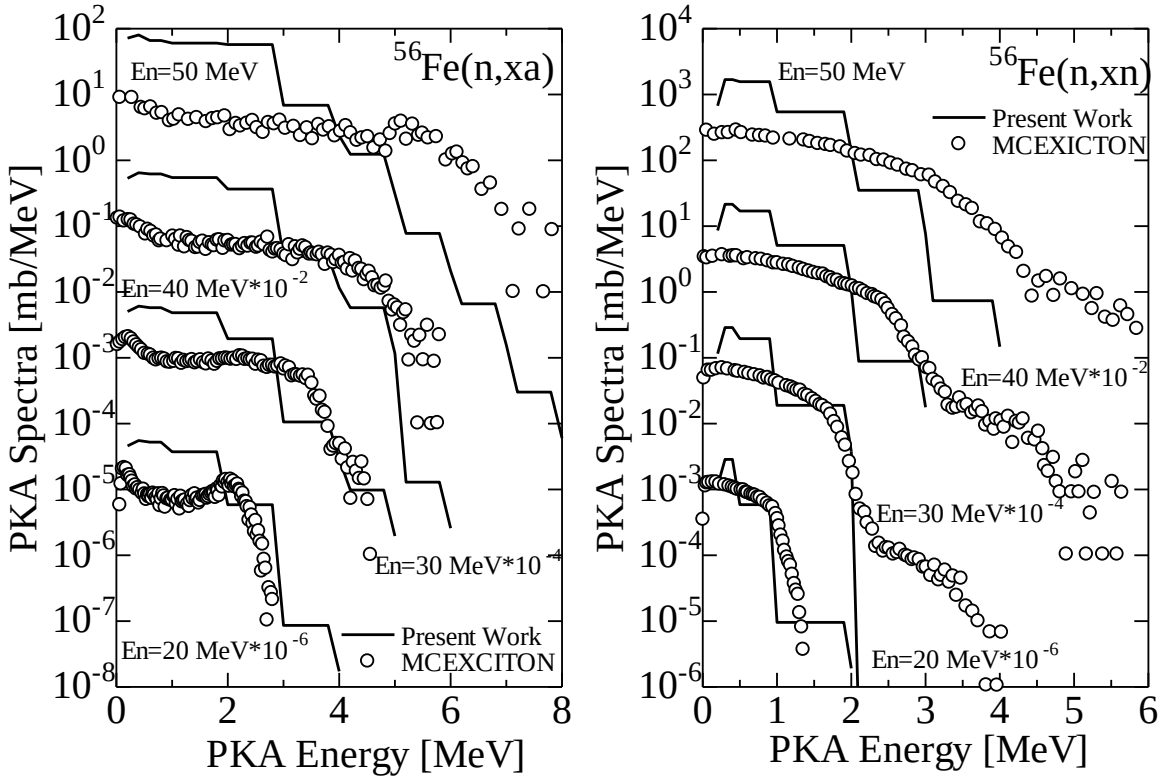

Fig. 7. PKA spectra related to reactions emitting neutrons and alpha-particles at the incident neutron energies of 20, 30, 40 and 50 MeV for ^{56}Fe.

3. Radiation damage model in PHITS

3.1 Overview

High-energy ions traveling a target lose their energy in three ways; nuclear reactions, electron excitations and Coulomb scattering. The lower projectile energy leads higher energy transfer to the target atom via Coulomb scattering. The target atom directly hit by the projectile has usually much lower energy than the projectile itself and therefore has a larger cross section for Coulomb scattering with other target atoms. Thus the target PKA creates localized cascade damage where many target

atoms are displaced from their original lattice site leaving same number of interstitials and vacancies. These point defects and their clusters affect the macroscopic material properties, such as hardness.

The conditions of various irradiations are described by using the damage energy to characterize the displacement cascade. This is defined as the initial energy of target PKA, corrected for the energy lost to electronic excitations by all of the particles composing the cascade. There are mainly three parts of calculations in the improved PHITS as shown in Fig. 8: 1) Transport calculation including nuclear reactions, 2) Coulomb scattering, and 3) Cascade damage approximation. We describe the main features of the calculation in the following sections.

3.2 Transport calculation including nuclear reaction

There are mainly two flows in the transport calculation to produce the target PKA as shown in Fig. 8. One is the Coulomb scattering due to PKA's directly created by the projectile, and the other is that due to PKA's created by the secondary particles. The energy of the secondary charged particles is obtained with PHITS calculations using a nuclear reaction model. In the event generator mode using a nuclear reaction, the conservation law on the energy and the momentum is sustained in each event. For proton-induced collisions, we use the simulation model JAM [11] above 1 MeV up to 10 GeV, whereas we only consider the ionization for charged particles below 1 MeV until they stop. PHITS can also transport nuclei in the materials. Below 10 MeV/c, we only take into account the ionization for nucleus transport, whereas above 10 MeV/u we describe heavy ion induced collisions up to 100 GeV/u with the simulation model JQMD [12]. JAM and JQMD calculations are stopped once it can be assumed that equilibrium has been achieved. After equilibration is reached, the Generalized Evaporation Model (GEM) [13] is applied to account for the process of the de-excitation and the associated particle emission from the highly excited nucleus remaining after the JAM and JQMD calculations.

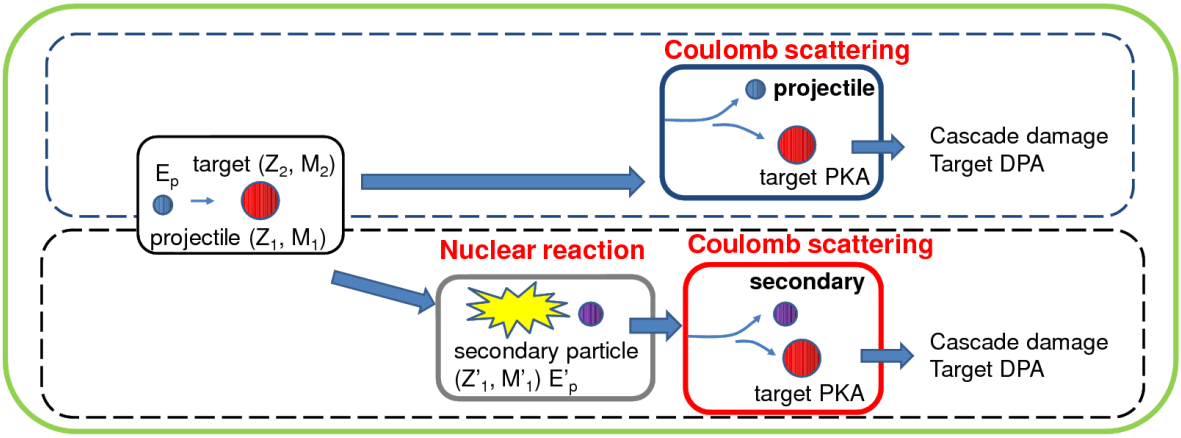

Fig.8. Overview of radiation damage model calculations in PHITS.

In the transport of low energy neutrons the "Event Generator Mode" has been used. In this mode, the evaluated nuclear data for neutrons and a special evaporation model are combined so as to trace all correlations of ejectiles keeping the energy and the momentum conservation in a collision. For the ionization process of the charge particles and nucleus, we have used the SPAR code [14] for the average stopping power dE/dx. For the total nucleus-nucleus reaction cross sections, the Tripathi's formula [15-17] has been adopted in PHITS.

3.3 Coulomb scattering with target atom

The Coulomb scattering part, which alone leads to the deflection of the projectile and secondary charged particles, is described with classical scattering theory using the screening functions $f(t^{1/2})$. A

universal one-parameter differential scattering cross section equation in reduced notation is expressed by J. Lindhard, et al. [18] as:

$$d\sigma_{\mathrm{sc}} = \frac{\pi a_{TF}^2}{2} \frac{f(t^{\frac{1}{2}})}{t^{3/2}}\, dt \tag{16}$$

where t is a dimensionless collision parameter defined by

$$t \equiv \varepsilon^2 \frac{T}{T_{\max}} = \varepsilon^2 sin^2\left(\frac{\theta_c}{2}\right) \tag{17}$$

T is the transferred energy to the target, and $T_{\max}$ is the maximum transferred energy as

$$T_{\max} = \frac{4M_1M_2}{(M_1+M_2)^2} E_p \tag{18}$$

where E_p is the projectile energy. ε is the dimensionless energy as

$$\varepsilon \equiv \frac{a_{\mathrm{TF}}}{d_c} = \frac{a_{\mathrm{TF}} E}{Z_1 Z_2 e^2} \tag{19}$$

In the above expression, d_c is the unscreened (i.e., Coulomb) collision diameter or distance of closest approach for a head-on collision (i.e., b = 0), and a_{TF} is the screening distance.

Lindhard et al. [18] considered the screening function, $f(t^{1/2})$, to be a simple scaling function and the variable t to be a measure of the depth of penetration into the atom during a collision, with large values of t representing small distances of approach. The function of $f(t^{1/2})$ can be generalized to provide a one parameter universal differential scattering cross section equation for interatomic potentials such as screened and unscreened Coulomb potentials. The general form is

$$f\left(t^{\frac{1}{2}}\right) = \lambda t^{\frac{1}{2}-m}[1+(2\lambda t^{1-m})^q]^{-1/q} \tag{20}$$

where λ, m, and q are fitting variables, with λ = 1.309, m = 1/3 and q = 2/3 [19] for the Thomas-Fermi version of $f(t^{1/2})$. Figure 9 shows a plot of the Eq.(20) for the Thomas-Fermi potential and the Rutherford scattering potential with respect to the dimensionless collision parameter $t^{1/2}$. We can see that the shape of the screening function is better than that of Rutherford scattering at low $t^{1/2}$. For high-energy collisions, at large $t^{1/2}$, screening effects are minimal since interactions primarily involve the inner parts of the atom, and $f(t^{1/2})$ decreases with increasing t [20]. The value of $t^{1/2}$ increases with increasing dimensionless energy ε, scattering angle in the CM system, and impact parameter.

3.4 Cascade Damage Approximation

To estimate the displacement cross sections the "NRT" formalism of Norgett, Robinson, and Torrens [21] is employed as a standard to determine that fraction of the energy of the target PKA producing damage, e.g., further nuclear displacements. The displacement cross sections can be evaluated using the following expression:

$$\sigma_{\mathrm{damage}} = \int_{t_{\mathrm{d}}}^{t_{\max}} d\sigma/dt \times \nu\left(Z_{\mathrm{target}}, A_{\mathrm{target}}, T_{\mathrm{target}}\right) dt \tag{21}$$

where Z_{target}, A_{target} are the numbers for the recoil target atom and T_{target} is the target PKA energy . Equation (21) indicates the scattering cross section multiplied by the number of defects. $t_{\max,}$ which is dimensionless, is equal to ε^2 from Eq. (17) when $\Theta = \pi$. t_{d} is the displacement threshold energy, also

dimensionless, given by Eq.(19). The displacement threshold energy $T_{\text{threshold}}$ is typically in the range between 20 and 90 eV for most metals [22].

Based on the Kinchin-Pease formula [23] modified by Norgett et al.[21] and the Lindhard slowing-down theory, the number of defects produced in irradiated material is calculated by

$$\nu\left(Z_{target}, A_{target}, T_{target}\right) = N_{NRT} \tag{22}$$

where N_{NRT} is the number of defects calculated by

$$N_{\text{NRT}} = \frac{0.8 \cdot T_{\text{damage}}}{2 \cdot T_{\text{threshold}}} \tag{23}$$

The constant 0.8 in the formula (23) is the displacement efficiency given independently of the PKA energy, the target material, or its temperature. The value is intended to compensate for forward scattering in the displacement cascade of the atoms of the lattice. The damage energy, T_{damage}, is the energy transferred to the lattice atoms and is reduced by the losses from electronic stopping in the atom displacement cascade and is given by [21]:

$$T_{\text{damage}} = \frac{T}{1 + k_{\text{cascade}} \cdot g(\varepsilon)} \tag{24}$$

where T is the transferred energy to target atom given by Eq. (17) as

$$T = T_{\text{max}} \times \frac{t}{\varepsilon_p^2} \tag{25}$$

where ε_p is the dimensionless projectile energy given by Eq.(19) and the projectile energy E_{p}. The parameters k_{cascade}, and $g(\varepsilon)$ are as follows:

$$k_{\text{cascade}} = 0.1337 Z_{\text{target}}^{\frac{1}{6}} \left(Z_{\text{target}} / A_{\text{target}}\right)^{1/2} \tag{26}$$

$$g(\varepsilon) = \varepsilon + 0.40244 \cdot \varepsilon^{3/4} + 3.4008 \cdot \varepsilon^{1/6} \tag{27}$$

The dimensionless transferred energy, ε, is given by Eqs. (19) and (25). The following equation was then derived using Eqs. (21), (23), and (24):

$$\sigma_{\text{damage}} = \int_{t_d}^{t_{\text{max}}} \frac{d\sigma_{\text{scat}}}{dt} \cdot \frac{0.8}{2 \cdot T_{\text{threshold}}} \frac{T}{1 + k_{\text{cascade}} \cdot g(\varepsilon)} dt \tag{28}$$

Figure 10 shows a displacement cross section (Eq. (28)) with displacement threshold energy of 90 eV for the Ge + W scattering as a function of Ge ion beam energy. As the cross section for Coulomb scattering ($T > t_d$) is much larger (~10^7 – 10^9 b) than the nuclear reaction cross section (of the order of ~ mb) treated in PHITS, it is difficult to calculate the DPA values using full Monte Carlo calculation with Coulomb scattering in PHITS because of significant calculation times. Therefore, only the energies of the projectile and secondary are calculated by using the dE/dx and nuclear reaction models in PHITS. The transferred energy to the target, T, is calculated using Eq. (25), and displacement cross section is estimated with Eq. (28).

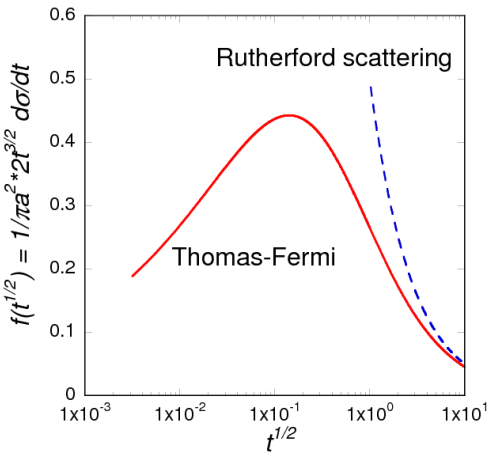

Fig. 9. The screening function $f(t^{1/2})$ of Coulomb scattering cross section is shown as a function of $t^{1/2}$ for the Thomas-Fermi potential and the Rutherford scattering potential.

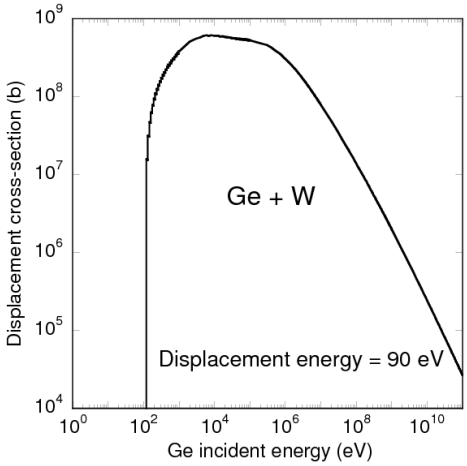

Fig. 10. Calculated displacement cross-sections are shown as a function of incident energy for Ge ions incident on a W target.

4. Summary

The displacement calculation method from evaluated nuclear data file has been developed by using effective single-particle emission approximation (ESPEA). The ESPEA can be used effectively below about 50 MeV, because of since multiplicity of emitted particles. These are also reported in the Ref. 24.

The displacement calculation method in PHITS has been developed. In the high energy region ($\geq$ 20 MeV) for proton and neutron beams, DPA created by secondary particles increase due to nuclear reactions. For heavy-ion beams, DPA created by the primaries are dominant to total DPA due to the large Coulomb scattering cross sections. PHITS results agree with FLUKA ones within a factor of 1.7. In the high-energy region above 10 MeV/nucleon, comparisons among codes and measurements of displacement damage cross section are necessary.

References

[1] K. Noda, *JAERI-Conf 95-008*, Japan Atomic Energy Research Institute, p.112 (1995).

[2] B. Yu, S. Chiba, T. Fukahori, *J. Nucl. Sci. Technol.* **29**, 677 (1992).

[3] S. Ganesan, P.K. McLaughlin, *IAEA-NDS-128 Rev.1*, International Atomic Energy Agency (1995).

[4] T. Fukahori, *JAERI-Conf 98-016*, Japan Atomic Energy Research Institute, p.37 (1998).

[5] J. Lindhard, et al., *Kgl. Danke Vidensk Selsk. mat-fis. Medd.* **33**, 10 (1963), N.T. Robinson, *Proc. BNES Conf. on Nuclear Fission Reactors, Culham 1969*, p.346 (BNES, London, 1969), P. Sigmund, *Rad. Eff.* **1**, 15 (1969), M.T. Robinson, I.M. Torrens, *Phys. Rev.* **B9**, 5008 (1974).

[6] N. Kishida, H. Kadotani, *Proc. Int. Conf. on Nuclear Data for Science and Technology, Mito, May 30-Jun. 3, 1988*, p.1209 (Saikon Publishing, Tokyo, 1988).

[7] D.G. Doran, N.J. Graves, *HEDL-TME* 7670, Hanford Engineering Development Laboratory, 1976.

[8] (Ed.) D. Garber, *BNL-17541*, 2nd Edition, Brookhaven National Laboratory, 1975.

[9] N. Yamano, et al., *JAERI*-1316, Japan Atomic Energy Research Institute (1989).

[10] R.J. Howerton, *UCRL-50400* Vol. 27 (1986).

[11] Y. Nara, et al., *Phys. Rev.* **C61(2)**, 024901 (2000).

[12] K. Niita, et al., *Phys. Rev.* **C52**, 2620-2635 (1995).

[13] S. Furihata, et al., *Nucl. Instr. and Meth.* **B171**, 251-258 (2000).

[14] T.W. Armstrong, K.C. Chandler, ORNL Report ORNL-4869, ORNL, Oak Ridge, TN, USA, May 1973.
[15] R.K. Tripathi, F.A. Cucinotta, J.W. Wilson, *Nucl. Instr. and Meth.* **B117**, 347-349 (1996).
[16] R.K. Tripathi, J.W. Wilson, F.A. Cucinotta, *Nucl. Instr. & Meth.* **B129**, 11-15 (1997) 11-15.
[17] R.K. Tripathi, F.A. Cucinotta, J.W. Wilson, *Nucl. Instr. and Meth.* **B155**, 349-356 (1999).
[18] J. Lindhard, V. Nielsen, M. Scharff, P.V. Thomsen, *Mat. Fys. Medd. Dan. Vid. Selsk.* **138**, No.A1815 (1965).
[19] K.B. Winterbon, P. Sigmund, J.B. Sanders, *Mat. Fys. Medd. Dan. Vid. Selsk.* **37** (no.14) (1970).
[20] M. Nastasi and J.W. Mayer, "Ion Implantation and Synthesis of Materials", Cambridge Solid State Science Series.
[21] M.J. Norgett, M.T. Robinson, I.M. Torrens, *Nucl. Eng. and Design*, **33**, 50-54 (1975).
[22] R.E. MacFarlane, NJOY99.0: Code System for Producing Pointwise and Multigroup Neutron and Photon Cross Sections from ENDF/B Data, RSICC Code Package PSR-480 (Report).
[23] G.H. Kinchin, R.S. Pease, *Rep. Progr. Phys.* **18**, 1 (1955).
[24] T. Fukahori, et al., *Reactor Dosimetry, ASTM STP 1398*, John G. Williams, David W. Vehar, Frank H. Ruddy, and David M. Gilliam, Eds., American Society for Testing and Materials, West Conshohocken, PA, 2000.

Calculation of gamma displacement cross sections / Generation of recoil spectra from ENDF/B-VII

Junhyun Kwon[1], and Yong Hee Choi[2]

1) Korea Atomic Energy Research Institute
2) Seoul National University
Korea

Background

Radiation damage in materials is caused by the transfer of energy from an incident particle to the target atoms, which results in the redistribution of target atoms. During the nuclear reactor operation, various kinds of radiation are produced, including fast neutron, gamma, beta, high-energy ions etc. These radiations may affect the properties of reactor structural materials in a direct and/or indirect way. It is well known that fast neutrons have an effect on the degradation of materials. Whereas the impact of fast neutrons (E_n > 1 MeV) on material property changes is clearly recognized, the impact of gamma ray damage to materials is usually not significant. However, there has been some interest in gamma ray damage in metals in promoting accelerated embrittlement of reactor pressure vessel steels in the HFIR (High Flux Isotopes Reactor) [1,2]. In situations where there is a large water gap between pressure vessel and fuel assembly, gamma damage can become comparable to that produced by neutrons, on the basis of displacements per atom (dpa) parameter. A recent analysis of gamma ray displacement damage in the RPV of the General Electric Advanced Boiling Water Reactor (ABWR) indicated that the ratio of calculated gamma- to neutron-induced displacement damage rates is over 100% at the RPV inner diameter [3]. Under a high gamma dose environment, embrittlement can be accelerated by radiation-enhanced mass transport mechanism. Because gamma rays are much more efficient than neutrons at producing freely-migrating defects [1], any radiation enhanced or induced processes that depend on the magnitude of defect fluxes to sinks, can be disproportionately affected by gamma. The direct evaluation of the contribution of gamma ray to damage in materials, quantified as a parameter of dpa, is made possible once the displacement damage cross section due to gamma rays are known. In this work, we present calculations for gamma ray displacement cross sections in various materials in the energy range from 0 to 14 MeV.

Neutrons can react with nuclei by neutron capture or simply by elastic scattering. During elastic scattering, neutrons transfer energy to atoms in the solid, creating energetic recoils which can interact with other atoms causing further displacements. Following neutron capture, the nucleus can

experience gamma emission (n,γ), charged particle (proton or alpha particle) reactions - (n,p) or (n,α), fission, or multiple neutron emission (n,xn). These reactions can generate other elements which are different from the target nucleus, which is referred to as transmutation. The transmuted elements tend to emit the characteristic gamma ray in the process of de-excitation. As a result of these reactions, energetic particles (p,α,γ) and recoil atoms are created. Energetic recoils created by the neutron-atom reactions will produce the radiation damage. The lattice atom initially struck during neutron scattering and displaced is called the primary knock-on atom (PKA). A PKA can induce additional displacements usually in a small region of space, called a displacement cascade. To fully characterize the damage, it is necessary to calculate the total number of displacements in the cascade and the number of surviving defects and defect clusters, following the cooling of the cascade. These quantities are strongly dependent on the recoil spectra, which are dependent on the neutron spectrum. Calculation of the neutron displacement damage can be carried out using the SPECTER computer code [4], which allows us to obtain various damage parameters such as spectral-averaged displacements, recoil spectra, gas production (hydrogen and helium), and total damage energy. The SPECTER code is compact and simple to use because data such as neutron cross sections for various reactions and PKA spectra are pre-processed and stored in its data file. Only the neutron spectrum is needed as an input source. In the SPECTER code, the energy transfer kernel is embedded, which was processed from the old-version of ENDF/B-V library. Although this code is efficient, it has a disadvantage that the direct access to the calculation routine is limited in that its master library was generated by another code. The user is not able to use the latest nuclear data in the damage calculation. In order to overcome this drawback, we developed a code for computing the recoil atom spectrum for given neutron spectra, which is called the RASG (Recoil Atom Spectrum Generator). The details on the code are presented at the IAEA technical meeting.

In case of neutron irradiation to materials, the probability of displacing lattice atoms due to interaction is expressed in terms of displacement cross section σ_d, which is given as:

$$\sigma_d(E) = \sum_i \sigma_i(E) \int_{T_{min}}^{T_{max}} f_i(E,T) \cdot \nu_{NRT}(T)\ dT\ , \qquad (1)$$

where E is the incident neutron energy, T the energy of recoil, $\sigma_i(E)$ is the nuclear cross section for i-type interaction at neutron energy of E, $f_i(E,T)$ is the neutron-atom energy transfer kernel, T_{min} and T_{max} are the lower and upper energy of a recoil atom, respectively and are determined by the type of interaction of interest, and $\nu_{NRT}(T)$ represents the secondary displacement function calculated using the Norgett, Robinson, and Torrens modification of the Kinchin-Pease formula [5]. Among various factors affecting the atomic displacement, one of the most important factors is the energy of recoil atoms (T) transferred by the incident neutron. This factor has an effect on the energy transfer kernel, f(E,T) and the number of secondary atomic displacement, $\nu_{NRT}(T)$, which finally determines the quantity of atomic displacement in units of dpa. It is, however, important to note that the meaning of dpa is a rough indicator of the complicated reactions produced by neutron irradiation. The majority of atomic displacements caused by neutron irradiation cause either recombination of defects of opposite type (interstitial and vacancy) or the clustering of defects of the same type. Only a small fraction of the total number of displacements survives as isolated point defects that are free to migrate over relatively long distances [6]. Many microstructural changes that take place during irradiation are directly related to these surviving defects and not to the total number of displacements. It is, therefore, important to quantify the net production rate of FMDs before any correlation between displacement damage and microstructural evolution is made. For several decades, such attempts have focused on the calculation of dpa. The dpa parameter has been widely used because the dpa is proportional to the total energy available for producing defects and is also proportional to the final number of stable defects that remain in the material. However, in some cases the dpa approach did not succeed in producing a quantitative correlation between the observed irradiation effect and the calculated damage. The FMD production is dependent on spatial aspects of defect distribution which the dpa approach does not consider. The fraction of point defects which survive recombination and clustering depends on the energy of primary recoil atoms. As the primary recoil atoms increase in energy up to an order of keV, more highly dense displacement cascades are created, which enhance defect recombination, thereby

reducing the FMD generation. Several experiments have demonstrated that cascade producing irradiation is not as efficient at producing FMD as light-ion or electron irradiation which produces lower energy recoils. In estimating the production of FMDs, we can apply the molecular dynamics (MD) computer simulation of displacement cascades. The application of MD simulation would be helpful to predict the net radiation damage in a more accurate way.

1. Calculation of gamma displacement cross sections

Gamma rays can displace atoms by first transferring energy to an electron, which transfers energy to a lattice atom through an electron-atom scattering. The energetic electrons can be produced from Compton scattering (CS), photoelectric effect (PE) and pair production (PP). Therefore, the total gamma displacement cross section consists of three components representing the sum of cross sections for three interactions. The calculated displacement cross sections show that for lighter elements the Compton displacement cross section dominates throughout the energy range, for heavier elements, the impact of photoelectric effect at lower energies and pair production at higher energies becomes more important. The following figure shows the gamma-ray displacement cross section for iron.

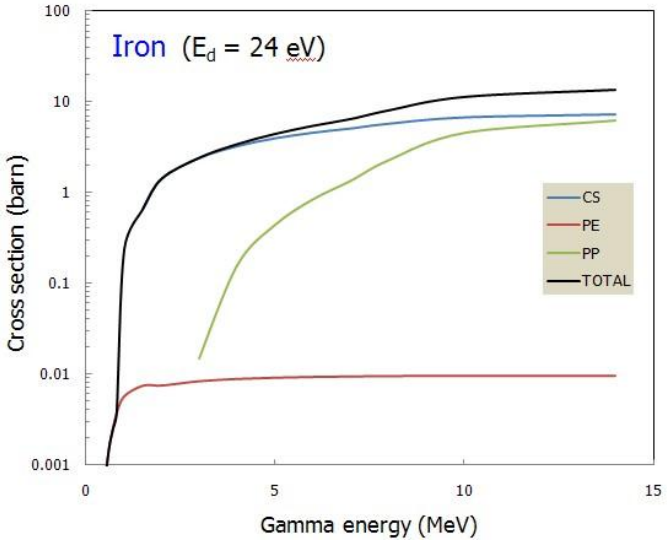

Fig. 1. The gamma-ray displacement cross section for iron.

2. Generation of recoil spectra from ENDF/B-VII

In estimating the effect of neutron irradiation on primary damage, we started with the calculation of recoil spectra by using the latest ENDF/B-VII library. The recoil atom spectrum can be obtained in two ways. The use of SPECTER code is an easy and simple way to produce results when the proper neutron spectrum is given. However, the latest nuclear data, which is available for damage calculation in the recent ENDF/B files, cannot be used since the master library had been processed several decades ago. Another way is to apply the NJOY99 code system that can access directly the cross section and energy transfer data stored in the ENDF/B-VII files [7]. The problem of using the NJOY code is, however, that it does not provide the differential recoil atom spectra but produce average recoil energy as a function of specified neutron energy. We have been developing a new code for generating the recoil atom spectra by using the recent ENDF/B files, which is named as RASG (Recoil Atom Spectrum Generator). This code generates the differential recoil spectrum, which represent the probability of recoil atom's having its kinetic energy between T and T+dT such as,

$$R(T)dT = \sum_i \int_0^{E_{max}} \phi(E) \cdot \sigma_i(E) \cdot f_i(E,T) dE\, dT \ , \qquad (2)$$

where E is the incident neutron energy in the laboratory system, T is the recoil atom energy, $\sigma_i(E)$ is the nuclear cross section for reaction channel i at the neutron energy of E, $f_i(E,T)$ represent the neutron-atom energy transfer kernel for reaction channel i and $\varphi(E)$ is the neutron flux.

We developed the code, named as RASG, which calculates the differential recoil spectra by combining three modules. Those modules include; 1) neutronics calculation to generate the neutron flux in the specific environments, 2) estimation of energy transfer kernel using the information in the ENDF/B library and 3) processing of nuclear microscopic cross sections from the NJOY system. In performing the neutron calculation, various neutron transport codes are applied, including MCNP, DORT etc. In this meeting, the emphasis is placed on the derivation of the energy transfer kernel based on the ENDF/B library and theoretical methods. Fig. 2 shows the recoil atom spectra of iron for the HFIR (High Flux Isotope Reactor) neutron flux, which is given in the SPECTER source code as an example. Since the code development is still underway, we present the recoil spectra for the target atom of iron.

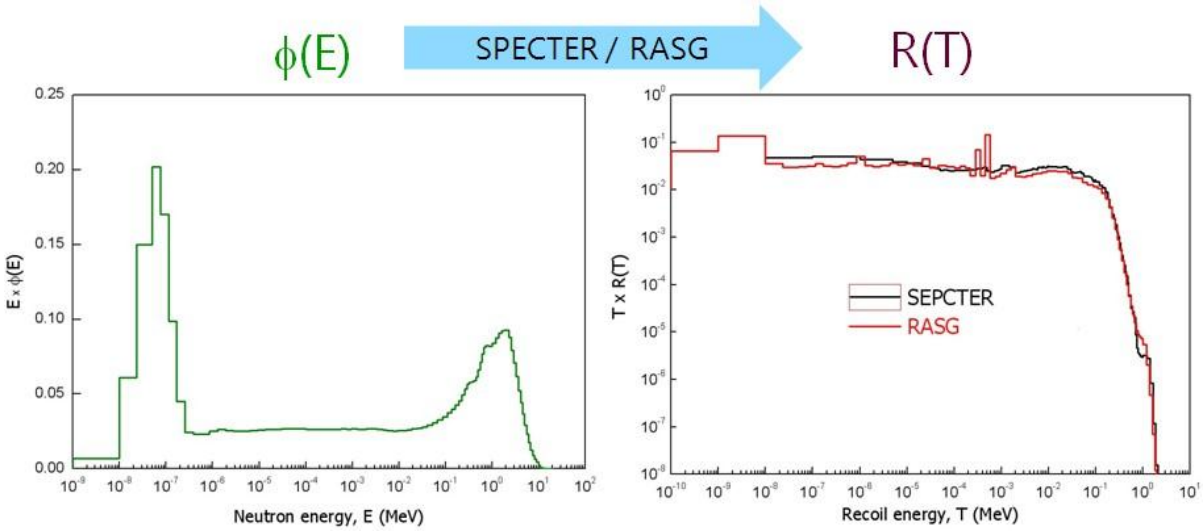

Fig. 2. The HFIR (High Flux Isotope Reactor) neutron flux and the recoil atom spectra of iron.

Proposed Work

In order to define the net radiation damage due to neutron irradiation to materials, it is necessary to determine the modified displacement cross section which represents the net damage production resulting from displacement cascades. The investigation of Eq. (1) gives us a direction to go. Two approaches are proposed for the future work.

First, we need to define the energy transfer kernel as accurately as possible. Although the calculation results of the SPECTER code produce the recoil atom spectrum in a convenient way, the use of the latest ENDF/B library would be a better choice to calculate the energy transfer kernel as well as microscopic cross sections. We have capability of dealing with the nuclear cross section processing with the NJOY system and generating the recoil atom spectrum. The latter work was partly demonstrated in this meeting.

The secondary displacement function, ν_{NRT} is a strong function of the recoil energy, T. Although the function of ν takes into account the energy loss to electronic interactions between PKA and target atoms, the calculation results still overestimates the net displacement damage. A number of molecular dynamics (MD) simulations have been made to quantify the residual defect production in the state of primary damage. The MD simulations can yield information about primary damage, particularly the spatial distribution of point defects and the number density of defect clusters. These results are very important to predict the microstructural evolution of materials in the reactor environments. We need to derive the information on the residual defects through the extensive MD simulations or the analysis of the previous results regarding cascade simulations. This trial was already made in estimating the cascade efficacy [8]. One of the drawbacks to the cascade simulation is purely theoretical, that is, lack of experimental verification. In order to overcome this problem, it is necessary to justify the MD results through the comparison to the experimental results. It is impossible to directly measure the amount of FMDs after the displacement cascade and the experimental information about the FMD production is not sufficient. However, we can collect the data on RIS (Radiation-Induced Segregation)

which relevant to FMD [9,10]. We believe that the proposed work will enable us to accurately estimate the net damage production and may assist in devising methods for mitigating the radiation damage process.

References

[1] L.E. Rehn and R.C. Birtcher. Experimental studies of free defect generation during irradiation – Implications for reactor environments. J. Nucl. Mater. 205 (1993) 31-39.
[2] K. Farrell, S.T. Mahmood, R.E. Stoller and L.K. Mansur, An evaluation of low temperature radiation embrittlement mechanisms in ferritic alloys. J. Nucl. Mater. 210 (1994) 268-281.
[3] D.E. Alexander and L.E. Rehn, Gamma-ray displacement damage in the pressure vessel of the advanced boiling water reactor. J. Nucl. Mater. 217 (1994) 213-216.
[4] L.R. Greenwood and R.K. Smither, SPECTER : Neutron Damage Calculations for Materials Irradiations, ANL/FPP/TM-197 (1985).
[5] M.J. Norgett, M.T. Robinson and I.M. Torrens. A proposed method of calculating displacement dose rates. Nucl. Eng. Des. 33 (1975) 50.
[6] L.E. Rehn. Production of Freely-Migrating Defects. J. Nucl. Mater. 174 (1990) 144.
[7] R.E. MacFarlane and A.C. Kahler. Methods for processing ENDF/B-VII with NJOY, Nucl. Data Sheets 111 (2010) 2739-2890.
[8] S.P. Simakov, A.Yu. Konobeyev, U. Fischer and V. Heinzel. Comparative study of survived displacement damage defects in iron irradiated in IFMIF and fusion power reactors, J.Nucl. Mater. 386-388 (2009) 52-55.
[9] T. Hashimoto, L.E. Rehn and P.R. Okamoto. Freely-Migrating Defect Production During Irradiation at Elevated Temperatures. Phys. Rev. B 38 (1988) 12868.
[10] R.A. Erck and L.E. Rehn. Kinetics of Radiation-Induced Segregation in Molybdenum-Rhenium Alloys. J. Nucl. Mater. 168 (1989) 208.

Neutron Damage Metrics and the Quantification of the Associated Uncertainty

P.J. Griffin

Sandia National Laboratories[1]
Albuquerque, NM 87185-1146
USA

Motivation

The motivation for this work is the determination of a methodology for deriving and validating a reference metric that can be used to correlate radiation damage from neutrons of various energies and from charged particles with observed damage modes. Exposure functions for some damage modes are being used by the radiation effects community, e.g. 1-MeV-Equivalent damage in Si and in GaAs [1] semiconductors as well as displacements per atom (dpa) and subsequent material embrittlement in iron [2]. The limitations with the current treatment of these energy-dependent metrics include a lack of an associated covariance matrix and incomplete validation. In addition, the analytical approaches used to derive the current metrics fail to properly treat damage in compound/poly-atomic materials, the evolution and recombination of defects as a function of time since exposure, as well as the influence of dopant materials and impurities in the material of interest. The current metrics only provide a crude correlation with the damage modes of interest. They do not, typically, even distinguish between the damage effectiveness of different types of neutron-induced lattice defects, e.g. they fail to distinguish between a vacancy-oxygen defect and a divacancy with respect to the minority carrier lifetime and the decrease in

[1] This work was supported by the United States Department of Energy under contract DE-AC04-94AL85000. Sandia is a multiprogram laboratory operated by Sandia Corporation, a Lockheed Martin Company, for the United States Department of Energy

gain in a Si bipolar transistor. The goal of this work is to facilitate the generation of more advanced radiation metrics that will provide an easier intercomparison of radiation damage as delivered from various types of test facilities and with various real-world nuclear applications.

One first needs to properly define the scope of the radiation damage application that is a concern before an appropriate damage metric is selected. The fidelity of the metric selected and the range of environmental parameters under which the metric can be correlated with the damage should match the intended application. It should address the scope of real-world conditions where the metric will be applied, e.g. with respect to material impurities or alloy composition. At one time the light water pressure vessel embrittlement community used the metric of a neutron fluence greater than 1-MeV to correlate with embrittlement damage in various light water reactors. This was sufficient as long as the damage correlation was restricted to a class of light water reactors that had a similar design – and little variation in the neutron spectrum at the critical weld locations. Once the iron radiation embrittlement community became interested in boiling water reactors, it quickly became evident that the iron dpa metric provided a much better correlation with the observed damage in the combined class of irradiation conditions. This same advantage of a more broadly applicable radiation damage metric is seen whenever a damage correlation is required for two radiation exposure conditions where the neutron spectra are different. The silicon 1-MeV(Si) displacement kerma was a good metric for bipolar transistor minority carrier lifetime and gain degradation as long as one restricted their interest to cases where the damage was dominated by fast neutrons. In heavily moderated low energy neutron exposures the observed damage is much less that predicted by the displacement kerma metric – probably due to a failure to distinguish between an electrical sensitivity in the device to the type of defect, e.g. a divacancy or a vacancy-oxygen defect. The correlation of fast neutron damage in GaAs was thought to correlate well with the displacement kerma until data was gathered in 14-MeV neutron fields. Here the dense damage clusters affected the resulting defect population and the observed damage to minority carrier heterojunction devices. The message here is that the application and applicable range of real-world conditions will dictate the level of sophistication required in the development of the damage metric and by its value to the community. It is also critical that the scope of environmental conditions under which the metric has been validated to correlate with a given damage mode be clearly defined and documented for the radiation community.

Terminology/Definitions

Before a procedure for calculating a damage metric is addressed, one has to establish a common lexicon for the words that will be used. It is appropriate to start with the definition of the general term "cross section". A cross section is the probability of interaction with a given atom and has units of area and is typically given in barns or cm^2. The important point to note here is that this is a microscopic quantity. There is an associated term, "macroscopic cross section", which is equal to the cross section multiplied by the atom density and has units of an inverse distance, typically given in cm^{-1}. The radiation effects community frequently switches back and forth between the macroscopic and microscopic representation and this can leave the reader confused concerning the relevant units. To address this issue the community often uses the term "microscopic cross section" rather than simply "cross section" in order to help orient the audience. The macroscopic cross section for photons is analogous to the macroscopic quantity termed the linear attenuation coefficient which is represented by the symbol μ. The mass attenuation coefficient has units of an area divided by a mass, e.g. cm^2/g, and is represented by the symbol μ/ρ [3]. For charged particles, one uses the term "linear stopping power" or "restricted linear electronic stopping power", notated by the symbol "S", to denote the energy loss per unit of length along the particle track. The related quantity S/ρ is called the mass stopping power and often is given with units of keV-cm^2/mg. The mass stopping power can be broken down into its electronic, radiative, and nuclear components. The unrestricted linear energy transfer (LET) is the linear electronic stopping power but the restricted stopping power is often indicated as a restricted LET where the LET term is corrected by subtracting the sum of the kinetic energy for all electrons emitted by the charged particle with energy greater than indicated value of the subscript.

Kerma is the basic quantity that underlies traditional metrics for radiation damage by neutrons. The kerma is the kinetic energy of all primary charged particles released by uncharged particles per unit mass. This

quantity is denoted with the symbol "K" and is equal to $[\mu_{th}/\rho]*\Phi*E$ and typically is given in units of Gy(matl) or rad(matl). Here "matl" stands for the material in which the dose/energy is deposited. Kerma should always be quoted with respect to a specific material. An important point here are that kerma is only defined for uncharged particles and that it is a macroscopic quantity related to the radiation delivered in a given scenario. The term "kerma coefficient" is now the recommended term for what was previously called the "kerma factor" and is equal to the kerma divided by the incident particle fluence, Φ. The kerma is often divided into an ionizing and a non-ionizing component. The non-ionizing term is called the "displacement kerma". Many in the radiation effects community use the term kerma loosely and refer to the microscopic analog of the kerma coefficient, $K*[A/N_o]/\Phi$ which is often given with units of MeV-mb. To avoid confusion, this quantity should be referred to as the "microscopic kerma". In this microscopic form, the units do not require that the material of the energy deposition be specified. An example of this type of usage is found in the manuals for the NJOY code [4] which refer to this quantity as kerma. The NJOY/HEATR module reports this microscopic parallel as the displacement kerma. An important point here is that the displacement kerma includes more than the energy that goes into breaking bonds in the target lattice. It also includes the energy that is delivered to the lattice in the form of phonons – and which ends up as heat. Table 1 shows the break down of energy loss from a 50 keV Si ion incident on a Si lattice. The primary ion, because of its higher particle energy and the dynamics of the energy partition between displacement and ionization, is responsible for most (30.5%) of the energy lost into ionization. The recoil atom is responsible for most of the energy that goes into displacements (vacancies + phonons). The largest component of this non-ionizing or displacement kerma corresponds to the energy that goes into the lattice in the form of phonons.

Table 1. Energy Partition for 50 keV Si Ion in Si Lattice

Energy Loss Mechanism	% Energy Loss	
	Primary Ion	Recoil Atoms
Ionization	30.50	25.67
Vacancies	0.23	3.38
Phonons	0.77	39.44

Dose is another macroscopic metric for the energy loss in a material. Dose takes into account the transport of secondary electrons. In the limit where one has charged particle equilibrium (CPE), it is identical to kerma for uncharged particles. Dose can also be broken into its ionizing and non-ionizing (or displacement) components. While this macroscopic quantity should be given in units of Gy(matl) or rad(matl), it is often cast into a microscopic form and presented with units of MeV-mb.

The scope for this paper calls for an investigation of the radiation damage equivalence between neutrons and charged particles. The fact that the traditional damage term "kerma" is only applicable to uncharged particles can make this mapping of radiation damage metrics to charged particle effects difficult. However, the radiation effects community does have a term analogous to kerma for charged particles – it is called cema. Cema is equal to the energy loss by charged particle, except for secondary electrons, per unit mass. Cema is typically given in units of rad(matl) or Gy(matl). This quantity is defined as the integral of the mass stopping power multiplied by the particle fluence as the particle slows down. Cema, like dose and kerma, can be broken down into displacement and electronic energy loss (ionizing) terms. Kerma and cema can be considered to be parallel quantities where one changes the mass stopping power into the mass attenuation coefficient multiplied by the energy.

The non-ionizing energy loss, or NIEL, is another term that is used by the radiation effects community. This is the rate at which energy of an incoming particle is lost per unit length in the material, through non-ionizing processes. This quantity is a microscopic term but is related to the macroscopic quantity of displacement dose and is frequently used by the space radiation effects community to characterize displacement damage modes in satellite materials (solar cells and electronics). This term is often broken down into its Coulombic and nuclear components. Note here however that the nuclear term is the energy lost due to nuclear reactions and is not to be confused with the partition of the stopping power into "electronic" and "nuclear" processes. The "nuclear" stopping power refers to elastic Coulomb collisions that impart recoil energy to the lattice atom.

Damage Metrics

Now that the basic terminology for the energy deposition in materials has been established, one can address how this energy is translated into quantities that can be readily related to specific damage modes of interest to the radiation effects community. While energy into ionization is typically related to the damage modes that depend upon the breaking of molecular bonds, the neutron effects community is typically more interested in effects that depend upon the introduction of displacements in the target lattice, or the introduction of Frenkel Pairs (FP), i.e. vacancy-interstitial pairs.

An important consideration here is the algorithm used to partition the energy into ionizing and non-ionizing energy loss. The early work in this area was done in 1963 by Lindhard, Scharff, and Schiot [5]. These authors treated elastic and inelastic energy loss where the elastic loss used the Thomas-Fermi potential and the inelastic loss used a non-local free uniform electron gas model. Their work is referred to as the LSS energy partition. In 1968 Robinson [6] derived an analytic expression that represented a good fit to the LSS energy partition using the atomic mass and atomic number for the incident ion and lattice atoms. Figure 1 shows the fraction of energy that goes into ionization as a function of the ion energy. For high ion energies almost all of deposited energy goes into ionization. For lower energy ions about 80% of the energy can go into creating displacements and into lattice phonons. Many applications, e.g. NJOY/HEATR module and ASTM standards, use this Robinson fit to partition the kerma into ionizing and displacement components.

Various types of reactions are possible when a neutron undergoes an interaction with a lattice atom. The probability of a given reaction is a function of the neutron energy and the lattice atom. Figure 2 shows the primary recoil ion spectrum for some representative neutron energies and reaction types in a silicon lattice. There is an analytic expression for the maximum energy a neutron can impart to a lattice atom in an elastic scattering process. This energy can be seen in the sharp cut-off energy in the high energy region of the recoil spectra for the two curves corresponding to elastic processes and is shown in Figure 2. The (n,α) transmutation reaction, by contrast, is seen to result in a smooth high energy tail in the primary recoil spectrum. In the case of the (n,α) reaction, in addition to the primary recoil atom, Mg, a high energy alpha particle is also generated. This alpha particle has a large range and will result in additional lattice displacements. Figure 3 shows the recoil spectra for the primary recoil atom, averaged over all reaction channels, for neutrons of various energies incident on a silicon lattice. At a neutron energy of 1-keV, the primary reaction is elastic scattering and the spectrum depicts the sharp high energy edge in the recoil spectra. For a 14-MeV neutron many reactions channels are possible and the recoil spectra depicts a much more complex shape. Figure 4 shows the LSS energy partition for silicon as a function of the incident neutron energy. This curve was generated using the ENDF/B/VII silicon cross sections, the NJOY representation of the reaction-dependent recoil atom spectra, and the LSS energy partition function.

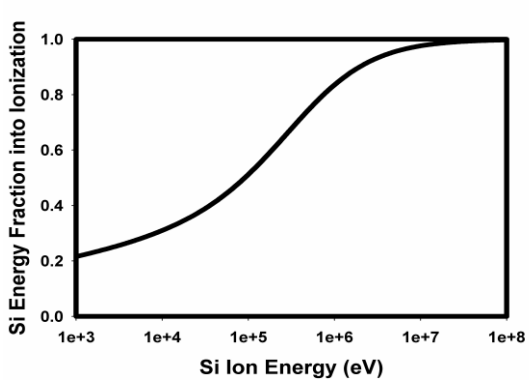

Fig. 1. LSS damage energy partition into ionization.

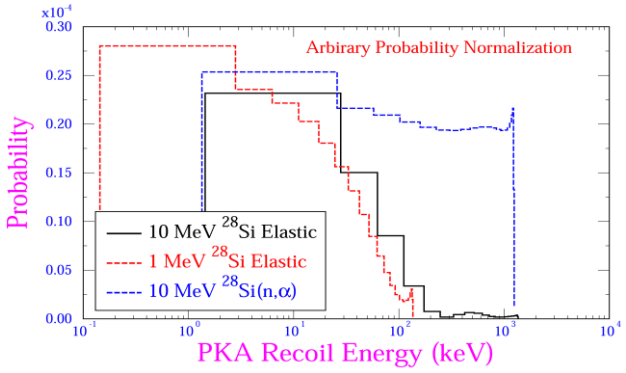

Fig. 2. Representative spectra for the neutron primary recoil atom in a silicon lattice.

The Thomas-Fermi potential is known to over-estimate the elastic energy loss. Recent (2006) work on silicon by Akkerman [7] treated the elastic process using a screened Coulomb interaction with the Ziegler-Biersack-Littmark (ZBL) potential [8] and a combination of local (impact parameter dependent) and non-local models for electronic scattering. This representation of the potentials better

represent current experimental data than do results using the traditional LSS potential. Akkerman used these potentials to provide a new damage partition function for silicon using an analytic expression in the same form as was used by Robinson. Use of the Akkerman damage partition for silicon results in changes of up to 15% in the damage energy as compared to that resulting from the use of the LSS energy partition.

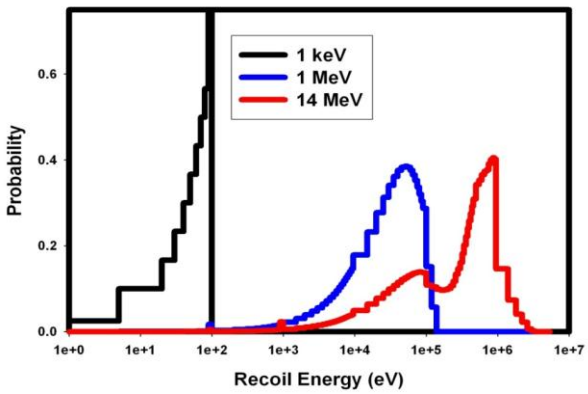

Fig. 3. Primary recoil atom spectra corresponding to various incident neutron energies.

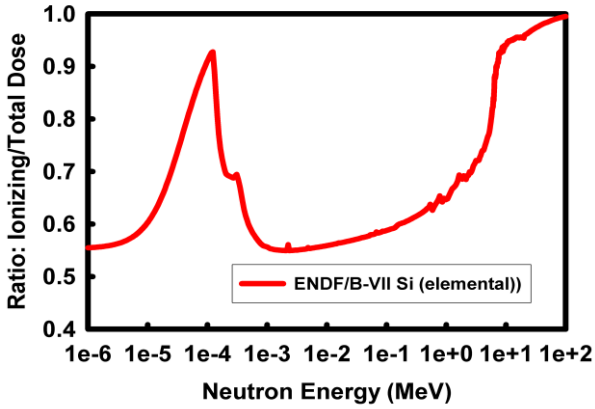

Fig. 4. LSS damage energy partition into ionization as a function of incident neutron energy

A common displacement damage metric is the number of displacements per atom or dpa. Dpa refers to the mean number of times each atom of a solid is displaced from its lattice site during an exposure to displacing radiation. To generate this computational metric, the displacement damage energy is converted to a number of displacements. The most common model used for this conversion was presented in 1955 by Kinchin and Pease (KP) [9]. Norgett, Robinson, and Torrens (NRT) [10] presented an update to the KP formulation that refined the creation of FPs in the threshold damage energy region where the damage energy was only sufficient to produce one or two discrete FPs. The problem with this metric, even with the refined NRT approach, is that, as demonstrated with MARLOWE simulations [11] using a simple binary collision approximation (BCA) of the ion-lattice interaction, closely spaced FPs have a large probability of recombining – thus significantly decreasing the effective/residual defect population. In fact, after the initial quenching of defects, which occurs in picoseconds, there can be a significant evolution in the types and quantities of defects. This evolution of the early-time defect population is commonly explored using molecular dynamic (MD) methods. The results of the MD analysis can be analyzed to statistically characterize the numbers and relative locations of different and complex defect types, e.g. dislocation loops and anti-site atom replacements. The application of MD techniques has been successfully applied to the study of defect evolution out to tens or hundreds of nanoseconds and for ion energies up to tens of keV. Often the high fidelity MD results for low energy ion interactions are spliced onto the results from BCA calculations in order to efficiently utilize both techniques in the regimes where they are accurate and computationally efficient. When the computational requirements of MD become too stressing, either in terms of cpu time or memory, even for massively parallel systems, kinetic Monte Carlo (kMC) techniques are used to track the further defect evolution. kMC approaches do not require the treatment of a large number of nodes in a discrete lattice volume sufficient to contain the complete spatial volume of diffusing atoms and only require the specification of defect mobilities and interaction probabilities. For the use of kMC for defect evolution in electronics, it may prove necessary to extend the kMC approaches to address boundary conditions for the electron flow and to explicitly treat the interaction of the charge state of defects.

With the more advanced treatment of the late-time evolution of the defect population the range of potential damage metrics greatly increases. For electronics, one will desire to distinguish the formation and persistence of defects that are electrically active, e.g. divacancies and vacancy-phosphorus defects in silicon, and ignore the presence of some defects, such as vacancy-oxygen defects. In this vein, some authors have proposed other damage metrics such as residual freely migrating defects or defect

clusters. What remains is to establish a correspondence of the damage metric with the observed damage mode under various irradiation conditions.

Related Work at Sandia National Laboratories

Work at Sandia National Laboratories had focused on neutron damage to electronics. Efforts here have used MD techniques to aid in the selection of the displacement threshold energy and to examine, with high fidelity, the defects that result from a low energy ion incident on the target lattice, typically Si or GaAs. While approaches have been explored that use BCA techniques to transport the primary and recoil atoms down to a predetermined energy and then to append on a defect cluster that is statistically representative of the MD results, the easier approach of extracting a normalization factor from the MD calculation and applying it to the final defect metric that results from the BCA analysis is typically used. Figure 5 shows the variety of defects than can result from the BCA representation of the initial defect population of an arsenic ion incident on a GaAs lattice. For a 10 keV incident ion into the GaAs lattice calculations showed a comparable number of Ga and As interstitials and vacancies, and about half as many Ga and As anti-site defects. A pair correlation function [12] can be used to describe the probability distribution for the separation between defects. The pair correlation function (PCF) can be used to determine if there is a different spatial clustering for different types of defects, e.g. vacancies and anti-site replacements. The PCF is computed for both the MD and BCA analysis and these distributions are compared to ensure that the dynamic aspects of the cascade are adequately captured in the specific application of the BCA approach. This approach, and its set of internal consistency checks, have proven to have sufficient fidelity and are all that is thought to be warranted until better data is available in order to refine the correlation of the selected computational metric with the observed damage mode of interest. This MD-complemented BCA analysis is typically performed using the MARLOWE code. MARLOWE is run for a set of scenarios varying the incident ion type, incident ion energy, lattice composition, and displacement threshold energy. For each case the results of selected metrics are captured and the results are built into a database. Figure 6 shows the probability of generating a specified number of Frenkel Pairs in a cascade generated from an incident silicon ion of a given energy into a silicon lattice.

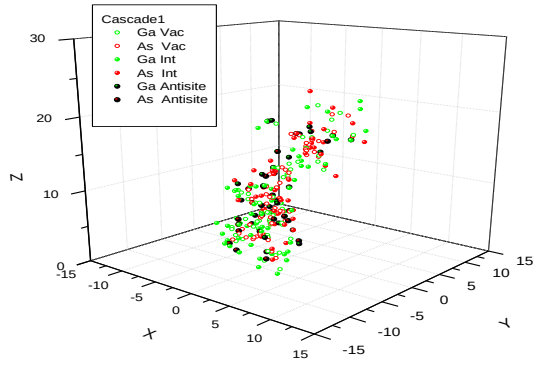

Fig. 5. One sample of the spatial configuration of different defect types resulting from a 10 keV As ion incident on a GaAs lattice.

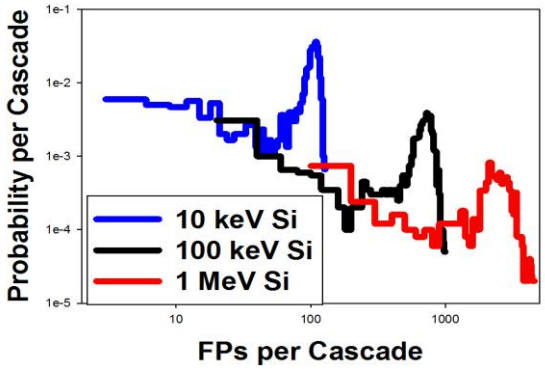

Fig. 6. Frenkel Pair distribution from silicon ions.

In support of the analysis of radiation damage from neutrons, once the damage metric has been selected and the computational metric completely parameterized for the range of relevant ions and energies, this information is folded in with the recoil spectrum. The NJOY code has been modified to employ the different energy partitions, e.g. the Akkerman partition for silicon, use of the NRT displacement formalism, and to permit the use of lattice-specific displacement threshold energies and a weighted treatment of composite (multi-atom) crystal lattices. For a radiation exposure of interest, MCNP [13] calculations are performed to determine the neutron spectrum at the location of interest, often at the emitter-base junction of a bipolar npn transistor. Given the neutron spectrum, the interaction probability with the relevant lattice atoms is calculation and convoluted with the recoil ion

spectrum. Recoil spectra are obtained using the SPECTER [14], TALYS [15], or EMPIRE [16] codes. The recoil spectrum resulting from summing over all of the neutron interactions is then folded with the computational metric. Figure 7 shows the probability distribution for Frenkel Pairs generated from the EMPIRE recoil spectrum for various monoenergetic neutron irradiations of a silicon lattice. Figure 8 convolutes this neutron energy-dependent FP production curve with the neutron spectrum from the Sandia Pulsed Reactor III (SPR-III). This figure shows that the Frenkel Pair distribution function for a reactor spectrum has a very broad distribution of the number of Frenkel Pairs. As part of this process, the cascade density in the area of interest is computed in order to flag cases where high neutron fluence irradiations may result in the overlap of cascades.

For small feature size semiconductor applications, the cascade density is also combined with feature size to determine the number of interactions in the relevant volume. In cases where there is a small number of neutron interactions and a (potentially) large variation in the damage metric between different neutron interactions, one can expect a significant device-to-device variation in the experimental data. For example, when one uses a metric of the number of FPs created, the probability density distribution for FP creation in the Sandia Annular Core Research Reactor (ACRR), a water moderated reactor, because of the broad neutron spectrum, the FP distribution is very wide. A maximum pulsed exposure at the White Sands Missile Range (WSMR) fast burst reactor is found, by calculation, to only result in ~20 defects in the active area of small feature size GaAs devices. If there are only a few neutron interactions in the sensitive volume of an electronics device, then the use of an average number of FPs created per neutron interaction requires consideration of the uncertainty (or variation) due to the sample size (number of interactions).

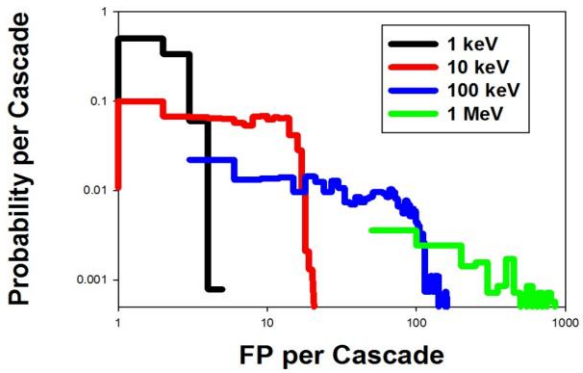

Fig. 7. Frenkel Pair distribution from monoenergetic neutrons.

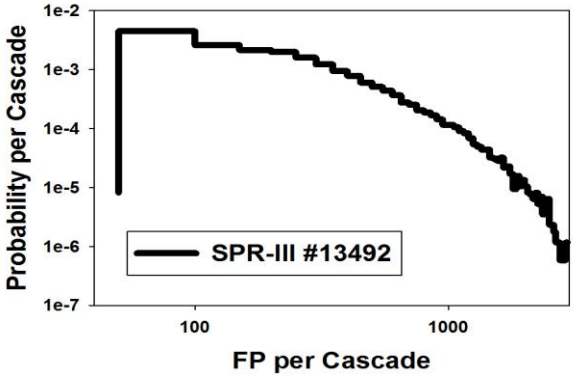

Fig. 8. Probability density distribution for Frenkel Pair creation in the SPR-III fast burst reactor neutron spectrum.

Another issue that can complicate correlating a computational metric with a given damage mode is the synergy that can exist between damage caused by neutrons and that caused by gammas. Most neutron exposures actually represent a mixed radiation field having both neutron and gamma components. Table 2 shows the neutron and gamma kerma from a representative exposure in the ACRR reactor field where a lead-boron shield/bucket is used to minimize the secondary gamma component. Even when an experimenter tries to reduce the gamma field, the gamma radiation component, there can be a significant dose to the parts – and the fraction of the dose attributed to the gammas is strongly dependent upon the material of interest. As shown in Table 2, with this shielded ACRR exposure configuration only 7% of the dose in silicon devices is attributed to the neutron environment, whereas 69% of the dose as recorded in an alanine dosimeter comes from the neutrons. This is due to the large hydrogen component in the alanine. One must be very careful to properly relate the dose as measured in a dosimeter with the dose as experienced within a part under test. When an active (time-dependent) diagnostics, such as a diamond/carbon photoconductive photodetector is used to record the time profile of an exposure, the detector, in this ACRR shielded configuration, records 28% of its temporal response as coming from the neutrons.

Table 2. Neutron/gamma response of various materials in an ACRR irradiation in a Pb-Boron bucket.

Matl.	Neutron Kerma	Gamma Kerma	% Dose from neutrons
Alanine	469.2	208.2	69%
Diamond	74.3	192.9	28%
Silicon	16.0	203.2	7%
CaF_2:Mn TLD	31.45	202.4	13%

Uncertainty Quantification

A damage metric has limited value if the user cannot associate an uncertainty with its application. This represents a major deficiency with the current community approach – and is an area which Sandia is trying to address. The correct way to represent the uncertainty is with an energy-dependent covariance matrix. Early work in this area generated a covariance matrix for silicon 1-MeV-equivalent damage using the variation seen in community representations of the silicon displacement kerma. Figure 9 shows the resulting energy-dependent correlation matrix [17]. The small sample size and the inability to address correlations in the underlying cross section evaluations limited the fidelity of this covariance matrix.

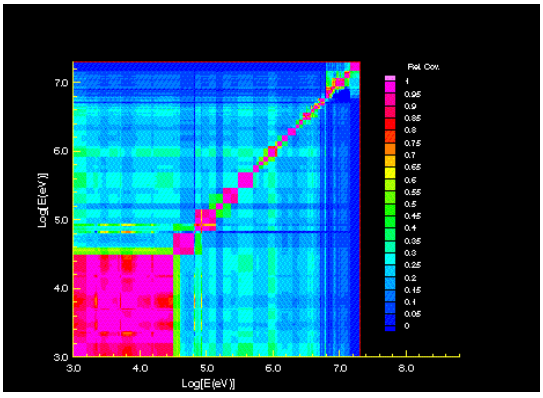

Fig. 9. Silicon correlation matrix based upon an examination of cross sections used within the radiation effects community.

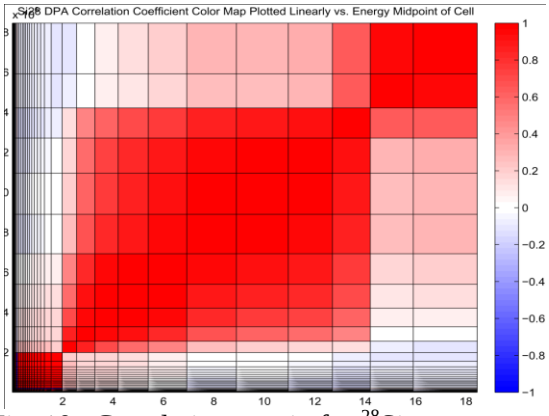

Fig. 10. Correlation matrix for ^{28}Si displacement kerma based upon TENDL-2010 random generation cross sections.

Another approach to formulating a covariance matrix is to use a Total Monte Carlo (TMC) approach [18]. The TALYS code and the randomly generated cross section evaluations available within the TENDL-2010 cross section library make it possible to explore this approach. The TENDL-2010 random library currently only presents a sample size of 30 for the random cross section evaluations. A sample size closer to 100 is desired in order to generate the energy-dependent covariance matrix using an energy grid of sufficient range and resolution for most applications, i.e. about 90 energy bins. Figure 10 shows the correlation matrix that is generated for the silicon displacement kerma using the TENDL-2010 cross sections and the TMC approach [19]. The shape of this correlation matrix for the displacement kerma is very similar to that seen for the total cross section. The correlated regions correspond to areas where one reaction channel tends to dominate the neutron interaction probability. An inspection suggests that the shape of the correlation matrix is not significantly influenced by the uncertainty in the recoil spectra. Work is ongoing to separate the displacement kerma covariance matrix into the cross section and recoil spectral components.

A critical issue associated with the use of calculated covariance matrices is the treatment of "model defect". This is an uncertainty component that is intrinsic to the models incorporated within the codes and may not be probed with the model parameter variation that is used to generate the random draws of the cross section evaluations. Previous comparisons of the TALYS-generated cross section uncertainty with the recommended data-driven dosimetry cross section evaluations as found in the IRDF-2002 library [20] and with EXFOR experimental data [21] suggest that the high energy portion of the TENDL cross sections significantly understates the uncertainty and exhibits a different energy-dependent shape [22]. The TENDL community addressed this issue for dosimetry cross sections in their 2010 release by renormalizing the baseline cross section shape to the best experimental-based cross section for the dosimetry reactions. Figure 11 shows that the TENDL-2010 random cross section evaluation correctly represents the parameter-driven variation about the renormalized baseline cross section. The challenge is how to correctly capture the non-parameter-drive model uncertainty in the covariance matrix for reactions channels where adequate experimental data does not exist to permit the use of this baseline renormalization approach.

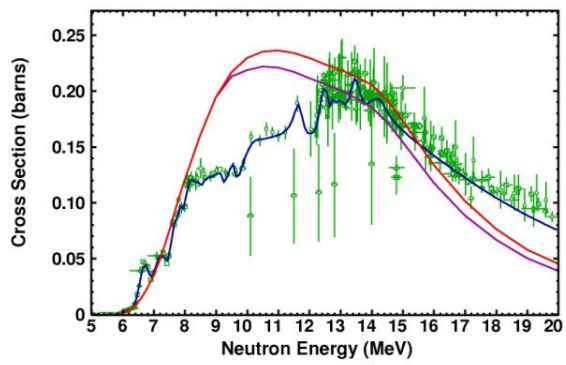

Fig. 11. Comparison of 2008 and 2009 TENDL calculated cross sections with the dosimetry-quality evaluation and experimental data for the $^{24}Mg(n,p)^{24}Na$ reaction.

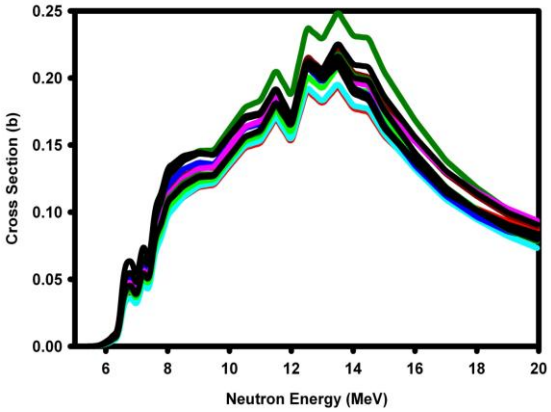

Fig. 12. TENDL-2010 parameter-driven variation in the computed re-normalized $^{24}Mg(n,p)^{24}Na$ cross section.

Work has shown that the effect of parameter variation of the interaction potentials used in the MD and BCA models can introduce a very large uncertainty in the model results for FP generation. Sandia's approach to this has been to eliminate the systematic portion of this uncertainty by using a calibration to a reference experimental point. This has been shown to drastically reduce the uncertainty that must be assigned to the computed metrics. This is consistent with the spirit incorporated into the 1-MeV(Si) and 1-MeV(GaAs) ASTM standards.

When one examines the uncertainty in the simulation of radiation damage under test reactor exposures, one needs to consider a wide range of uncertainty components, including:

- uncertainty in the incident neutron spectrum, typically derived from a least squares spectrum adjustment
- uncertainty in the neutron cross section, typically provided by the covariance matrices in ENDF or TENDL evaluations
- uncertainty in the recoil atom energy spectrum, currently modeled by the parameter variation within the TENDL-2010 random draws for the cross sections
- uncertainty in the energy partition function due to:
    - knowledge of the displacement threshold energy and its angle dependence
    - knowledge of the interaction potentials used to model the MD or BCA ion transport
    - model defect in the MD or BCA codes used to model the ion transport.

Parameter variations in the BCA and MD codes has demonstrated that the variation in the interaction potentials and displacement threshold energy can result in a large uncertainty, but the largest share of

this uncertainty is systematic and can be removed by an energy calibration. We calibrate at a fast neutron energy using a fast fission reactor spectrum, so the uncertainty is small until we transition to thermal neutron energies or up to the high energy regions (> 8 MeV). Through the use of a double ratio technique, calibration in the ACRR Pb-Boron shielded configurations has been shown to produce only a 1% variation in the FP generation due to the displacement threshold energy and 1% due to the atom interaction potential when one makes a prediction for a fast fission spectrum representative of the SPR-III reactor. We have not yet found a way to calibrate out the systematic uncertainty due to the recoil atom spectrum. The correlations in the TENDL/TALYS models are not used for this since we have not found a way to account for model defect. When we compare the effect of recoil atom spectra using different codes, we are forced to accept an uncertainty of ~12%. Efforts are underway to find a way to extract the systematic component from this uncertainty. The uncertainty in using an average number for the FP generation per cascade has not yet been factored into our approach. For cases with a large number of neutron interaction sites this uncertainty should be small, but the FP distribution has been shown to be very non-Gaussian, so simulations are needed in order to quantify how this uncertainty will be propagated. The effect of dopants (P or B typically for silicon devices) has been shown to not be important in the initial defect population from MD or BCA analysis, but can be large when kMC codes are used to model the evolution of the defect population.

There are a number of other complicating factors that must be studied. These include the effect of the incident neutron fluence rate, the effect of impurities, long-term defect migration, and synergistic effects from ionization or helium accumulation. Whether these complications are addressed with modeling or through experiments demonstrating the correlation between the damage metric and the observed damage mode depends upon the needs for the given application and the acceptable uncertainty.

Conclusions

There are many remaining challenges to the development of good computational damage metrics that can be used to compare the damage from different irradiation scenarios involving neutrons and charged particles. This paper has outlined an approach being pursued at Sandia National Laboratories to add an uncertainty treatment to the generation of the damage metrics. Key elements of our approach are the use of a Total Monte Carlo technique built upon the TENDL cross section library and use of an experimental calibration point in order to limit the uncertainty in the metric. The first step is to define the damage modes that are of interest. Different computational metrics may be valid for different damage modes. Another consideration in the path forward regards how the correlation of the damage metric can be validated and the specification/documentation of the range of conditions under which the correlation has been validated.

References

1. ASTM Standard E722-09e1, Standard Practice for Characterizing Neutron Fluence Spectra in Terms of an Equivalent Monoenergetic Neutron Fluence for Radiation-Hardness Testing of Electronics,Vol. 12.02, ASTM International, West Conshohocken, PA, 2009.
2. ASTM Standard E693-12, Standard practice for characterising neutron exposure in iron and low alloy steels in terms of displacements per atom (dpa), Vol. 12.02, ASTM International, West Conshohocken, PA, 2012.
3. ICRU Report 60: Fundamental Quantities and Units for Ionizing Radiation. International Commission on Radiation Units and Measurements, Bethesda, MD, USA (1998) ISBN 0-913394-59-9
4. R.E. MacFarlane, D.W. Muir, R.M. Boicourt, The NJOY nuclear data processing system: Volume 1, User's manual, Los Alamos National Laboratory, report LA-9303-M-Vol.1, published May 1, 1982. Updated on Feb. 7, 2008.
5. J. Lindhard, M. Scharff, and H. E. Shiøtt. Range concepts and heavy ion ranges. Mat. Fys. Medd. Dan. Vid. Selsk., 33(14):1, 1963.

6. M. Robinson, I. Torrens, "Computer simulation of atomic-displacement cascades in solids in the binary-collision approximation". *Physical Review B* **9** (12), 1974.
7. A. Akkerman, "New Partition Factor Calculations for Evaluating the Damage of Low Energy Ions in Silicon", IEEE Transactions on Nuclear Science, Vol. 53, Issue 6, December 2006.
8. J. F. Ziegler, J. P. Biersack, and U. Littmark, The Stopping and Range of Ions in Matter, volume 1, New York, Pergamon Press, ISBN 0-08-022053-3, 1985.
9. G. H. Kinchin and R. S. Pease, "The Displacement of Atoms in Solids by Radiation", Reports on Progress in Physics, Volume 18, 1955.
10. M. J. Norgett, M. T. Robinson, and I. M. Torrens, A proposed method of calculating displacement dose rates, Nucl. Engr. and Design Vol. 33, 1975.
11. M. T. Robinson, "MARLOWE Binary Collision Cascade Simulation Program, Version 15b, A Guide for Users", December 5, 2002.
12. S.M. Myers, P.J. Cooper, W.R. Wampler, "Model of defect reactions and the influence of clustering in pulse-neutron-irradiated Si", Journal of Applied Physics, Vol. 104, issue 4, August 2008.
13. F.B. Brown, (Team Leader) and X-5 Monte Carlo Team, MCNP – A General N-Particle Transport Code, Version 5, Volume 1: Overview and Theory, LA-UR-03-1987, Los Alamos National Laboratory, Los Alamos, NM, April 2003.
14. L.R. Greenwood, R.K. Smither, "SPECTER: Neutron Damage Calculations for Materials Irradiations", Argonne National Laboratory, report ANL/FPFP/TM-197, 1985.
15. A. Koning, S. Hilaire, S. Goriely, TALYS-1.4: A nuclear reaction program, User manual, Nuclear Research and Consultancy Group (NRG), Dec. 28, 2011.
16. M. Herman, in *Workshop on Nuclear Reaction Data and Nuclear Reactors: Physics, Design and Safety*, edited by N. Paver, M. Herman and A. Gandini, March 13 - April 14 2000, Trieste Italy, p. 137, 2001.
17. M. Danjaji, P.J. Griffin, J.G. Williams, Reactor Dosimetry, Proceedings of the 9th ISRD, World Scientific, pp. 611-618, 1996.
18. A. Koning, "Total Monte Carlo and related applications of the TALYS code system", Technical Meeting on Neutron Cross Section Covariances, September 27-30, 2010, IAEA, Vienna, Austria.
19. R. Middleton, Sandia National Laboratories, private communication, August 2012.
20. International Reactor Dosimetry File 2002 (IRDF-2002), IAEA, Technical Reports Series No. 452, 2006.
21. EXFOR Exchange Formats Manual, Atomic Energy Agency, Vienna Austria, report IAEA-NDS-207, February 2008.
22. P. J. Griffin, "Use of Model-based Covariance Estimates in Dosimetry Applications," presented at the ND2010 conference and accepted for publication in the Journal of Korean Physical Society.

NJOY/HEATR: What It Calculates Now, What Should It Calculate?

A. C. (Skip) Kahler

Theoretical Division
Los Alamos National Laboratory
USA

We provide a summary report that accompanies the LA-UR-12-25154 oral presentation made at the October 2012 IAEA Technical Meeting on "Primary Radiation Damage: from Nuclear Reactions to Point Defects" held in Vienna, Austria.

The NJOY Nuclear Data Processing System [1,2] is used worldwide to create application specific nuclear data libraries from Evaluated Nuclear Data File (ENDF) formatted [3] files.

In this summary report we briefly review the ENDF system, then discuss use of NJOY to calculate "radiation damage".

ENDF is the United States' national nuclear data file. The ENDF system was initially developed in the 1960s, and currently is in its seventh generation. Candidate data files are reviewed by a standing committee known as the Cross Section Evaluation Working Group (CSEWG) which advises Brookhaven National Laboratory's (BNL) National Nuclear Data Center (NNDC) as to ENDF's recommended content. This file is formally known as ENDF/B. A lesser known file, ENDF/A, contains files that contain candidate evaluations for a future ENDF/B release, or partial evaluations that remain under development.

As a product of the 1960's, the ENDF format is product constrained by the limits of computer card technology. The data (resonance parameters, cross sections, angular distributions, secondary distributions, and more) are defined to fit within a fixed 80 character per record format. Specifically, numerical data and ascii text strings occur in the first 66 columns and the final 14 columns contain a set of four control integers; matn(i4), mf(i2), mt(i3) and ns(i5). Matn, or material number, is a flag associated with a specific nuclide. Mf, or file number, is used to identify a specific type of data. The 66 column data region consists of 6 eleven column fields containing a mix of real and integer data. Most relevant to this topic are the data given in mf=3 (neutron cross sections), mf=4 (outgoing neutron angular distributions), mf=5 (secondary neutron energy distributions), and mf=6 for coupled energy-angle distributions for multiple emitted particles. Mt, or section number, identifies a specific reaction. Examples are mt = 1 for the total cross section, mt = 2 for elastic scattering, mt's 51 to 89 for discrete level inelastic scattering, and mt's 102 through 107 for the (n,γ), (n,p), (n,d), (n,t), (n,^{3}He) and (n,α) reactions, respectively.

The mt numbers cited above constitute "fundamental" data, i.e., data that are the result of the evaluator's analysis of the underlying microscopic data, usually supplemented with model calculations to fill in the gaps in the experimental database. Another class of mt number constitutes "derived" data. These mt numbers define data that are obtained by a summation of other mt values or other calculations. For example there are a number of mt's that define reactions where a proton (or deuteron, triton, ^{3}He or α) is the only emitted particle, or one of multiple emitted particles. The summation of the appropriate cross sections defines a "proton production" cross section and the ENDF system has defined a specific mt value, 203, where these data may reside. Mt values of 204 through 207 are reserved for production of deuterons through α particles. Collectively these mt's allow for the calculation of "gas production". Note however, we say "may". There is no requirement that these data types be defined in any specific evaluation; rather a derived cross section is usually the product of a processing code such as NJOY and most likely is only calculated if requested by the end user.

Mt numbers are reserved for derived quantities such as the kinetic energy release in materials, or KERMA (mt = 301), with other mt's defined for the KERMA associated with specific reactions and damage.

The ensuing discussion is derived largely from that given in the NJOY manual [1,4]. Damage to materials is caused by the effects of neutron irradiation. Gas production (i.e., helium embrittlement) and production of lattice defects are examples of such damage. Lattice defects are produced by the primary recoil nucleus of a nuclear reaction as it slows down, or loses energy, in the lattice. Furthermore, there is an empirical correlation between the number of displaced atoms (DPA, displacements per atom) and various material properties. The number of displaced atoms depends on the total energy available, E_a, and the energy required to displace an atom from its lattice position, E_d. Since the available energy is used up in producing pairs,

$$DPA \sim \frac{E_a}{2E_d}$$

The values of E_d built into NJOY vary by element from about 25 eV to 90 eV while the energy available, E_a, is calculated by NJOY using nuclear data obtained from ENDF evaluations. The actual energy available to cause lattice displacements depends upon the recoil spectrum and the partition of recoil energy between electronic excitation and atomic motion. The partition function used is that given by Robinson[5], based upon the electronic screening theory of Lindhard [6],

$$P(E) = \frac{E_R}{1 + F_L(3.4008\varepsilon^{1/6} + 0.40244\varepsilon^{3/4} + \varepsilon)}, if\ E_R \geq 25\ eV,$$

or zero otherwise.

Terms appearing in this formula include:

$$E_R = the\ primary\ recoil\ energy;$$

$$\varepsilon = \frac{E_R}{E_L},$$

$$E_L = \frac{30.724 Z_R Z_L (A_R + A_L)\sqrt{Z_R^{2/3} + Z_L^{2/3}}}{A_L},$$

$$F_L = \frac{0.0793 Z_R^{2/3} Z_L^{1/2} (A_R + A_L)^{2/3}}{\left(Z_R^{2/3} + Z_L^{2/3}\right)^{3/4} A_R^{3/2} \sqrt{A_L}},$$

and Z_i and A_i are the charge and atomic number of the lattice nuclei (L) and recoil nuclei (R).

Specific formulas for E_R depend upon the reaction and the type of data available from the ENDF/B evaluation. For example, the recoil nuclei energy following elastic (mt = 2) or two-body discrete level (mt=51 to 89) inelastic scattering is

$$E_R(E, \mu) = \frac{AE}{(A+1)^2}(1 - 2R\mu + R^2), where$$

$$R = \sqrt{1 - \frac{(A+1)(-Q)}{AE}}$$

and μ is the CM scattering cosine. With this, NJOY/HEATR computes a damage energy production "cross section", with units of eV-barns, as

$$D(E) = \sigma(E) \int_{-1}^{1} f(E, \mu) P_R(E_R[E, \mu]) d\mu$$

where *f* is the angular distribution from (mf) file 4. A more complex reaction representation might include continuum spectra. In this case the damage energy production cross section becomes a double integral over both angle and energy, where the secondary energy distribution function comes from (mf) file 5. Refer to the NJOY manual and recent Nuclear Data Sheets paper on ENDF/B-VII processing [1,2], for a more comprehensive discussion of these calculations and the approximations made if not all expected data are available or for more complex reactions with multiple particle emission.

The total damage energy production cross section is a "derived" quantity and is assigned mt = 444 by NJOY. Individual components of this total include elastic (mt = 2) damage, assigned mt = 445; inelastic (mt = 51 to 89) damage, assigned mt = 446 and neutron disappearance damage (mt = 102 to 120), assigned mt = 447. Calculated damage energy production for ENDF/B-VII.1's ^{56}Fe is shown:

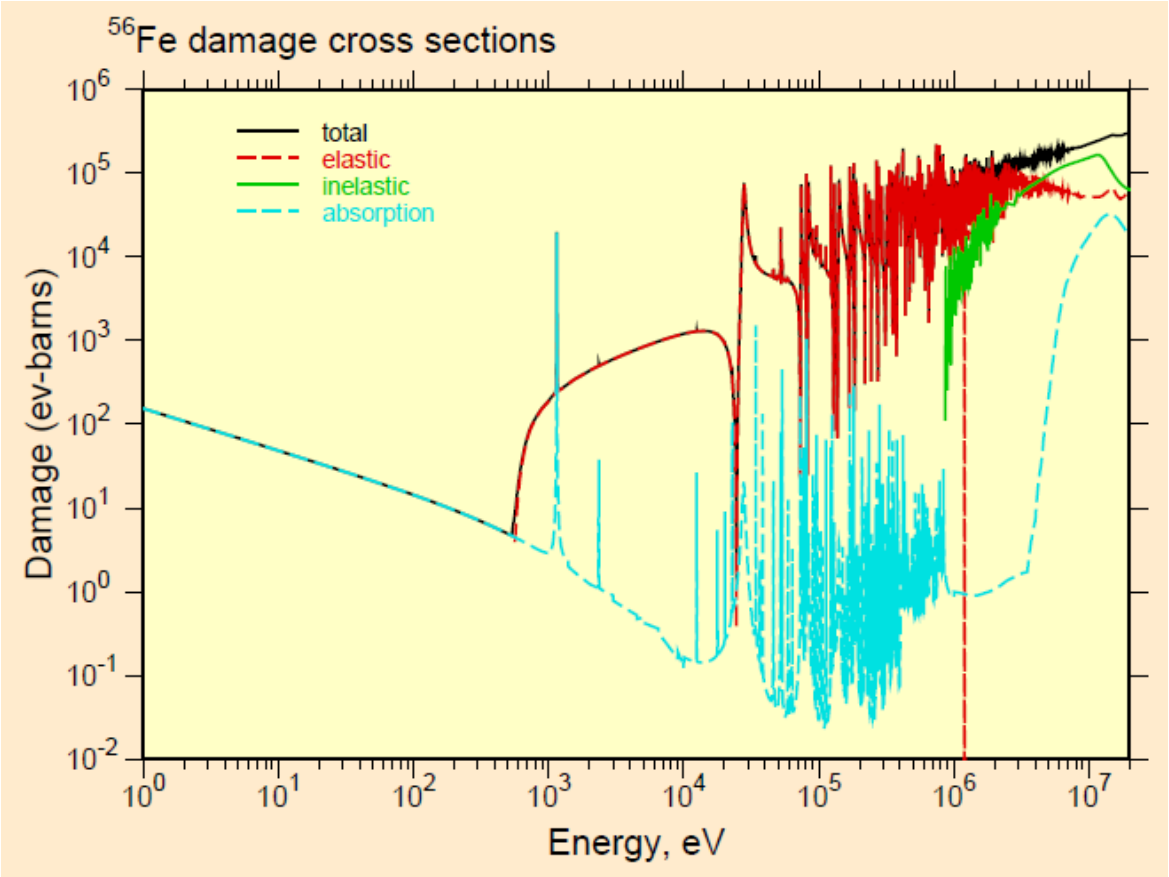

As might be inferred from the publication date for Reference 4, the methods and techniques employed by NJOY to calculate damage have remained unchanged for many years. NJOY can adapt to new methods, or implement new formulas for calculation of the damage energy production cross section, and the NJOY development team stands ready to implement any such alternate representations that may appear in future years and receive broad acceptance within the technical community.

That said, it must be remembered that NJOY is an ENDF-formatted file nuclear data processing code and there are no plans to expand NJOY's capability to read fundamental data from non-ENDF formatted sources.

References

1. R.E. MacFarlane and D.W. Muir, "The NJOY Nuclear Data Processing System, Version 91," Los Alamos National Laboratory report LA-12740-M (1994).
2. R.E. MacFarlane and A.C. Kahler, "Methods for Processing ENDF/B-VII with NJOY," *Nuclear Data Sheets*, **111**, 2739-2890 (2010).
3. A. Trkov, M. Herman and D.A. Brown, Eds., "ENDF-6 Formats Manual, Data Formats and Procedures for the Evaluated Nuclear Data Files ENDF/B-VI and ENDF/B-VII," Brookhaven National Laboratory report BNL-90365-2009 Rev.2, December 2011 (http://www.nndc.bnl.gov/csewg/docs/endf-manual.pdf)
4. R.E. MacFarlane, D.W. Muir and F.M. Mann, "Radiation Damage Calculations with NJOY," *J. Nucl. Materials* **122** and **123**, 1041 (1984).
5. M.T. Robinson, "The Energy Dependence of Neutron Radiation Damage in Solids", in the Proceedings of the British Nuclear Energy Society Nuclear Fusion Reactor Conference at Culham Laboratory, September 1969.
6. J. Lindhard, V. Nielsen, and M. Scharff, "Range Concepts and Heavy Ion Ranges," *Mat. Fys. Medd. Dan. Vid. Selsk*, **33**(14) 1-42 (1963).

Direct observation of radiation defects: experiment and interpretation.

S.L. Dudarev

**EURATOM/CCFE Fusion Association, Culham Centre for Fusion Energy,
UK Atomic Energy Authority, Oxfordshire OX14 3DB
UK**

Electron microscopy is arguably the only available experimental method suitable for the direct visualization of nano-scale defect structures formed under irradiation. Images of dislocation loops and point-defect clusters in crystals are usually produced using diffraction contrast methods. For relatively large defects, a combination of dynamical imaging and image contrast simulations is required for determining the nature of visible radiation defects [1].

At the same time, density functional theory (DFT) models developed over the last decade have provided unique information about the structure of nano-scale defects produced by irradiation, including the defects that are so small that they cannot be observed in an electron microscope, and about the pathways of migration and interaction between radiation defects. DFT models, involving no experimental input parameters and being as quantitatively accurate and informative as the most advanced experimental techniques for the direct observation of defects, have created a new paradigm for the scientific investigation of radiation damage phenomena. In particular, DFT models offer new insight into the origin of temperature-dependent response of materials to irradiation, a problem of pivotal significance for applications. By combining information derived from the first-principles models for radiation defects with information derived from small-scale experimental observations it may be possible to acquire quantitative knowledge about how materials respond to irradiation and, using this knowledge, develop materials suitable for advanced applications in fission and fusion.

It now appears possible to pose the question about the development of integrated fusion power plant models, combining neutron transport calculations and microscopic models for microstructural evolution of materials, for example models for *ab initio* prediction of helium embrittlement [2]. Such models, based on scientific principles and quantitative data, and developed at low cost in comparison with the mock-up tests, offer scientific insight and make it possible to perform, in combination with experimental information derived from fission and ion-beam irradiation experiments, the preliminary assessment of power plant operating scenarios.

Defining the limits of visibility of small defect clusters and dislocation loops, and optimal diffraction conditions for electron microscope imaging, remains one of the central problems of electron microscopy of irradiated materials. Using computer image simulations based on the propagation–interpolation algorithm for solving the Howie–Basinski equations, it is possible to investigate the relation between the actual and the 'observed' size of small loops, the part played by many-beam dynamical diffraction effects, and limitations of electron microscope imaging in identifying the structure of small defects [3].

A particularly impressive and useful application of electron microscopy is given by recent *in situ* electron microscope observations, providing real-time visualization of dynamics of defects produced by ultra-high-energy electron irradiation, or showing microstructural evolution occurring under ion beam irradiation. Such observations have revolutionized our understanding of how properties of metals and alloys change in the extreme radiation and thermal environments of a fission or a fusion power plant.

The key feature of *in situ* electron microscopy is its ability to exhibit the time-dependent dynamics of migration, interaction, and transformation of radiation defects, and to visualize the entire complexity of evolving defect and dislocation networks. For example, *in situ* electron microscope observations provided evidence of violation of the Burgers vector conservation law for dislocations on the nanoscale. This gave a vital clue needed for modeling microscopic processes responsible for the formation of unusual high temperature dislocation structures in iron, and for explaining the origin of the loss of strength of ferritic-martensitic steels at high temperatures.

The development of *in situ* electron microscope techniques was partially stimulated by the application of large-scale molecular dynamics (MD) simulations to modeling mobile defects and clusters of defects (for example, nano-dislocation loops) in iron and other metals. A hypothesis stating that clusters of point defects play a significant part in microstructural evolution of irradiated materials was proposed in 1990s within the framework of the "production bias" radiation damage model. However, it is only recently that *in situ* electron microscope observations confirmed the fact that mobile and immobile clusters of point defects form an integral part of the microstructure of an irradiated material.

Somewhat surprisingly, interpreting *in situ* real-time electron microscope observations still remains genuinely problematic. The ten orders of magnitude mismatch between the nanosecond (10^{-9}s) time scale accessible to an MD simulation, and the 10–1000 s time scale of a typical *in situ* electron microscope observation, impedes meaningful quantitative analysis. The need to develop such a model has recently stimulated the development of a novel approach to modeling defect evolution in real time (Langevin dynamics [4]).

In situ electron microscope observations visualize the dynamics of microstructure corresponding to the limit of high irradiation dose rates, approaching 10-3 dpa/s (80 dpa per 24 h) for the ultrahigh-voltage electron irradiation case, and ($6x10^{-4}$ dpa s^{-1} to $8x10^{-4}$ dpa s^{-1} (50–70 dpa per 24 h) for the *in situ* ion-beam irradiation case. These dose rates are similar to the 10 dpa per 24 h to 100 dpa per 24 h range of dose rates characterizing irradiation conditions in *ex situ* ion-beam facilities. *In situ* electron microscopy and *ex situ* ion-beam irradiation experiments generate similar microstructures, corresponding to a similar range of high irradiation dose rates. These dose rates are several orders of magnitude higher than the rates associated with the irradiation environment of a fission nuclear reactor, an accelerator-driven system such as the International Fusion Materials Irradiation Facility or a fusion power plant.

The dose rate effects – somewhat surprisingly – are observed even in the very low dose rate limit, for example, dose rate effects are seen in swelling experiments performed using conventional fission reactors. This highlights the dynamic nature of microstructural evolution, and the need to understand the parameters determining this evolution, at quantitative level. The refinement of nuclear cross-section data, and the development of an integrated approach describing how materials evolve under irradiation, from the treatment of neutron scattering by atomic nuclei to the development of defect microstructures in materials, is a timely objective for fission and fusion materials research.

References

1. L.M. Peng, S.L. Dudarev, and M.J. Whelan. *High-Energy Electron Diffraction and Microscopy* (Oxford University Press, 2011).
2. M.R. Gilbert, S.L. Dudarev, S. Zheng, L.W. Packer and J.-Ch. Sublet, Nucl. Fusion 52 (2012) 083019
3. Z. Zhou, M.L. Jenkins, S.L. Dudarev, A.P. Sutton and M.A. Kirk, Philos. Mag. 86 (2006) 4851
4. S.L. Dudarev, M. R. Gilbert, K. Arakawa, H. Mori, Z. Yao, M. L. Jenkins, and P. M. Derlet, Phys. Rev. B **81** (2010) 224107

Primary damage characteristics in metals under irradiation in the cores of thermal and fast reactors

V.A. Pechenkin

SSC RF Institute of Physics and Power Engineering, Obninsk
Russia

Introduction

For an analysis and forecasting of radiation-induced phenomena in structural materials of WWERs, PWRs and BN reactors the fast neutron fluence is usually used (for structural materials of the reactor cores and internals the fluence of neutrons with energy > 0.1 MeV, for WWER and PWRs vessel steels the fluence of neutrons with energy > 0.5 MeV in Russia and East Europe, and with energy > 1.0 MeV in USA and France). Displacements per atom (dpa) seem to be a more appropriate correlation parameter, because it allows comparing the results of materials irradiation in different neutron energy spectra or with different types of particles (neutrons, ions, fast electrons). Energy spectra of primary knocked atoms (PKA) and "effective" dpa, which are introduced to take into account the point defect recombination during the relaxation stage of a displacement cascade, can be still better representation of the effect of irradiation on material properties.

In this work the results of calculating dose rates (dpa/s, NRT-model), PKA energy spectra and PKA mean energies in metals under irradiation in the cores of Russian reactors WWER-440, WWER-1000 (both power thermal reactors) and BN-600 (power fast reactor) and BR-10 (test fast reactor) are presented. In all the reactors Fe and Zr are considered, with addition of Ti and W in BN-600. "Effective" dose rates in these metals are calculated. Limitations and uncertainties in the standard dpa formulation (the NRT-dpa) are discussed. IPPE activities in the fields related to the TM subject are considered.

Calculation of damage dose characteristics

At an arbitrary location in the material the dose rate K (dpa/s) is given by the following expression:

$$K = \int_{E_{min}}^{E_{max}} \sigma_d(E)\varphi(E)\, dE\,, \qquad (1)$$

where E_{min} and E_{max} is minimum and maximum boundaries of neutron spectrum, φ(E) is the neutron energy dependent flux, and σ_d(E) is the displacement cross section

$$\sigma_d(E) = \int_{T_d}^{T_{max}} \frac{d\sigma\ (E,T)}{dT}\ \nu(T)dT\,, \qquad (2)$$

where $\nu(T)$ (the cascade function) is the number of displaced atoms per PKA of the energy T, $\frac{d\sigma\ (E,T)}{dT}$ is the differential cross section for the transfer of energy T to the struck atom from the incoming particle of energy E, T_{max} is the maximal energy transferred to the struck atom from the neutron of energy E, T_d is the effective displacement energy.

An analysis indicates that the main errors in dose rate calculations are introduced by uncertainties in T_d and ν(T) evaluation. Since displacement energy T_d is a strong function of recoil direction [1] then some averaged recommended values of the effective displacement energies are used in dose rate calculations (see e.g. [2]). Now the *NRT* – model (Norgett, Robinson and Torrens [3]) for cascade function (ν_{NRT}(T) in (2)) with Lindhard's partitioning between elastic and electronic PKA energy losses [4] is widely used in dpa calculations. Extensive molecular dynamics (MD) simulations of cascades created by PKAs with energies up to 200 keV in Fe [5-8] and other metals (see references in

[9]) have revealed that a significant part of point defects (PD) created in the collision stage (< 0.1 ps) of cascade development is annihilated during the subsequent quenching stage (~ 10 ps) when the temperature of cascade region is decreased to the thermodynamical one. The cascade functions calculated for a number of metals using MD simulations of cascades will be denoted as $\nu_{MD}(T) = \nu_{NRT}(T)\cdot\eta(T)$, where $\eta(T)$ is the cascade efficiency.

The number of displacements per atom calculated with account of only defects surviving after in-cascade recombination during quenching stage will be called as "effective" dpa. Note that the low temperature electrical resistivity rate in a number of metals and in 300 series SS after irradiation in different neutron spectra [9] agrees with "effective" dpa rate. It should be noted that the value of $\eta(T)$ is dependent on the interatomic potentials chosen in the MD simulations. For example, MD displacement cascade simulations in Ref. [10] resulted in $\nu_{MD1}(T) = 6{,}2\ T^{0{,}697}$ (E is the PKA energy in keV) for E ranging from 1 to 10 keV in Fe. In Ref. [11] such simulations using a different interatomic potential for Fe resulted in $\nu_{MD2}(T) \approx 8{,}25\ T^{0{,}967}$ that is much closer to the result $\nu_{NRT}(T) = 10\ E$ of the NRT-model. At E = 10 keV $\nu \approx 31$, 77 and 100 according to Refs [10], [11] and NRT-model, respectively. At elevated temperatures some part of "effective" dpa is additionally annihilated during the subsequent annealing stage (> 1 ns) of cascade development because of correlated recombination [12]. This stage lasts until all mobile defects (PD and their clusters) escape the cascade region. Just these free-migrating defects determine the microstructure evolution during irradiation at elevated temperatures. Correlated recombination can be evaluated using kinetic Monte Carlo simulation. However the results could depend not only on material parameters (cascade arrangement, PD and their clusters diffusivities), but also on temperature, cascade producing rate, material pretreatment, microstructure development.

In difference with T_d and $\nu(T)$ the values of $\varphi(E)$ and $\frac{d\sigma\ (E,T)}{dT}$ are known now with much more accuracy. Changing the order of integration in the equations for the dose rate, one can find:

$$K = \int_{T_d}^{T_{\max}} dT \cdot \ \nu(T) \cdot \int_{E_{\min}}^{E_{\max}} \varphi(E)\ \cdot \frac{d\sigma\ (E,T)}{dT}\ \ dE \qquad (3)$$

The integral over E is the spectrum of recoil energies transferred to lattice atoms (if $T > T_d$, then it is the spectrum of primary knocked atoms, PKA spectrum). Substitution of $\nu_{NRT}(T)$ or $\nu_{MD}(T)$ in (3) allows to calculate NRT dpa or "effective" dpa respectively.

Neutron fluxes with various lower energy boundary and primary damage characteristics: NRT-dpa, "effective" dpa, recoil- and PKA-spectra were calculated in different locations of the cores and internals of WWER-440, WWER-1000, BN-600 and BR-10. Recoil spectra were calculated using the SPECTER code [13] with T_d = 40 eV in α-Fe, Zr and Ti and T_d = 90 eV in W. Cascade efficiencies for these metals were taken from [9]. Calculated mean PKA energies (T_m) in Fe in the center of cores are as follows: BN-600 (T_m = 7.2 keV), WWER-440 (T_m = 15.6 keV), WWER-1000 (T_m = 15.9 keV) and BR-10 (T_m = 17.2 keV). Contrary to expectations, the mean PKA energy in the core center of the thermal reactors is twice of that in the power fast reactor BN-600. However it is even greater in the test fast reactor BR-10. Because of the reasonably high mean PKA energy in Fe the "effective" dpa rates comprise about 1/3 of NRT–dpa ones in these locations of the reactors considered. However this energy is decreased significantly with increasing the distance from the core center, so an above simple proportionality cannot fulfil in distant locations of the reactors. This conclusion holds to a greater extent for other metals considered, where mean PKA energy is less than in Fe.

IPPE activities in the fields related to the TM subject

Calculation of neutron fluxes and primary damage characteristics in metals and structural materials under irradiation in different locations of Russian reactors.

WWER-440,-1000; BN-600, -800, -1200, BREST; BR-10, BOR-60, MBIR are under consideration.

Calculation of primary damage characteristics in metals and alloys along projected range under ion irradiation.

Irradiation with heavy metal ions leads to spatially high non-uniform radiation damage in materials. Comparison of NRT–dpa and "effective" dpa rates, calculation of PKA-spectra along the projected range under ion irradiation are important.

Irradiation with 7 MeV Ni^{++} ions (accelerator EGP-15, IPPE) and with 1.8 MeV Cr^{+3} ions (accelerator ESUVI, KIPT) are under consideration.

Molecular dynamics (MD) simulations to compute diffusional and energetic characteristics of elements, PD and their clusters in alloys.

Diffusivities of elements, PD and their clusters in metals and alloys obtained on the base of MD simulations [14] are the input parameters for kinetic Monte Carlo simulation of correlated recombination during cascade relaxation and for modeling of radiation-induced segregation in alloys under neutron and ion irradiation.

Fe, Cr, Fe-Cr, Fe-C(N), Fe-Cr-W are under consideration.

Modeling of radiation-induced segregation (RIS) in alloys under neutron and ion irradiation.

RIS during spatially uniform (in reactors) irradiation leads to significant changes in alloy composition near main microstructural features acting as point defect sinks, namely grain boundaries, free surfaces, dislocations, precipitates and voids (see e.g. [15-18]). If there is a pronounced dependence of displacement and gas production cross sections on the alloy content than the difference for displacement and gas production rates in the matrix and near PD sinks can be calculated.

Cascade efficiency and "effective" dpa rate in near surface region of alloys under ion irradiation depends on ion energy. Modeling of RIS in this region and comparison with experimental data could give some estimates on cascade efficiency in alloys.

Gas production: estimation of (n,α) reaction cross section for chromium isotopes.

The (n,α) reaction cross section of chromium isotopes is of considerable importance in radiation resistance of structural materials. In EXFOR there is only limited number of experimental data for this reaction and mainly they relate to 14 MeV. The experimental data for (n,α) reaction probability in fission neutron energy range are almost absent. In this work results for $^{50}Cr(n,\alpha)$ and $^{52}Cr(n,\alpha)$ reaction excitation function investigations are presented [19]. It is shown that ENDF/B-VII library for $^{50}Cr(n,\alpha)$ reaction holds estimations, which are more than 20 times higher than the results of our measurement. Furthermore, we observe irregularity in energy dependence of $^{50}Cr(n,\alpha)$ cross section which is not predicted by any library. The experimental data for $^{52}Cr(n,\alpha)$ reaction in reactor neutron energy region are obtained for the first time. Other chromium isotopes could be under consideration.

References

1. G.S. Was, Fundamentals of Radiation Materials Science: Metals and Alloys, Springer-Verlag, New York, 2007.
2. ASTM E521 ASTM International, West Conshohocken, PA, 1996.
3. Norgett M.J., Robinson M.T., Torrens I.M. A Proposed Method of Calculating Displacement Dose Rates. - Nuclear Engineering and Design, 1975, 33, pp. 50-54.
4. J. Lindhard, V. Nielson, M. Scharff and P. V. Thomsen, Kgl. Dan. Vidensk. Selsk. Mat.-Fys. Meld. 33 (1963) 1-42.
5. Stoller R.E. Point defect survival and clustering fractions obtained from molecular dynamics simulations of high energy cascades. - Journal of Nuclear Materials, 1996, 233-237, pp.999-1003.
6. Stoller R.E., Odette G.R., Wirth B.D. Primary damage formation in bcc iron. - Journal of Nuclear Materials, 1997, v. 251, pp.49-60.
7. Stoller R.E., Greenwood L.R. An Evaluation of Neutron Energy Spectrum Effects in Iron Based on Molecular Dynamics Displacement Cascade Simulations. - Effects of Radiation on Materials:

19th International Symposium, ASTM STP-1366, American Society for Testing and Materials, West Conshohocken, PA, 2000, pp. 548-559.
8. R.E. Stoller, Primary Radiation Damage Formation, in Comprehensive Nuclear Materials, R. J. M. Konings, T. R. Allen, R. E. Stoller, and S. Yamanaka, Editors, Elsevier Ltd., Amsterdam, 2012, pp. 293-332.
9. Broeders C.H.M., Konobeev A.Yu. Defect production efficiency in metals under neutron irradiation. - Journal of Nuclear Materials, v. 328, 2004, pp. 197 – 214.
10. Stoller R.E., Simulation of primary damage formation in irradiated materials, Fusion Materials. Semiannual Progress Report for Period Ending June 30, 2000, DOE/ER – 0313/28, pp. 227-236.
11. Doan N.V., Interstitial cluster motion in displacement cascades, Journal of Nuclear Materials, 283 – 287 (2000) 763 – 767.
12. S. Zinkle, B. Singh, Analysis of displacement damage and defect production under cascade damage conditions, Journal of Nuclear Materials, 1993, vol. 199, no. 3, pp. 173-191.
13. Greenwood L.R., Smither R.K. SPECTER: Neutron damage calculations for materials irradiations - ANL/FPP-TM-197 (1985).
14. V.A. Pechenkin, V.L. Molodtsov, V.A. Ryabov, D. Terentyev, On the radiation - induced segregation: contribution of interstitial mechanism in Fe-Cr alloys, accepted for publication in Journal of Nuclear Materials.
15. Pechenkin V.A., Stepanov I.A. Modeling the radiation-induced segregation of undersized solutes near grain boundaries // Mater. Science Forum, 1999, v.294-296, p.771-774.
16. Pechenkin V.A. Stepanov I.A., and Konobeev Yu.V. Modeling of phosphorus accumulation on grain boundaries in iron alloys under irradiation // Effects of Radiation on Materials: 20th Int. Symp., ASTM STP 1405, 2001, p. 174-187.
17. Stepanov I.A., Pechenkin V.A., and Konobeev Yu.V. The modeling of radiation-induced phosphorus segregation at point defect sinks in dilute Fe-P alloys // Effects of Radiation on Materials: 21st Int. Symp., ASTM STP 1447, 2004, pp. 579-589.
18. Stepanov I.A., Pechenkin V.A., Konobeev Yu.V. Modeling of radiation-induced segregation at grain boundaries in Fe-Cr-Ni alloys // J. Nucl. Mater., 2004, Vol. 329–333, pp. 1214-1218.
19. Khryachkov V.A., Bondarenko I.P., Ivanova T.A., Kuzminov B.D., Semenova N.N., Sergachev A.I. Investigation of $^{50}Cr(n,\alpha)^{47}Ti$ reaction cross section for neutron energy less than 7.2 MeV, Proc. of XIX Int. Seminar on Interaction of Neutrons with Nuclei, ISINN-19, Dubna 2011, pp. 163-166.

Primary displacement damage calculation induced by neutron and ion using binary collision approximation techniques (MARLOWE code)

F. Mota, C. J. Ortiz, R. Vila

Laboratorio Nacional de Fusión – CIEMAT, Madrid
Spain

1. Introduction

The level of damage expected in future fusion reactors conditions is such that the performance of materials and components under these extreme irradiation conditions is still unknown. Considering this scenario, the study of the effects of energetic neutrons generated in fusion reactors on materials is one of the most important research topics to be carried out during next years.

The effects of neutron irradiation on materials involve, from a fundamental point of view, two physical phenomena: i) the displacement of atoms from their equilibrium positions in the lattice, which creates point defects, and ii) the generation of nuclear transmutation reactions that contribute to the formation of impurities inside the material, with He and H as the most important ones. The ratio between the levels of He and H, and the amount of point defects is one of the main parameters to understand the effect of the radiation on materials

In order to emulate the neutron irradiation that would prevail under fusion conditions, two approaches are contemplated:

a) on one hand different kinds of current neutron sources to emulate the fusion irradiation environment are available, as for example
   - Fission power reactor
   - Spallation sources
   - Striping Sources: The objective of t*he International Fusion Materials Irradiation Facility (IFMIF*) [1] will be to provide an intense neutron source with adequate energy spectrum to test the suitability of candidate materials for future nuclear fusion power reactor (DEMO). IFMIF will constitute an essential tool in the international strategy towards the achievement of future fusion reactors.

b) on the other hand, as these neutron sources have a number of problems and very strict operating conditions, (e.g. the radiological risks), to emulate the effects of fusion neutron on materials, some other facilities can be used. One example is the Spanish initiative TechnoFusión facility [2] which purpose is to serve as technological support for IFMIF and DEMO. The Material Irradiation Experimental Area of TechnoFusion will emulate the extreme irradiation fusion conditions in materials by means of three ion accelerators: one used for self-implanting heavy ions (Fe, Si, C,…) to emulate the displacement damage induced by fusion neutrons and the other two for light ions (H and He) to emulate the transmutation induced by fusion neutrons. This Laboratory will play an essential role in the selection of functional materials for DEMO reactor since it will allow reproducing the effects of neutron radiation on fusion materials. Ion irradiation produces little or no residual radioactivity, allowing handling of samples without the need for special precautions.

Currently, two different methods are used to calculate the primary displacement damage by neutron irradiation or by ion irradiation. On one hand, the displacement damage doses induced by neutrons are calculated considering the NRT model [3] based on the electronic screening theory of Linhard. This methodology is commonly used since 1975. On the other hand, for experimental research community the SRIM code is commonly used to calculate the primary displacement damage dose induced by ion irradiation. Therefore, both methodologies of primary displacement damage calculation have nothing in common. However, if we want to design ion irradiation experiments capable to emulate the neutron fusion effect in materials, it is necessary to develop comparable methodologies of damage calculation for both kinds of radiation. It would allow us to define better the ion irradiation parameters (Ion, current, Ion energy, dose, etc) required to emulate a specific neutron irradiation environment.

Therefore, our main objective was to find the way to calculate the primary displacement damage induced by neutron irradiation and by ion irradiation starting from the same point, that is, the PKA spectrum.

2. Methodology

Neutron irradiation induces elastic and inelastic nuclear reactions. The subsequent displacement of ions (Primary Knock-on Atoms [PKA] spectrum) is generated by both elastic and inelastic nuclear reactions, the elastic nuclear reactions contributing generally in more than 90% to the displacement damage [4]. This varies with the isotope analyzed. However, the PKA spectrum itself (displacements atomic induced by neutron irradiations) mainly induces elastic atomic reactions producing displacement damage. The combination of the neutron irradiation and PKA spectra (induced by neutrons) will produce different types of defects; on one side Interstitials, Vacancies and Clusters thereof can be produced by elastic and inelastic reactions whereas impurities - such as He, H, T-are only produced in materials by inelastic reactions, i.e. transmutation reactions. Hence, it is very important to predict/simulate the defects created by neutron and PKA spectrum induced by neutron, and the long-term evolution of defects and impurities. Therefore, the calculation of damage generated by fusion neutrons requires a dedicated methodology which can combine the effects of fusion neutron and ion irradiations (PKA spectrum induced by neutron).

The methodology used in this work to calculate the damage generated in materials due to the combined effects of fusion neutron irradiation and the damage generated by ion displaced by neutron irradiation was developed in previous works [5,6] by the authors, and it is based on a methodology previously developed by Vladimirov et al. [7,8]. This methodology allows us to calculate several damage parameters (PKA spectrum, database of displacement cascades, damage profile, damage function, and damage dose (dpa-new concepts)) for the materials analysed.

This methodology consists on a combination of Nuclear Data Libraries Processing, Neutronic transport and Monte Carlo Binary Collision codes. First, the neutron spectrum for the desired area is obtained using the neutron transport codes (MCNP5 code). This neutron spectrum and the nuclear data libraries (FENDL 3.0) are used as input for the Nuclear Data Libraries Processing code NJOY [9] to obtain the PKA spectrum. The recoil matrices are obtained using the module GROUPR of NJOY code. The Nuclear Data libraries used to obtain the recoils matrices are FENDL-3/SLIB release 2. Then, the recoil matrices are weighted by neutron spectra to get an averaged PKA energy spectrum for each facility and irradiation spot under consideration. The PKA differential cross sections weighted with neutron spectrum defines the Kinetic energy distribution of the PKAs induced by a specific neutron spectrum, that is, the PKA spectrum describes how the damage is actually produced during irradiation, since it defines the probabilities to generate each PKA with a specific kinetic energy.

In the case of ion irradiation PKA spectrum was calculated using Marlowe code. The PKA spectrum is obtained for both codes with a specific subroutine developed by us. But, currently we have developed a subroutine to be able to calculate either the PKA spectrum in the total implantation profile as the PKA spectrum on different depth bins.

Afterwards, to evaluate the fraction of Frenkel pairs generated by PKA with energy T, $N_d(T)$, Marlowe code is used. Marlowe is a displacement damage simulations code based on the Binary Collision Approximation (BCA) [10,11].

In order to quantify the energy lost to electronic excitation in the low energy range, several models are available. In the Lindhard, Scharff and Schiøtt (LSS) theory [12], the electronic system of the material is regarded as a continuum and has the consequence that the energy loss cross-section is proportional to the ion velocity, just as depicted by the Ohm's law.

In addition, the binding energies used to calculate the displacement of atoms is obtained from first-principles calculations or molecular dynamics calculations depend on the material assessed.

This model proved to work remarkably well in a broad range of conditions and may expectedly apply in conditions where electron localization effects on ion trajectories are small. They are not when the ion velocity is comparable or higher than the Bohr velocity, which is typically the case for ion energies above 25 keV per amu. With further increasing velocities, the transition from the Lindhard to the Bethe regime governed by Rutherford scattering is met. The physical understanding of this transition gave rise to an extensive literature that is rationalized in [13]. The whole range of velocities and masses is captured in a semi-empirical way by J. Ziegler [14], which we implemented as a specific module in the Marlowe code. To do so, the so-called heavy ion scaling rule can be used to calculate the stopping power of atoms with energies above 25 keV per amu [15]. However, a more computationally efficient way was found and that consists in using directly the stopping power data found in the SRIM code, where the typical stopping powers in nuclear materials (Fe, W, …) are available. Therefore, MARLOWE now allows to simulate the stopping of ions in materials with energies of MeV (or even GeV), such as those formed by collision with energetic fusion neutrons or transmutation reactions.

One of the advantages of MARLOWE is that it allows simulating displacement of atoms in materials much faster than Molecular Dynamics (due to BCA) and exploring much higher energies (MeV-GeV). In particular, it allows defining the lattice structure of the materials and thus allows simulating displacements in monocrystal, polycrystal and amorphous materials, in contrast to SRIM. Therefore, it is possible to take into accounts effects such as channelling, replacements, linear collision sequence, etc. The binding energies of atoms to their lattice sites used to calculate the displacement of atoms are obtained either from first-principles calculations or from molecular dynamics calculations. In order to take into account the recombination of defects that takes place during thermal spike (like MD) an

effective capture radius I-V is assumed. Simply, when two defects are within a distance smaller than the capture radius, it is assumed that these defects would recombine during the cooling phase during the cascade, and are thus eliminated. This capture radius is adjusted on MD results.

In addition, a subroutine to be able to calculate either the PKA spectrum in the total implantation profile as the PKA spectrum on different depth bins was developed by us.

After the number of defects corresponding to a given PKA spectrum are calculated, the PKA spectrum is weighted with the damage profile, that is, the Number of Frenkel pairs versus PKA energy to obtain the damage function and the damage dose.

The damage function (W(T)) is calculated using the following equation:

$$W(T) = \frac{1}{D/t}\int^{T} \sigma_{PKA}(T')N_d(T')dT' \qquad (1)$$

where σ_{PKA} (T) is the PKA spectrum, N_d(T) is the number of Frenkel pairs by PKA of energy T, and D/t is the rate of damage created by the atomic displacement.

It is well known that different primary recoil energy spectra can produce completely different damage morphologies. Hence, the damage function converts the PKA spectra to the total damage in the materials and therefore W(T) indicates the cumulative damage production by all PKAs up to the energy T. It gives us information of how the damage is produced and of the average PKA kinetic energy generating the damage. It is a very useful function as it allows us to compare different neutron sources in a simple manner. This is because it is an integrated function which is normalised to the maximum value of each damage function.

In addition, the damage dose, which is, the concentration of vacancies as a function of neutron dose, [dpa values] is calculated using equation 2:

$$dpa = t\phi_{Total}\int_{T_O}^{T_{MAX}} \sigma_{PKA}(T)N_d(T)dT \qquad (2)$$

where Φ_{Total} is the total neutron fluence rate and *t* is the exposition time.

3. Conclusion

A methodology was developed to calculate the damage due to fusion neutrons in Materials (monocrystal, polycrystal and amorphous systems). This methodology is based on the methodology developed by KIT laboratory. It consists of a combination of Nuclear Data Libraries Processing, Neutron Transport and Monte Carlo Binary Collision codes.

This methodology allows to design irradiation experiments with ions to emulate neutron fusion effects in materials. It is possible because the displacements damage generation have been calculated using the same methodology for both neutron and ion irradiations (starting from PKA spectra).

The resulting damage profile used to calculate damage function and damage dose was calculated using MARLOWE code.

- A dedicated module developed at CIEMAT was used to account for energy loss of Ions in materials at energies in the Bethe regime (>> 25 keV / amu).
- Allows defining the lattice structure and accounts for effects such as channelling, replacements, linear collision sequence, recombination of I-V, etc….
- In order to take into account the recombination of defects, the capture radius is generally adjusted on experiments or MD calculations.
- A subroutine to be able to calculate either the PKA spectrum in the total implantation profile as the PKA spectrum on different depth bins was developed.

Mainly, a methodology to develop displacement damage data libraries using the MARLOWE code is proposed in order to standardize the calculation of primary displacement damage on compound materials.

4. Related Publications

- M. Hou, C.J. Ortiz, C.S. Becquart, C. Domain, U. Sarkar and A. Debacker, "Microstructure evolution of irradiated tungsten: Crystal effects in He and H implantation as modelled in the Binary Collision Approximation" Journal of Nuclear Materials, Volume 403, Issues 1-3, August 2010, pages 89-100
- F.Mota, R. Vila, C. Ortiz, A. Garcia, N. Casal, A. Ibarra, D. Rapisarda. V. Queral, "Analysis of displacement damage in materials in nuclear fusion facilities (DEMO, IFMIF and, Technofusion)" Fusion Engineering and Design 86 (2011) 2425 - 2428
- F. Mota, C. J. Ortiz, R. Vila, N. Casal, A. García, A. Ibarra, "Calculation of damage function of Al2O3 in irradiation facilities for fusion reactor applications", to be published in Journal of Nuclear Materials, (ICFRM-15 - 2011)

References

1. Comprehensive Design Report, an Activity of the International Energy Agency (IEA) Implementing Agreement for a Program of Research and Development on Fusion Materials, January 2004
2. A. Ibarra, M. Perlado et al., "TechnoFusión, National Centre for Fusion Technologies", Scientific-Technical Report, September 2009, ISBN:978-84-7834-628-8
3. M.T. Robinson, Journal of Nuclear Material 216 (1994) 1
4. S.P. Simakov, A.Yu. Konobeyev, U.Fischer, V. Heinzel, "Comparative study of survived displacement damage defects in iron irradiated in IFMIF and fusion power reactor", Journal of Nuclear Materials 386-388 (2009) 52-55
5. F. Mota, R. Vila, C. Ortiz, A. Garcia, N. Casal, A. Ibarra, D. Rapisarda. V. Queral, "Analysis of displacement damage in materials in nuclear fusion facilities (DEMO, IFMIF and Technofusion)", Fusion Engineering and Design 86 (2011) 2425 - 2428
6. F. Mota, C.J. Ortiz, R. Vila, N. Casal, A. García, A. Ibarra, "Calculation of damage function of Al2O3 in irradiation facilities for fusion reactor applications", to be published in Journal of Nuclear Materials (Proc. of ICFRM-15, 2011)
7. P.V. Vladimirov, Yu.D. Lizunov, A.I. Ryazanov, "Damage calculations in compound materials under neutron and ion irradiation", Rad. Eff. 139 (1996) 109-123
8. P.V. Vladimirov, S. Bouffard, "Displacement damage and transmutations in metals under neutron and proton irradiation", C.R. Physique 9 (2008) 303-322
9. R.E. MacFarlane, NJOY 99 Nuclear Data Processing system. http://t2.lanl.gov/codes/NJOY99/index.html
10. M.T. Robinson, Phys. Rev. B 40 (1989) 10717–10726
11. M.T. Robinson, Rad. Eff. Def. 130-131 (1994) 3-20
12. J. Lindhard, M. Scharff, H.E. Schiøtt; Mat. Fys. Medd. Dan. Vid. Selk. **33**, 14 (1963) 1
13. P. Sigmund, "Particle Penetration and Radiation Effects", Springer-Verlag Berlin, Heidelberg, 2006, ISBN3-540-31713-9
14. J.F. Ziegler, J.P. Biersack, and U. Littmark, *Stopping Powers and Ranges of Ions in Matter* (Pergamon, New York 1985)
15. M. Hou, C.J. Ortiz, C.S. Becquart, C. Domain, U. Sarkar and A. Debacker, Journal of Nuclear Materials, 403 (2010) 89-100

Development of theoretical modeling of point radiation defects, cascades and sub-cascades formation in diatomic materials (Al_2O_3) irradiated by fast charged particles on accelerators and fast neutrons in atomic reactors.

Alexander I. Ryazanov

Institute of General and Nuclear Physics, National Research Centre "Kurchatov Institute"
123182, Moscow, Kurchatov Sq. 1
Russia

Objective

The main aim of this presentation is a description of modern theoretical models and obtained numerical results for radiation damage production inculing point defects, cascade and sub-cascade formations in different monoatomic materials irradiated by fast ions and fast neutrons taking into account elastic and inelastic processes. The special topic of this presentation is oriented on the theoretical modeling and numerical calculations of radiation damage formation (point defects, cascades and subcascades) in diatomic materials (Al_2O_3) irradiated by fast charged paricles on accelarators and fast neutrons in atomic reactors using exested nuclear data base.

Neutron damage calculation

To calculate the accumulation of primary radiation damage in sapphire NRT model modification for diatomic materials is used. This model is based on the concepts of cascade function (the total number of defects formed by the primary knock-on atom (PKA) with energy E) and cross section of neutron scattering by atomic lattice of the material. A simple expression for the cascade function was obtained by Kinchin and Pease [1] using two-particle approximation for interactions between atoms. Later this theory was developed by Norgett, Robinson and Torrens [2], where an analytical expression for the energy dissipated only in elastic collisions between the PKA and atoms of crystal lattice of the material instead of the kinetic energy E of the PKA was used. This approach is called NRT model. The obvious disadvantage of NRT model is the fact that it is not applicable or only partially applicable to materials composed of atoms of several types. for extension to polyatomic materials. An obvious method of applying NRT model to polyatomic materials is to use average atomic mass and atomic numbers to determine number of displaced atoms. This approach is generally reasonable in the case of close elements in the periodic table. Development of a model for investigation of primary radiation defects in diatomic and polyatomic systems was proposed by Parkin and Coulter [3] and later modified by Greenwood [4]. The study was based on the general equation of PKA's slowing-down in polyatomic materials taking into account electronic stopping power for PKA. Solution coupled integro-differential equations can be calculated numerically for the cascade function for each type of atoms. The Thomas-Fermi interatomic potential was used to determine the number of displacements for each pair of atoms. The main feature of this approach proposed by Lindhard in these works is the relationship between the impact parameter and the deflecting angle. He extended the momentum approximation relationship between these values for case of hard collisions with large deflecting angles. Thus, one can treat the differential cross section which, in fact, depends upon two values: the deflecting ion energy E and the transferred energy T. The electronic stopping power for multicomponent targets was calculated by applying Bragg's additivity rule to electronic stopping powers of individual types of atoms taking into account Lindhard and Bethe-Bloch theories.

The data on the scattering cross sections were obtained using nuclear database ENDF/B-VII (information on elastic and inelastic cross sections for neutron interactions with the atoms of aluminum and oxygen, as well as angular distributions of the particles) in sapphire (Al_2O_3). Threshold energy values for the formation of point defects in sapphire correspond to values of 18 eV for aluminum and 76 eV for oxygen. In addition, a number of calculations were made here to estimate the influence of temperature on the threshold energy of formation of point defects in sapphire, using the data obtained by Pells and Phillips in HVEM microscopy experiments [5,6]. The results for

temperature dependence of threshold energies for point defect production for Al and O atoms into Al_2O_3 [6] are presented in Fig. 1.

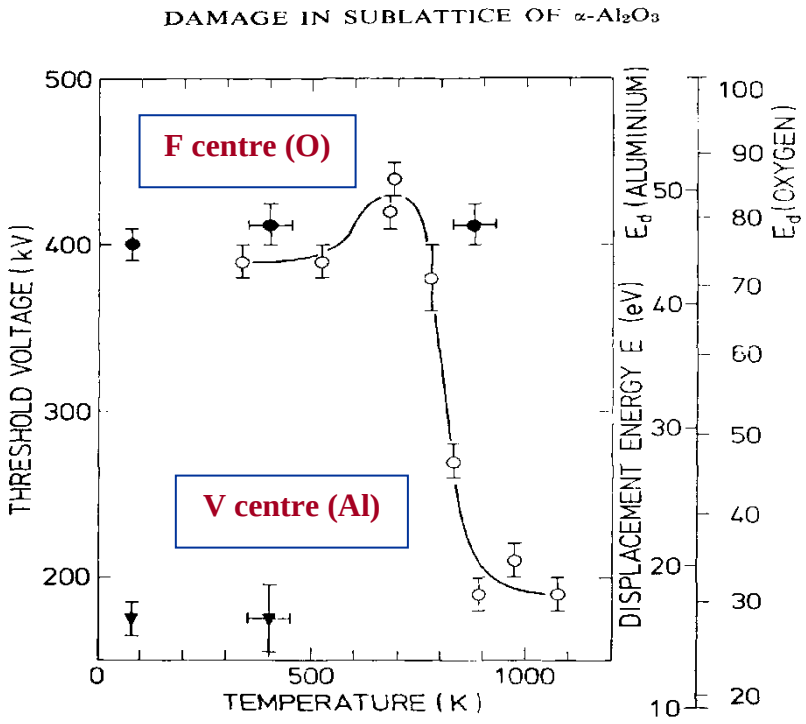

Fig. 1. Temperature dependence of threshold energies for point defect production for Al and O atoms into Al_2O_3.

Cascade functions are calculated for each type of atoms at different temperatures corresponding to T_1 = 500 K and T_2 = 1000 K based on the data [5,6]. On the basis of the cascade functions and cross-sections, the generation rates of primary radiation defect formation produced by neutrons in sapphire were calculated too.

Ion damage calculation

A set of equivalent dose accumulation in displacements per atom (dpa) in the sapphire irradiated with protons, α-particles and oxygen ions with energies from 5 MeV to 30 MeV, 60 MeV and 25 MeV respectively was calculated by simulation experiments. Calculations were made using the program SRIM-2010 [7], which is based on the Monte Carlo method to calculate the interaction of ions with different materials using the ZBL-potential for the elastic interactions and experimental data for inelastic electronic losses. As a result of SRIM calculations we obtain the densities as well as the total numbers of displaced atoms for each type of target atoms. The obtained distribution profiles for point defects due to displacements of O and Al atoms into Al_2O_3 under 5 MeV oxygen ion irradiation with the total ion fluence $\Phi = 10^{17}$ ion/cm^2 at two irradiation temperatures: T_1 = 500 K and T_2 = 1000 K are presented in Fig. 2. We can see, that the average dose of irradiation <D> (dpa level) after ballistic stage practically in two times higher <D> = 6.67 dpa at irradiation temperature T_2 = 1000 K comparing with irradiation tempewrature T_2 = 500 K where <D> = 3.75 dpa. For practical applications one should express these values in terms of relative damage of the particular target material sublattice for certain irradiation environments. In the case of one component targets this leads to the well known notion of the atomic damage in Displacements-Per-Atom (DPA) units. For multicomponent targets the extension of the DPA notion is not straight forward due to the fact that the relative damage rates are different for individual sublattices of the target. Although for some polyatomic materials relevant aspects of the irradiation damage like the PKA-energy dependence of the displacement efficiency [3]

have been already developed in detail, sublattice specific dpa-rates for relevant irradiation sources are practically not available. In principle, the displacement damage density of each component can be either normalized to the related atomic density of that constituent, or it can be normalized to the total density of the polyatomic target. In this particular case, the latter approach is used.

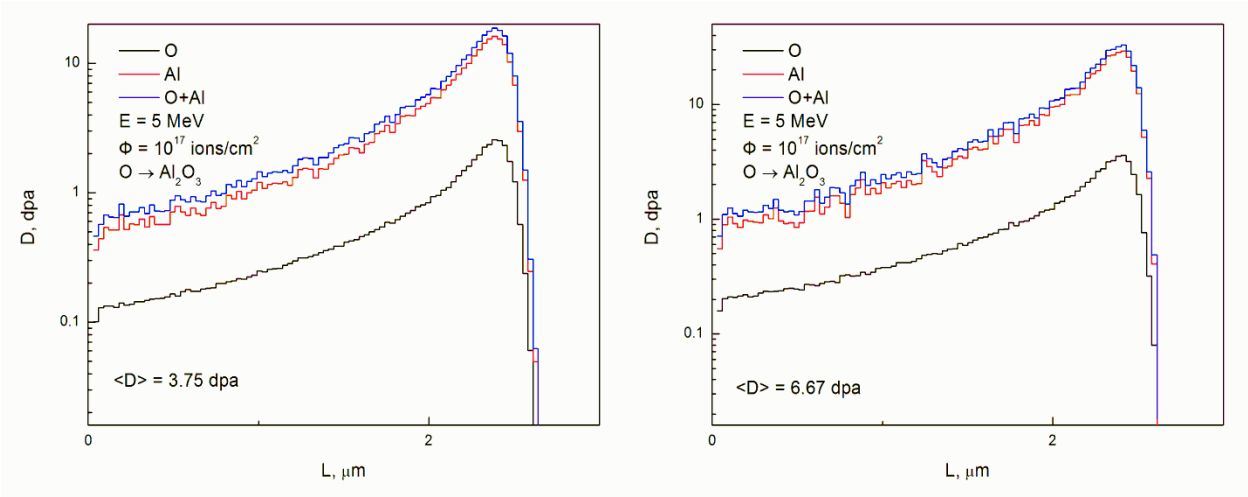

Fig. 2. Distribution profiles of point defects due to displacements of O and Al atoms into Al_2O_3 under 5 MeV oxygen ion irradiation at T_1 = 500 K (left) and at T_2 = 1000 K (right).

The obtained results for specific ions were compared with the data received using Boltzmann transport equation for ion stopping calculations. This method is equaly suitable for one- and multi- component targets, and is about hundred times faster than Monte-Carlo base methods. Most of the results presented here show the abilities of the developed method.

The problem of ion transport in matter is of great importance for solid state physics and for different new technological applications. Ion beams now are widely used for modification of different materials as well as for their scientific investigations. That is why the majority of questions, standing before ion transport theory can be formulated in terms of one dimensional or cylindrical beam geometry. First of all it is the problem of calculation of ions range and damage distributions. In whole ion transport theory can be divided into two parts. One of them treats the individual collisions of ions with target atoms. The other one studies the statistical properties of ion movement.

Consider system of Boltzmann transport equations in the simple case of one-component uniform target bombarded by ions of different mass and charge than that of the target. In this case the system consists of two equations. The equation for moving ions (the first component) does not depend upon the distribution function of moving atoms of the target (the second component). So, it can be solved separately. its solution determines the source of the second type particles for another equation. If one is interested in values connected with knock-off of atoms of the target he must solve the second equation. It looks like the first one differing from it by the term describing the knocking out atoms of the target. The situation is different in the case of two or multi-component targets. In this case the system consists of more than two equations. Now all the components with non-zero atomic concentration in the target enter the system symmetrically. Moreover, if the matter consists of the components with differing atomic masses the ranges of light components can be much greater than those of the heavy ones and can approach to the ranges of the bombarding ions. Thus, in this case one should solve all the equations with spatial derivatives.

Most of the features of this algorithm by the BOLT program were described in details earlier [8-11]. The code solves the time independent system of linear Boltzmann transport equations for slowing down ions and knocked-on atoms in one-dimensional plane geometry. We define the *X* axis directed perpendicular to the target surface along with the incident beam. The slowing down of particles is described in the program by two independent processes: (i) the continuous slowing down due to

interaction with the electron subsystem described by the electronic stopping power and (ii) the discrete binary elastic collisions with target atoms.

The system of equations is solved numerically by a multigroup method from high energies down for low energies. The main feature of this method that it treats all the types of moving atoms in the same manner. Bombarding ions are treated like target atoms but their concentration in the target is set to zero. Such approach allows to calculate the kinematics of collisions between atoms of different masses in an accurate manner. The code treats correctly different threshold energies for various components of the target. It makes the approach highly suitable for radiation damage calculations in multicomponent ceramics. The method correctly treats the boundary conditions on the surface of matter. It can be used for reflecting ratio calculations and recoil implantation calculations with minor improvements in surface model. The developed method is potentially suitable for ion stopping catculations in two- and three-dimentional geometry. Even in complicated cases it will be more efficient than Monte Carlo calculations. In the case of complicated geometry the time needed for ingroup transport calculations will increase strongly, but not the total running time.

Subcascade formation in monatomic irradiated materials

Irradiation of materials with high-energy particles causes atoms in a crystalline lattice to receive energy greater than some displacement threshold and thus to leave their equilibrium states. Later exchange of energy as a result of elastic collisions between primary knock-on atoms and atoms inside the crystalline lattice sites leads to formation of cascade of atomic collisions. For PKA having some threshold energy cascade is represented as a series of regions not overlapping among themselves, so called sub-cascades. During development of cascades and sub-cascades in solids point defects such as vacancies and interstitials are produced that define accumulation of radiation damage in the irradiated material. The number and structure of the cascades (size, number of subcascades, number of point defects created) depend on materials and PKA energy spectra, the latter being linked to neutron spectra. It is difficult to characterize experimentally the displacement cascades and subcascades because their lifetime is very short (some ps) and their size is very small (about 10 nm). Nevertheless, it is possible to get some information on their structure with numerical simulation tools such as the binary collision method of Monte-Carlo and the Molecular Dynamics method. Such tools allowed in particular to study the subcascades formation process. However, they require a large statistic (particularly for high PKA energy) to give precise data, which is time consuming. Another way to characterize cascades is to use a theoretical approach based on the numerical solution of the Boltzmann transport equation in a binary collision approximation. This approach was used to calculate the volumic distribution of subcascades by taking into account the neutron energy spectrum. In these calculations, the threshold energy for subcascades formation was chosen as a free parameter. This work can be performed by comparing the mean free path $\lambda(E)$ between two successive collisions of a PKA with target atoms (Secondary Knock-on Atoms: SKA) and the average size R of the damage zones resulting from the two collisions. Subcascades are formed when $\lambda(E) > R$. The theory of cascades and sub-cascades of atomic collisions in the irradiated materials was developed in [12].

The detail comparison of obtained numerical results for subcascade formation with experimental data is very difficult. Because our calculations describe only a collisional phase of atomic cascade (ballistic stage) and don't take into account cluster formation of point defects into cascades on quenching stage of cascade. The experimental observations of cascades [13] base on using TEM and observation of small visible clusters of point defects in materials after penetrating of cascades. For consideration of cluster formation of point defects into cascade we have to take into account the value of formed density of point defects (vacancies and interstitials) and diffusion migration of their into cascade. So our calculations show that the number of subcascades as a function of PKA energy decreases with increasing of atomic number, but defect densities (vacancies) has opposite dependence and increase with increasing of atomic number. The number of observed clusters will be depend not only on the number of subcascades on ballistic stage but also on the value of migration energy barrier of point defects and their diffusivity into cascade on quenching stage.

This approach allowed to determine the main characteristics of subcascades, such as: threshold energy for subcascades formation, generation rate of subcascades for a given neutron spectrum, average number of subcascades per PKA, average distance between subcascades, average subcascade size. The effect of two neutron spectra on some of these characteristics was also can be studied.

Subcascade formation in irradiated Al_2O_3

As the number of different types of atoms and PKA-SKA pairs in irradiated material increaces, the analysis of the problem in the framework of the Boltzmann transport equation does not lead to an analytical solution despite the simplicity of the geometric criterion for determining the formation of subcascades of atomic collisions. Simultaneously, the analysis of the problem using Monte Carlo method still requires significant computing power. Therefore, energy criterion was selected to simplify the task of collection of statistics as a criterion for the formation of subcascade on the basis of monatomic approximation. In this case, a value of PKA energy 1.4 keV the was chosen in our calculations as threshold energy for the formation of subcascades, which corresponds to those in pure aluminum (corresponding energy for oxygen - 0.4 keV). A set of statistics and numerical calculations for sapphire irradiated with different types of ions have been made and produced using the program SRIM-2010 [7], which is based on the Monte Carlo method for calculating the interaction of ions with different materials using ZBL-potential for the elastic interactions and experimental data for electronic inelastic losses. To evaluate the effectiveness of the energy criterion was conducted additional research. It was shown that the presence of PKA with energy more than 1.4 keV gives an indication of the separation cascade of atomic collisions on individual subcascades. On the basis of this criterion a set of important characteristics of subcascades in Al_2O_3 was obtained under fast ion irradiation, such as subcascade spectra for different types of atoms for both aluminum and oxygen knock-on atoms and distribution of subcascades along the penetration depth of diferent types of fast ions in target material.

Conclusion

The theoretical model and numerical calculations of the displacement cross sections and the generation rate of the primary radiation point defects in mono materials (C, Be, Al, Fe, V, W) and binary systems, such as sapphire (Al_2O_3), under the influence of irradiation by fast nions and fast neutrons (ITER, DEMO and IFMIF energy spectra) with energies up to 20 MeV based on ENDF/B-VII nuclear library with the elastic and inelastic scattering. Number of displaced atoms were calculated depending on the type of primary knocked-out atoms (PKA) as a function of their energy on the basis of double integral-differential equations. In addition, cascade function and the displacement rate of point defects were studied in Al_2O_3 for each type of atoms at different temperatures in the range of 500 K and 1000 K using the experimental data of Pells and Phillips.

A set of equivalent dose simulations was performed for sapphire at temperatures 500 and 1000 K under irradiation by protons with energies ranging from 5 to 30 MeV, by α - particles with energies ranging from 5 to 60 MeV and by oxygen ions with energies ranging from 5 to 25 MeV. Displacement damage calculations for Al_2O_3 was performed by the method based on the direct solution of Botzmann transport equation for knock on atoms. Obtained results were found to be similar betweet SRIM and proposed approach using the Botzmann transport equation. This method was applied to some neutron and high energy light ion sources which are available to qualify ceramics for fusion reactor applications. Direct comparison of neutron and ion irradiations within one and the same physical and numerical approach has been done.

The obtained results show that binary collision model allows to investigate the subcascades formation in the collision stage of cascade and gives reasonable results for the main important characteristics of subcascades as a function of PKA energy. Subcascade structure was analyzed on the basis of criterion for subcascascade formation for monatomic materials and SRIM-2010 program under different irradiation conditions. The sublattice specific displacement damage rates neither follow the stoichiometric ratios of polyatomic materials nor the ratio of the displacement threshold energies. In this case the ratios of the sublattice specific damage rates can slightly vary for different irradiation

environments. The analysis of the formation subcascade structure along the direction of ion propagation and the energy spectra of subcascades obtained for fast ions with the different energies.

The new aproaches and development of new theretical modeling should be done in the future investigations including improving of NRT standart model for mono materials (W, Fe) and polyatomic materials such as Al_2O_3 and SiC under irradiation of these materials by fast ions and neutrons taking into account elastic and inelasic processes based on existed nuclear data base including the comparison of obtained theoretical and numerical results with Molecular Dinamic, Monte Carlo methods and experimental data.

References

1. G.H. Kinchin and R.S. Pease, The Displacement of Atoms in Solids by Radiation, Reports on Progress in Physics, vol. 18, pp. 1-51, 1955.
2. M.T. Robinson, J. Nucl. Mater. 216 (1994) 1.
3. Parkin and Coulter, J. Nucl. Mater. 117 (1983) 340-344.
4. H.L. Heinisch, L.R. Greenwood, W.J. Weber, R.E. Williford, J. Nucl. Mater. 307–311 (2002) 895–899.
5. G.P. Pells, D.C. Phillips, J. Nucl. Mater. 80 (1979) 207.
6. G.P. Pells, A.Y. Stathopoulos, Radiat. Eff. 74 (1983) 181.
7. J. F. Ziegler, Nucl. Instr. Meth. B (2004) 219-220.
8. Yu.D.Lizunov, A.I. Ryazanov, Radiat.Eff., 60 (1982) 95.
9. Yu.D. Lizunov, A.I. Ryazanov, Rad. Eff. 107 (1989) 185-196.
10. Yu.D. Lizunov, A.I. Ryazanov, Preprint IAE-5298r11, 1991, Moscow.
11. P.V. Vladimirov, Yu.D. Lizunov, A.I. Ryazanov, A. Moslang, J. Nucl. Mater., 253(1998) 104-112.
12. A.I. Ryazanov and E.V. Semenov, J. Nucl. Mater., 417 No. 1–3 (2011)1074–1077.
13. M. Kiritani et al., Radiat. Eff. Defects Solids 113 (1990) 75–96.

The interest of dpa to handle the microstructure of irradiated materials

Laurence Luneville[1], David Simeone[2], Yves Serruys[4], S. Bouffard[5]

1) CEA/DEN/DANS/DM2S/SERMA/LLPR, Matériaux Fonctionnels pour l'Energie, Equipe Mixte CEA-CNRS-ECP, CE Saclay, Gif sur Yvette, 91191, France
2) CEA/DEN/DANS/DMN/SRMA/LA2M, Matériaux Fonctionnels pour l'Energie, Equipe Mixte CEA-CNRS-ECP, CE Saclay, Gif sur Yvette, 91191, France
3) CNRS, Matériaux Fonctionnels pour l'Energie, Equipe Mixte CEA-CNRS-ECP, SPMS, ECP, Chatenay-Malabry, 92292, France
4) CEA/DEN/DANS/DMN/SRMP, CE Saclay, Gif sur Yvette, 91191, France
5) ENSIOCAEN/CIMAp 7 boulevard du general Le Clerc, 14000 Caen, France

Abstract

Even if the Binary Collision Approximation does not take into account relaxation processes at the end of the displacement cascade, the amount of displaced atoms calculated within this framework can be used to compare damages induced by different facilities like pressurized water reactors (PWR), fast breeder reactors (FBR), high temperature reactors (HTR) and ion beam facilities on a defined material. In this paper, formalism is presented to evaluate the displacement cross-sections pointing out the effect of the anisotropy of nuclear reactions. From this formalism, the impact of fast neutrons (with an kinetic energy E_n superior to1 MeV) is accurately described. This point allows calculating accurately the displacement per atom rates as well as primary and weighted recoil spectra. Such spectra provide useful information to select masses and energies of ions to perform realistic experiments in ion beam facilities.

Introduction

Over more than 50 years, many experimental works were performed to study radiation damage in materials. Submitted to important neutron fluxes, materials in nuclear plants exhibit unusual micro structures and subsequent properties [1]. Many works in 1980s have clearly shown a large shift of the brittle ductile transition temperature in steel under irradiation [2]. Looking back into history, we find prominent names like Bohr, Fermi and Bethe associated with the early development of this field of research. Many works are devoted to capture key parameters responsible for the unexpected micro structures of solids observed under irradiation. Even if primary damage due to neutron - atoms interactions are produced at the atomic scale, the spatially inhomogeneous distribution of these primary defects, their diffusion and their agglomeration act over different length scales giving rise to complex micro structures. Many works were devoted to study the slowing down of ions in the matter [4-8]. However, few works in the material field were comparatively performed to quantify the primary damages induced by neutrons in solids [9,14,18,20]. This point explains why ion beam experiments then remain the most powerful tool to study the structural stability of solids under irradiation [4-8]. From this short introduction, a question naturally arises: can we select peculiar ions to simulate the micro structure induced by neutron irradiations occurring in nuclear plants?

The answer to such a question is quite complex. The neutron-atom cross sections are 8 orders of magnitude smaller than the ion-atom cross sections. This point implies that:

- the displacement per atom rate due to neutron fluxes is thus about 3 orders of magnitude smaller than the displacement per atom rate induced by ion beams. Neglecting the diffusion of point defects at low temperature, a correct scaling of the irradiation time in particle accelerators can easily overcome this effect in a first approximation. In practice, experimentalists increase the temperature during an irradiation by ions to erase possible overlapping between collisions cascades.
- the neutron mean free path between two collisions in the target (few centimeters) is larger than the ion mean free path (few nanometers). The localization of primary defects in the medium should then be drastically different. This remark can also be largely overcome. As the neutron ion mean free path is large, the characteristic length between two cascades in neutron irradiations is so large than displacement cascades (symbolized by large grey dots on figure 1) can be considered as independent events. They do not overlap each other over a few nanometers. In ion beam experiments, the penetration depth of incident particles with kinetic energy below a few MeV is about few nanometers. This analysis points out the fact that both irradiations generate the same localization of primary defects over few nanometers.

Figure 1 summarizes the characteristic lengths associated with the micro structural evolution of solids under ion and neutron irradiations.

As the ion-atom interatomic cross sections are much more important than the neutron atoms ones, penetration depths R(E) of ions is of the same order of magnitude as the displacement cascade L produced by neutrons [27]. This point ensures that ion beams can efficiency simulate the evolution of materials irradiated by nuclear plants.

As pointed out on Figure 1, all characteristic lengths depend only on the energy of incidents projectiles. It appears that criteria based only on the energy of recoils atom would thus give some clues to select the energies and masses of ions to simulation radiation damages dues occurring in materials in nuclear plants. In this work we describe in detail a new formalism to take into account different peculiar inelastic neutron atoms cross sections in the calculation of the displacement per atom rate and the primary and recoils spectra associated with a defined neutron irradiation. Thanks to this formalism, we exhibit some criteria to select the mass and the energy of incident ions able to reproduce in metals and ceramics the same microstructures as those created in nuclear facilities.

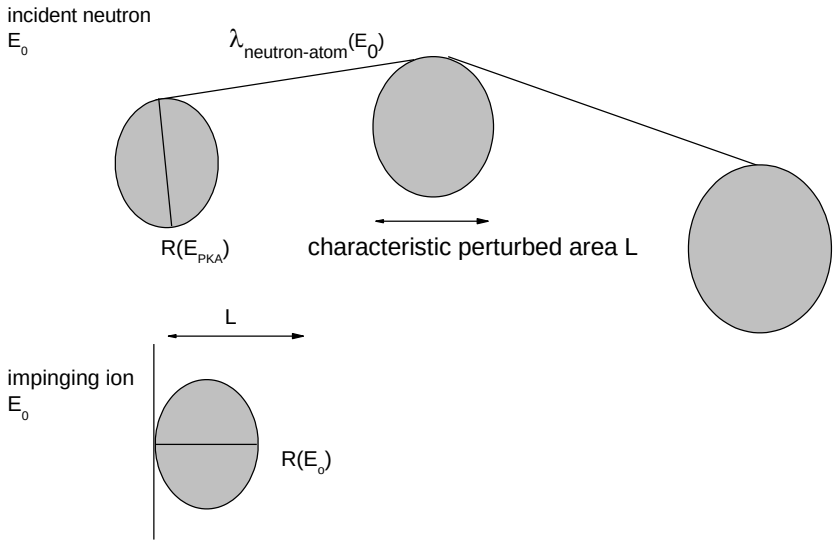

Fig. 1. This graph sketches the different length scales associated with the penetration of particles in a medium (top: penetration depth of a neutron in the medium, bottom: penetration depth of an ion in the medium).

Theory

When a material is bombarded by a neutron, atoms are displaced from their lattice sites with a large amount of energy [11,12] leading to the apparition of a displacement cascade and then to point defects and extended defects in well localized area. So, a precise description of neutron-atoms inelastic interactions is essential to calculate accurately the amount of energy transferred to primary knocked on atoms (PKA). The Isotropic Emission Compound Nucleus model (IECN) [13,14], was usually used to perform these calculations. Although for elastic scattering, the complete angular distribution is used, for inelastic processes, such as inelastic diffusion or emission of particles, the angular distributions of recoils is assumed isotropic in the center of mass system within this framework. However, recent nuclear evaluations (ENDFB6, JEFF3) [15,16] contain accurate angular distributions of recoils for all neutron-atom interactions. We present in this paper a new formalism to take into account this information. This formalism highlights the impact of this anisotropy on the recoil energy distribution [25,26].

An incident neutron of energy E generates recoil of energy T for a specific reaction (as for example inelastic scattering). Defining θ as the angle between the incident and the recoil particle, the corresponding differential cross section for this nuclear reaction is directly obtained from nuclear evaluations in the following way:

$$\sigma(\mu, E, E') = \sigma(E)\, f(\mu, E, E') / 2\pi \qquad \text{(Eq. 1)}$$

Where μ = cosθ ie the cosine of the angular defection in the center of mass frame, σ(E) is the neutron reaction cross section, E' the energy of the emitted particles and f(μ,E,E') is the angular emission probability density function. The differential PKA cross, χ(E,T), is then expressed as :

$$\chi(E,T) = \sigma(E)\int_0^{+\infty} dE' \frac{f(\mu, E, E')}{2\pi} \frac{1}{\left|\frac{\partial T}{\partial \mu}\right|}. \qquad \text{(Eq. 2)}$$

In the IECN model, f(μ,E,E') is independent of μ. In many inelastic nuclear reactions, this function is peaked and sharp. From Eq. 2, it appears clearly that the shape of f(μ,E,E') modifies drastically

χ(E,T). Figure 2 displays the evolution of χ(E,T) as a function of the recoil energy T for a given neutron energy E. The function χ(E,T) calculated within our formalism exhibits large discrepancy with χ(E,T) derived from the IECN model. This point highlights the effects on the anisotropy on the recoil energy distribution for high energy neutrons.

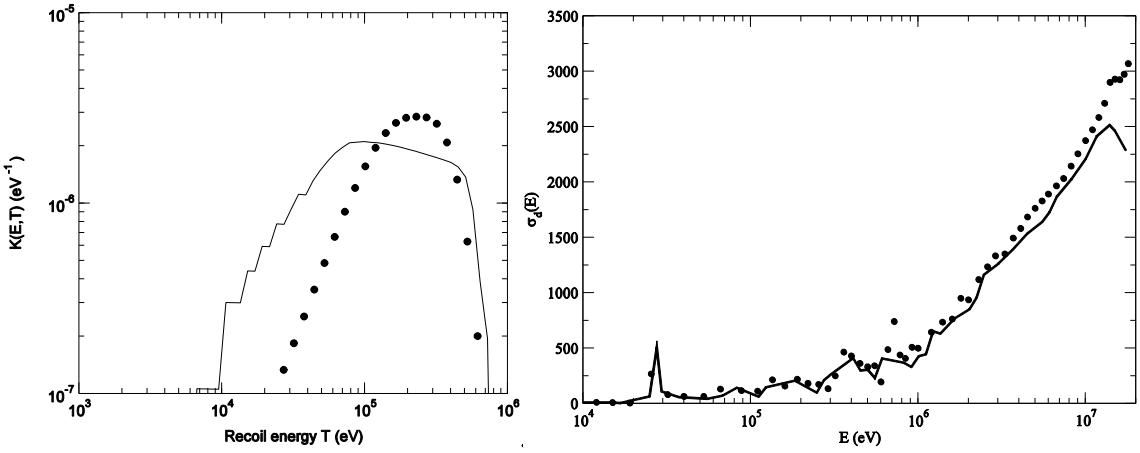

Fig. 2. Comparison between the PKA cross section and the displacement cross section as a function of the energy of recoils (left) and the energy of incident neutron (right) calculated for a Fe target irradiated under a 14 MeV neutron flux. The large discrepancy between χ(E,T) derived from our formalism (dots) and calculated within the IECN approximation (full line) appears clearly on figure 2 (left). This discrepancy of χ(E,T) leads to large variation of the displacement cross sections calculated according to our formalism (dots) and within the IECN approximation (full line). This discrepancy is equal to 20% in the high energy domain (above E_n > 1 MeV) where the neutron spectra exhibits large values in nuclear facility.

From the calculation of χ(E,T), it is possible to derived the displacement cross section $\sigma_d(E)$ according to:

$$\sigma_d(E) = \int_0^{T_{max}} \chi(E,T)\nu(T)dT \qquad \text{(Eq. 3)}$$

Where T_{max} is the maximum energy transferred to the recoil atom and ν(T) is the mean number of displaced atoms calculated within the BCA[17,18,19]. From this equation, it appears clearly that our formalism describes accurately the high energy part of $\sigma_d(E)$ associated with inelastic neutron-atom collisions. The displacement per atom rate P is obtained summing the displacement cross section weighted by the neutron spectrum over the neutron energy:

$$P = \int \sigma_d(E)\phi(E)dE \qquad \text{(Eq. 4)}$$

Where $\sigma_d(E)$ is the displacement cross section and φ(E) is the neutron spectrum (n cm^{-2} s^{-1} eV^{-1}). As $\sigma_d(E)$ is an increasing function and the neutron spectrum exhibits a sharp shape around few MeV, $\sigma_d(E)$ for E_n > 1 MeV gives the main contribution to the displacement per atom rate [3]. This point highlights the need of an accurate description for inelastic neutron collisions taking into account the anisotropy of these reactions.

To compare different irradiations performed in ion beam facilities with irradiation in nuclear plants, the primary and recoil spectra were calculated. A program called DART has been achieved to provide accurate displacement cross sections, displacement per atom rates as well as different spectra for a polyatomic solid irradiated by neutrons, ions or electrons.

Discussion

The renewed interest in nuclear energy production is bringing about a renaissance in materials sciences. In order to test new concepts, the structural stability of SiC and Oxides Dispersed Strengthens (ODS) steels need to be studied in great detail. From the knowledge of neutron spectrum of generation IV plants, displacement cross sections and different spectra can be calculated from DART. To simulate the structural stability of ODS under irradiation, the masses of energy of particles (ions or electrons) must be chosen to give similar spectra. Figure 3 displays the evolution of primary and recoil spectra induced by a neutron flux extracted from a FBR reactor, an ion beam facility and an electron flux. Whereas only an irradiation performed with 1.2 MeV Kr ions seems to give the same primary spectrum than a High Temperature Reactor, only an irradiation performed with 600 keV Ar ions gives the same recoil spectrum than an irradiation performed in an HTR plant as clearly pointed out on Figure 3.

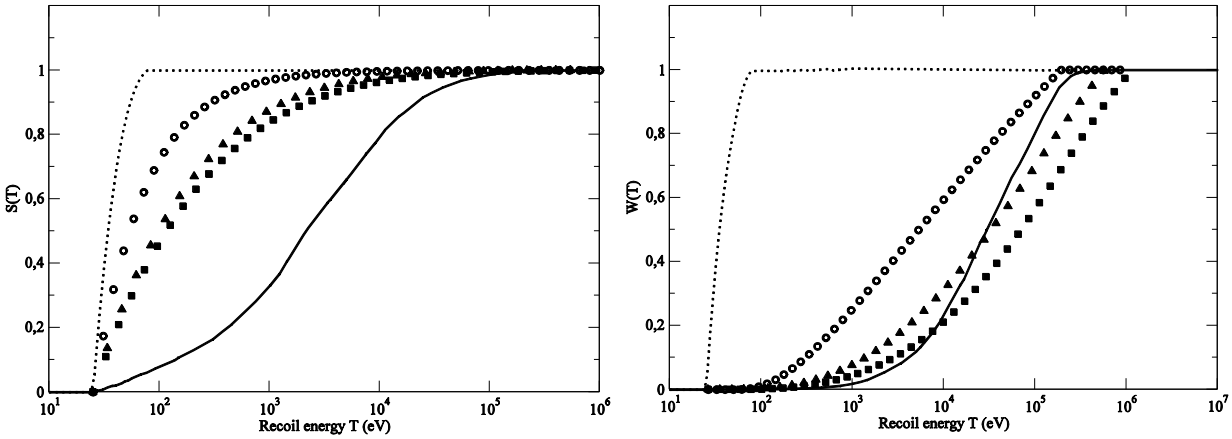

Fig. 3. Evolution of the primary and recoil spectra in ODS steel as a function of the recoil energy for different projectiles: 1 MeV electrons (dots), 1.2 MeV Krypton ions (square), 1 MeV Helium ions (circles), 600 keV Argon ions (triangles) and Phenix neutron flux (solid line).

Transition Electron Microscopy observations performed on ODS steels irradiated at 30 dpa under a FBR neutron flux, and 1.2 MeV Kr and 600 KeV Ar irradiations clearly assesses that only similar recoil spectra give the same microstructure in this kind of material [22,23].

Conclusion

Many works were devoted to study the slowing down of ions in matter to simulate radiation damage produced in nuclear plants. Few works described in details the energy transfer from neutrons to atoms during neutrons atom collisions. The IECN model is usually used to quantify the impact of neutron atom collisions. However, the anisotropy of inelastic neutron atom collisions, preponderant in a nuclear plant, are not accurately described in this model. In this paper, we present a formalism to overcome this point. We developed a program (DART) to calculate the displacement per atom rate as well as primary and recoil spectra induced by high energy neutrons in a polyatomic target. This paper highlights the fact that this anisotropy is responsible for a large increase of the displacement cross section and a drastic modification of primary and recoil spectra. The calculation of accurate primary and recoil spectra allows to select the mass and the energy of ion able to simulate radiation damage induced by neutrons in an ODS steel. The analysis of this spectra reveals that 600 keV Ar ions are able to similar evolution of the microstructure in this complex materials than neutron irradiations in FBR. TEM observations of the irradiated microstructures assess this point.

This work points out that tools are now available to select ions produced in ion beam facility to simulation radiation damage of solids occurring in nuclear plants. Taking into account the peculiar feature of neutron atom inelastic collisions, the comparison of recoil spectra gives clues to choose the mass and the energy of impinging ions in a realistic way.

References

1. G. Martin, P. Bellon, *Solid State Phys*. **50**, 189 (1997).
2. E. Balanzat, S. Bouffard, *Materials under Irradiation*, Trans Tech. Publication (1993).
3. R. Averback, T. Diaz de la Rubbia, *Solid State Phys.* **50**, 189 (1997).
4. C. Abromeit, J. *of Nucl. Mat.* **216**, 78 (1994).
5. M. Bleiberg and J. Bennet, Int. Conf. on *Radiation Effects In Breeder Reactor Structural Materials*, ASTM Scottsdale (1977).
6. H. Brager and J. Perrin, Int. Conf. on *Effects of Radiation on Materials*, ASTM Scottsdale (1982).
7. F. Garner, N. Packan and A. Kumar, Int. Conf. on *Radiation Induced Changes in Microstructure*, ASTM Seattle (1986).
8. *see for a comprehensive review of the problem, fundamental of radiation damage, I. Robertson, R. Averback, D. Tapin, L. Rehn J of Nucl Mat.* **216,** (1994).
9. R. Averback, J. of Nucl. Mat. **33**, 108 (1971).
10. J. Ziegler, J. Biersack, U. Littmark, *The Stopping Power and Range of Ions in Solids*, Pergamon press (1985).
11. W. Meyerhoff, *Elements of Nuclear Physics*, Dunod (1970).
12. K. Kikuchi, M. Kawai, *Nuclear Matter and Nuclear Reactions*, North Holland (1968).
13. L. Greenwood, J of Nucl. Mat. **206**, 25 (1994).
14. G. Odette, D. Doiron, Nuclear technology **29**, 346 (1976).
15. V. MacLane, ENDF-102 Data Formats and Procedures for the Evaluated Nuclear Data file ENDF-6, *Cross Section Evaluation Working Group*, BNL-NCS-44945-02/04-Rev (2001).
16. The JEFF3.0 Nuclear Data Library, JEFF Report **19**. NEA, OECD (2000).
17. A. Albermann, D. Lesueur, Am. Soc. for Tes. and Mat. **19**, 19103 (1989).
18. D. Simeone, O. Hablot, V. Micalet, P. Bellon, Y. Serruys, J of Nucl. Mat. **246**, 206 (1998).
19. J. Lindhard, V. Nielsen, M. Schraff, Kgl. Dan. Vid. Mat. Fys. Medd. **36**, 1 (1968).
20. L. Greenwood, R. Smither, SPECTER: Neutron Damage Calculation For Materials Irradiations, *ANL/FPP/TM*-**187** (1985).
21. S. Jumel, J. Van Duysen, J. of Nucl. Mat. **328**, 151 (2004).
22. I. Monnet, Ph. D. (2000).
23. C. Chen, J. Sun, Y. Xu, J. of Nucl. Mat. **283-287**, 1011 (2000).
24. M. Klimiankou, R. Lindau, A. Möslang, J. of Crystal Growth **249,** 381 (2003).
25. D. Simeone, L. Luneville, C. Jouanne, J. of Nucl. Mat **353,** 89 (2006).
26. L. Luneville, D. Simeone, D. Gosset, Nucl. Instr. Meth. B **250**, 71 (2006).
27. D. Simeone, L. Luneville, J. P. Both, Euro. Phys. Let. **83**, 56002 (2008).

Primary damage in ceramics: complexity and inapplicability of the NRT dpa

Jean-Paul Crocombette

CEA Saclay, DEN/DANS/DMN/SRMP
France

The NRT dpa is a measure of the primary state of ballistic damage. It has been designed for pure metals. Even in these very simple situations it faces some problems, as it will discussed thoroughly by others experts more competent than me. From what I understand, these problems are:

- the determination of the value of the Threshold Displacement Energy (E_d) entering NRT law
- the linearity of the NRT law while the amount of surviving Frenkel pairs consistently exhibits a sublinear behaviour
- the difficulty to account for mixing in alloys.

My contribution will focus on materials quite different from metals. Indeed I shall deal with the primary damage that appears in ceramics and more precisely in amorphizable ceramics. Specifically I

shall describe what one can lean from molecular dynamics (MD) simulations of displacement cascades in such materials. Some of the results have been obtained by me and some by others. Considering a material after another I will show that the NRT formula is in fact inapplicable in much of these materials and that even the concept of dpa is sometimes irrelevant in ceramics.

Under irradiation some ceramics induce an amorphization process, sometimes called metamictization (Ewing 1994). The metamict state is a state of high disorder, with a loss of long range crystalline order. Metamict state is close to the glassy state. However in some compounds noticeable differences exist between metamict state and thermally obtained glassy state**.**

MD simulations of cascades in ceramics are basically no different from simulations of cascades in other materials (Crocombette 2005). One builds a large simulation box containing atoms initially in the crystalline state; after a thermalization time, one introduces an impulsion to one of the atoms of the crystal (the PKA) and follows the subsequent displacement cascade. MD simulations are much heavier computationally than BCA calculations. However they enable to describe both the ballistic and thermal phase on equal footage and are based on empirical potentials that describe the atomic bonding and as such give much more detailed and relevant information about the atomic structures at the end of the cascades. The main information lies of course in the final atomic structure of the material.

The main specificity of these simulations for ceramics lies in the types of empirical interatomic potentials one has to use to describe the inter-atomic bonding. Oxides are commonly described by pair potentials with Coulombic long range and repulsive short range interactions. One may have to complement these pair potentials by three body terms to account for the iono-covalency of the bonding. Bonding in carbides is often more complex than in oxides with more covalency involved and sometimes even a part of metallic bonding. The potentials are then of more complex forms with many body terms, e.g. SiC is best described by Tersoff-Brenner potentials (Tersoff 1988)

Zircon: direct impact amorphization.

Zircon (formula $ZrSiO_4$), is a natural mineral which has been contemplated for long term disposal of actinide radioactive waste. Zircon is well-known to become amorphous under irradiation. Such metamictization is even observed in natural zircons containing either uranium or thorium. We performed MD simulations of cascades initiated by uranium atoms to model the effect of the recoil nucleus created by of α disintegrations (Crocombette and Ghaleb 2001). These simulations were complemented by calculations of threshold displacement energies. These studies were performed a few years ago and were thus restricted to low PKA energies. However more recent studies performed by others (Devanathan, Corrales et al. 2005) basically show the same picture.

One can clearly see (Figure 1) that the crystalline order is lost in the cascade track, showing amorphization of the cascade core. This behaviour defines materials which amorphize by so-called direct impact mechanism. This prediction by calculations of direct impact amorphization is consistent with the measured evolution of swelling under irradiation in the material and was subsequently confirmed by experimental observation (Rios, Salje et al. 2000). Note that not all amorphizable materials do amorphize by direct impact mechanism. Other possible mechanisms include the point defect accumulation up to a threshold value triggering amorphization and the double- (multi-) impact mechanisms where two (multi) cascade tracks must overlap to achieve amorphization.

Considering such primary state of damage in direct impact amorphizable materials, one may wonder how to quantify the amount of damage. My first idea was to count the number of atoms displaced from their original positions by more than a certain distance. In the submitted draft of this study, I put without details this number of displaced atoms. The referee did not believe these numbers as they were much larger than the ones deduced by the NRT formula. Indeed I found about ten times more displaced atoms than expected with the E_d I gave in the paper. I had trouble understanding the remarks of the referee, as, at that time, I was not aware that dpa are not really *displacements* per atoms but rather *defects* per atoms. It also took time to have the referee admit that the concept of (surviving vacancy-interstitial) Frenkel pairs was meaningless in the present case. Indeed one cannot properly define replacements, vacancies or interstitials in a metamict track. If one proceeds by comparison with

the perfect crystal one obtains that the number of defects is close or equal to the number of atoms in the track which invalidates the applicability of the concept of point defects.

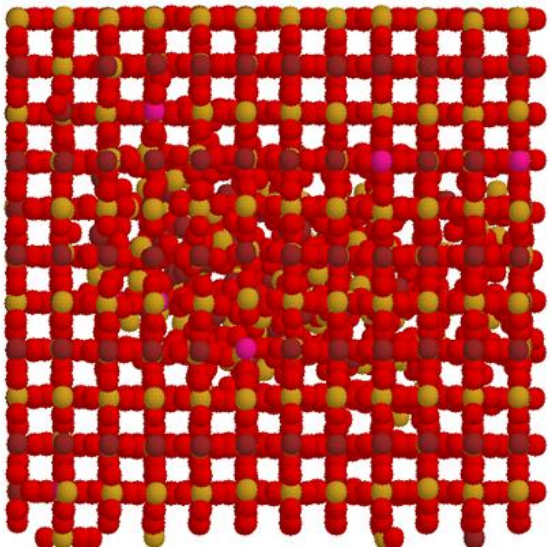

Fig. 1. Final structure after an uranium 5 keV cascade in zircon from (Crocombette and Ghaleb 2001).

The indication of the number of displaced atoms gives an estimation of the size of the amorphous track but does not characterize its structure. Eventually I defined disordered and distorted cations. Disordered cations are the ones which have in the final structure a different number of neighbours than in the crystal while distorted cations have the same number of neighbours but with strong angular distortions. Using these definitions one can realize that the center of the amorphous track contains disordered cations while distorted ones appear also at the periphery (see Figure 2).

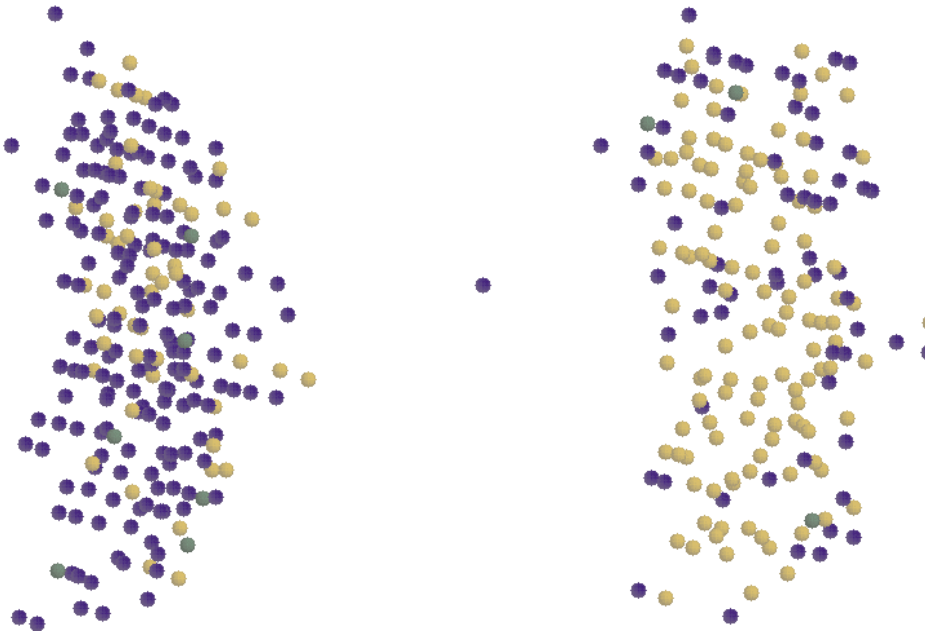

Fig. 2. Disordered cations after a cascade in zircon and distorted cations after a cascade in zircon from (Crocombette and Ghaleb 2001).

One can clearly see that the NRT dpa fails completely to measure the amount of damage in irradiated zircon. First the number of surviving Frenkel pair is meaningless and second the number of displaced

atoms (strictly speaking) is much larger than estimated by the NRT formula, which is quite normal. However the number of displaced atoms, in the raw sense, gives an estimate of the size of the cascade track.

Zirconolite: point defects and amorphous clusters

The second example I would like to mention is zirconolite $CaZrTi_2O_7$, also a candidate for radioactive waste disposal. Simulations of cascades initiated by uranium PKAs were modelled in this compound (Veiller, Crocombette et al. 2002). Cascade in this material basically show a damage of mixed nature (see Figure 3). First along the trajectory of the uranium, one obtains an amorphous core. Second at the periphery of the track as well as disconnected from it one can see point defects. Some Replacement Collision Sequences (RCS) have even been observed in some cases (in the titanium planes, not shown).

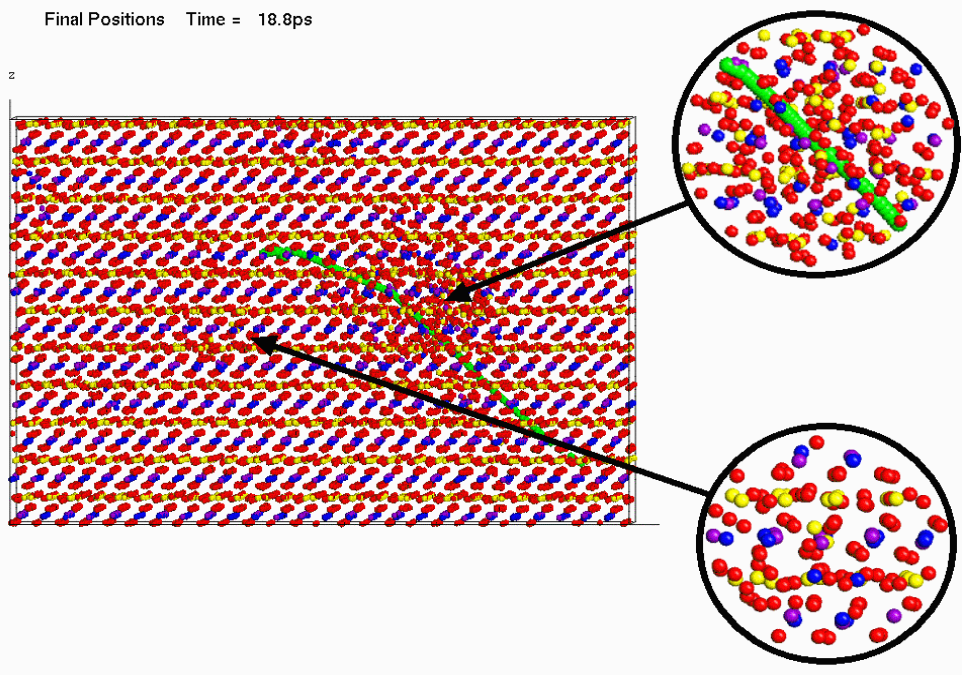

Fig. 3. Final structure after uranium 12 keV cascade in zirconolite. The path of the uranium atom is in green (from (Veiller, Crocombette et al. 2002)).

How the measure the damage then? On one hand, the number of point defects is difficult to define as the track is amorphous and so the number of point defects becomes close or equal to the number of atoms in this area. On the other hand giving the number of displaced atoms is OK for the amorphous core but irrelevant for the periphery where RCS will be counted as damage while in fact they are not. In this part of the damaged region the situation is close to what it is in metals, namely surviving point defects with some mixing as in alloys. All in all, I could not find a satisfactory "number" to measure the damage.

Silicon carbide: nature of damage depends on the atomic type of the PKA

SiC is a major candidate material for future fusion or fission nuclear reactors. It is, for instance, contemplated for plasma facing coatings and structural components in fusion reactors and as inert fuel coating or matrix in high temperature fission reactors. MD simulation of cascades in this material has been performed by many groups especially the Gao-Weber team (e.g. (Gao, Weber et al. 2001)). They find that the damage depends on the nature of the PKA.

For Si PKA, after one cascade, the damage is made of both isolated defects and pockets of nano-amorphized materials. They choose to analyze these clusters in terms of point defects with the perfect crystal as a reference frame for defect detection. This choice may be questioned as it appears clearly that, in these clusters, the number of defects is close to the number of atoms in the cluster which invalidates the concept of point defects. They assess the applicability of the NRT formula, with an assumed value of Ed and find, as in metals, that the number of Frenkel pairs is less in MD than suggested by NRT. Moreover, the evolution of the number of Frenkel pairs with energy is sublinear with a power of 0.82.

For Au PKA the damage is quite different: Although some small isolated defects can be seen, a large disordered region is created by the Au PKA which consists of interstitials, vacancies and anti-sites defects. Examination of the cascade shows that this disordered region has a very high defect concentration and contains 105 displaced atoms, with 93 antisites and 35 interstitials. This part is therefore directly amorphized. One then has damage comparable to what we observed in zirconolite.

The SiC case therefore shows that the number of defects and beyond that the very nature of damage depends on the type of PKA. While it is of common knowledge that neutrons, ions and electrons irradiations induce different kinds of damage, this is an example where different ions or atomic PKA induce different types of damage in a given material.

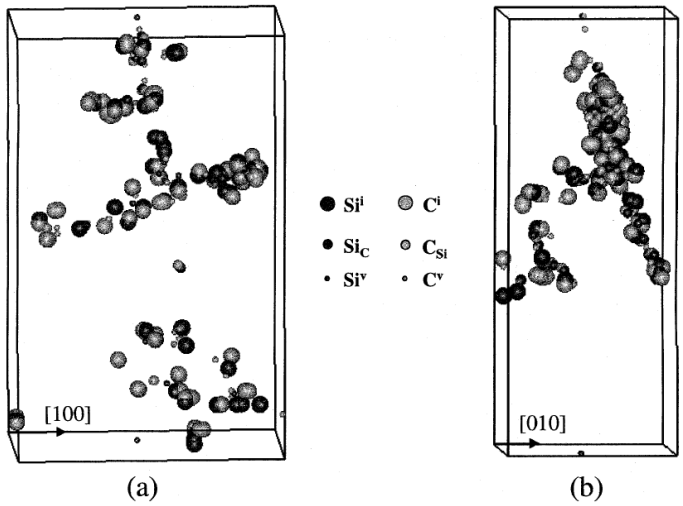

Fig. 4. The final damage in SiC at 300K due to (a) the 10 keV Si recoil and (b) the 10 keV Au recoil from (Gao, Weber et al. 2001).

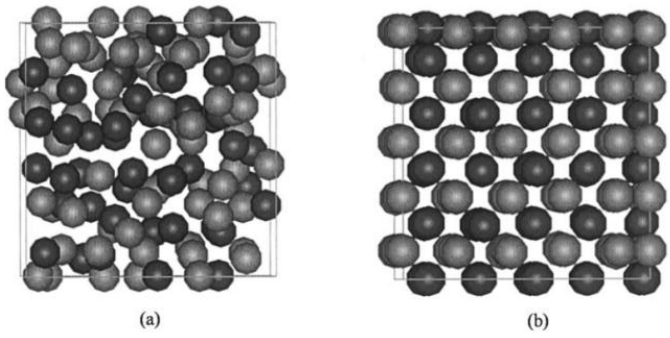

Fig. 5. (a) the local disordered region created by a 10 keV Au PKA; (b) the perfect SiC structure from (Gao, Weber et al. 2001).

Zirconium carbide, uranium oxide and pyrochlore: apparently regular situation

I finally mention the situation in ZrC (Van Brutzel and Crocombette 2007), UO_2 (Van Brutzel, Delaye et al. 2003) and pyrochlore compounds (Chartier, Meis et al. 2003) (pyrochlore is family of oxides of general formula $A_2B_2O_7$). In these materials the damage created by cascades is regular. As in metals or metallic alloys cascades produce only point defects. The amount of damage is then satisfactorily described by the dpa concept. One is then brought back to the usual problems of the NRT formula. For instance in UO_2, the number of Frenkel pairs after a cascade varies $E^{0.94}$ for uranium atoms and $E^{0.84}$ for oxygen atoms respectively.

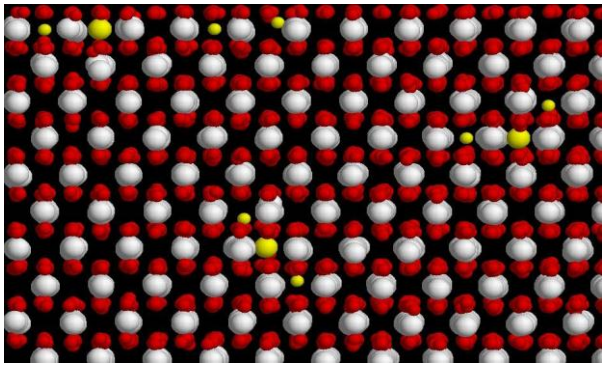

Fig. 6. Part of the final structure of UO_2 after a 10 keV cascade.

Finally it is worth returning to the fact that the eventual amorphization of ceramics under irradiation is not always related to direct impact damage. For instance, cascades in pyrochlore create point defects only, but these compounds amorphize or not depending on composition. We have been able to show that when amorphization occurs it is created by the accumulation of point defects created by successive cascades (Chartier, Meis et al. 2005). In non amorphizable pyrochlore, as well as in UO_2 which has a very similar structure, the amorphization is prevented by the fast recombination of close Frenkel pairs. In amorphizable pyrochlore, a critical temperature exists above which amorphization is prevented. We showed that is related to the high temperature enhancement of the Frenkel pair recombinations which is a thermally activated process (Crocombette, Chartier et al. 2006; Chartier, Catillon et al. 2009).

This last point may be of general interest. Even in the regular situation where cascades create only Frenkel pairs. The surviving fraction of these may vary with temperature. This can be rationalized approximately in terms of an increase of the spontaneous recombination volume of these pairs with temperature, or more precisely as the thermal activation of recombinations at intermediate distances with an associated energy barrier (Van Brutzel, Chartier et al. 2008).

Summary

I have tried to show that the studies on ceramics bring even more complexity is an already difficult situation about the NRT dpa. First in ceramics amorphized by direct impact, the very concept of surviving FPs which is what the NRT dpa is supposed to measure is meaningless. One then has to return to the bare number of displaced atoms to quantify the damage. Second in more complex situations where the damage is mixed between amorphization and creation of point defects, it is almost impossible to define a quantity to measure atomic disorder induced by cascades. Finally it was shown that the amount and nature of damage depends not only on the energy of the PKA but also on its nature. Finally one should keep in mind that even in the regular cases, the number of surviving Frenkel pairs may vary with temperature as their recombinations can be thermally activated.

Routes of improvements for the definition of the dpa

With such a complex picture of damage in ceramics, it appears difficult to suggest an improvement of the definition of the dpa which would satisfactorily described the complexity of irradiation damage in ceramics. In my opinion it is basically impossible to get a definition of damage or dpa that will work for every situation. Involved studies are needed for each material of interest to determine what is the damage induced by ballistic loses under irradiation. However I would suggest two leads to make progress in the reform of the dpa. These are iconoclastic and rather paradoxical suggestions.

First one could change nothing in the NRT definition of the dpa. It is now widely realized that this measure is not perfect, but improvements are too much material and irradiation dependent to allow an effective redefinition of the norm.

The second suggestion would be to realize that the complexity of the observed damage lies in the variety of materials response. Various materials respond differently (according to their composition, structure, temperature, etc.) to a certain amount of deposited ballistic energy. We may thus consider going one step backwards and just quantify the amount of deposited ballistic energy. A first version of this would be to give exactly that "amount of ballistic energy deposited per atom". In practice that would mean replace the "dpa" by a "bEpa" for ballistic energy deposited per atom (in eV per atom). A second, less severe version would be to continue to talk in terms of dpa using an NRT formula with an Ed constant and common to all elements in all materials. One can for instance choose 20 eV. The new formula would then be that the number of dpa is E(in eV)/50. This drastic choice would allow continuing talking in terms of dpa, but would stress that the dpa is just an artificial measure of the ballistic energy deposited, a very gross estimation of the amount of damage and that if one is serious about the amount and nature of damage one should go way beyond such crude formulas

References

Chartier, A., G. Catillon, et al. (2009). "Key Role of the Cation Interstitial Structure in the Radiation Resistance of Pyrochlores." Physical Review Letters **102**: 155503.

Chartier, A., C. Meis, et al. (2005). "Molecular dynamic simulation of disorder induced amorphization in pyrochlore." Phys. Rev. Lett **94**: 025505.

Chartier, A., C. Meis, et al. (2003). "Atomistic modeling of displacement cascades in La2Zr2O7 pyrochlore." Physical Review B **67**: 174102.

Crocombette, J. P. (2005). "Cascade Modeling" in Handbook of Materials Modeling. S. Yip. Berlin, Springer**:** p. 987.

Crocombette, J. P., A. Chartier, et al. (2006). "Atomistic simulation of amorphization thermo-kinetics in lanthanum pyrozirconate." Applied Physics Letters **88**: 051912.

Crocombette, J. P. and D. Ghaleb (2001). "Molecular dynamics modeling of irradiation damage in pure and uranium doped zircon." Journal of Nuclear Materials **295**: 167-178.

Devanathan, R., L. R. Corrales, et al. (2005). "Molecular dynamics simulation of defect production in collision cascades in zircon." Nucl. Instrum. Meth. Phys. Res. B **228**: 299.

Ewing, R. (1994). "The metamict state: 1993 - the centennial." Nucl. Instr. and Meth. B **91**: 22.

Gao, F., W. J. Weber, et al. (2001). "Atomic-scale simulation of displacement cascades and amorphization in beta-SiC." Nucl. Instrum. Meth. Phys. Res. B **180**: 176-186.

Rios, S., E. Salje, et al. (2000). "Amorphization in zircon : evidence for direct ompact damage." Journal of Physics: Condensed Matter **12**: 2401-2412.

Tersoff, J. (1988). "New Empirical approach for the structure and energy of covalent systems." Physical Review B **37**(12): 6991.

Van Brutzel, L., A. Chartier, et al. (2008). "Basic mechanisms of Frenkel pair recombinations in UO2 fluorite structure calculated by molecular dynamics simulations." Physical Review B **78**(2):.

Van Brutzel, L. and J. P. Crocombette (2007). "Classical molecular dynamics study of primary damage created by collision cascade in a ZrC matrix." Nuclear Instruments & Methods in Physics Research Section B-Beam Interactions with Materials and Atoms **255**(1): 141-145.

Van Brutzel, L., J. M. Delaye, et al. (2003). "Molecular dynamics studies of displacement cascades in the uranium dioxide matrix." Philosophical Magazine **83**(36): 4083-4101.

Veiller, L., J. P. **Crocombette**, et al. (2002). "Molecular dynamics simulation of the alpha-recoil nucleus displacement cascade in zirconolite." Journal of Nuclear Materials **306**(1): 61-72.

Specific effects of ionizing energy on the displacement damage calculation in insulators.

R. Vila, F. Mota, C. J. Ortiz

Laboratorio Nacional de Fusión – CIEMAT, Material group, Madrid Spain

Introduction

The level of damage expected in functional materials for future fusion reactors is generally much lower than structural materials, but the degradation of their physical properties is also generally observed at very low dose levels compared to the latter. Normally the properties of interest (DC Electrical resistivity, HF dielectric absorption, optical transmission etc.) degrade long before mechanical integrity is an issue.

This weakness is in part related to the more important effects of ionizing energy on both, covalent and ionic, insulators or semiconductors.

As irradiation in fission and fusion reactors (even spallation sources) also involves the participation of gamma radiation, it has to be taken into account for total damage calculation. In the case of ions, the energy partition provides the amount of electronic (ionizing) energy lost in the material.

In general and regarding radiation, insulating materials can be divided in two groups depending on whether they experience *radiolysis*, (i.e. purely ionizing radiation can produce noticeable amounts of atomic displacements) or not. First group includes for example alkali halides and fluorides. But, although radiolysis is negligible in the second group (radiation-hard materials), collateral effects of ionizing radiation have been observed (when combined with displacement damage). Therefore it is important to make some comments about the concept and use of *dpa (displacements per atom)* in this large family of materials.

Relevance of dpa concept to damage in insulators.

Currently, there are two main methods used to calculate the primary displacement damage by neutron irradiation or by ion irradiation. First, the displacement damage doses induced by neutrons are calculated considering the NRT model [1] based on the electronic screening theory of Linhard [2]. Second, for experimental research community, SRIM code is commonly used to calculate the dpa damage dose induced by ion irradiation. Since in both cases ionizing energy is not used to calculate the dpa, errors are introduced for insulators/semiconductors as it will be now presented.

An important aspect related to early damage creation is that ionizing radiation can promote the recovery of displacement damage in many ceramic insulators by enhancing the mobility of point defects (ionization-induced diffusion) [3,4,5] because charge state of SIAs' depend on the ionizing level. Enhanced point defect annealing and coalescence due to ionization-induced diffusion processes have been observed for both self-interstitial atoms and vacancies. Although exceptions may occur, in general this enhancement in diffusion leads to improved radiation resistance since many of the produced point defects are annihilated via recombination events or at sinks such as grain boundaries.

On the other hand, high ionizing levels can contribute to enhance Frenkel pairs production in insulators. Therefore, as a general conclusion, when comparing different irradiation conditions (electronic stopping powers), ionizing radiation can lead to either a substantial enhancement or suppression of radiation resistance in ceramics, but certainly to differences with NRT dpa formula.

As a clear example the results for conductivity degradation, known as RIED (Radiation Induced Electrical Degradation) are presented in Figure 1 for Al_2O_3, a typical "radiation resistant" insulator. This figure summarizes the observed results using different radiation sources but measuring the same property (and using approximately the same conditions of temperature and electrical field…). Although still a bit controversial, it is a perfect example of previous discussion.

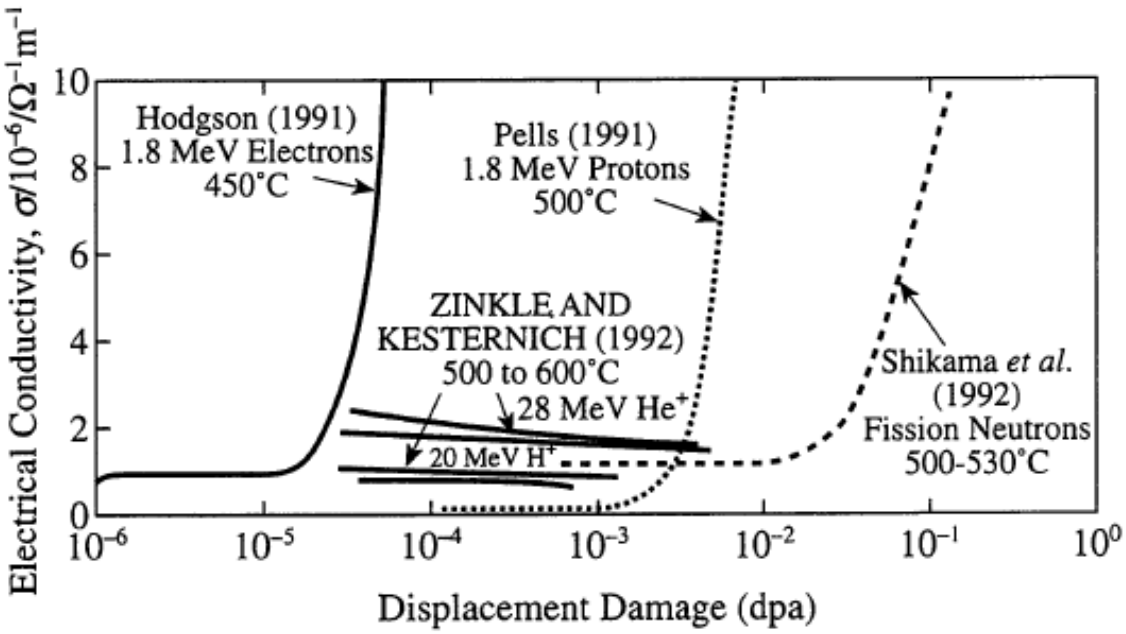

Figure 1. Summary of electrical conductivity degradation (RIED) in alumina as a function of classical *dpa* dose for several irradiation particles (from electrons to neutrons) [6].

When using the classical dpa formula to compare the damage, it becomes dramatically evident that RIED does not scale at all with dpa, but depends on ionization level of incident radiation. It can be seen that results depend strongly on it producing shifts of several orders of magnitude in dpa dose. High levels of ionization, as is the case for electrons induce earlier degradation of the conductivity, followed by protons, alpha particles and finally neutrons (with the lower % of ionization).

Another interesting result is the previously commented low level of dose where degradation appears, around only 3 10^{-5} dpa for electrons. The best case (neutrons) is around 0.1 dpa. Therefore, although it can be argued that previous results are not just primary damage, these effects appear at very low damage levels and are triggered by a different damage production rate.

In Figure 2 the data are presented in a different way, demonstrating that a good agreement for the level of electrical degradation can be obtained when plotted as a function of total ionizing dose (Gy) instead of dpa. Figure shows in-reactor conductivity measurements for a high purity alumina. The figure also shows the estimated RIED contribution extrapolated back to the low dose region, which cannot be directly measured in-reactor. This now allows one to compare the in-reactor RIED with values obtained for electron, proton, and alpha particle accelerator irradiations of similar alumina grades. When all these data are plotted in terms of ionizing dose (Gy), the RIED values, except for one of the alpha particle data, now agree very well, highlighting the importance of the ionizing component for RIED degradation. For details reader can consult reference [7].

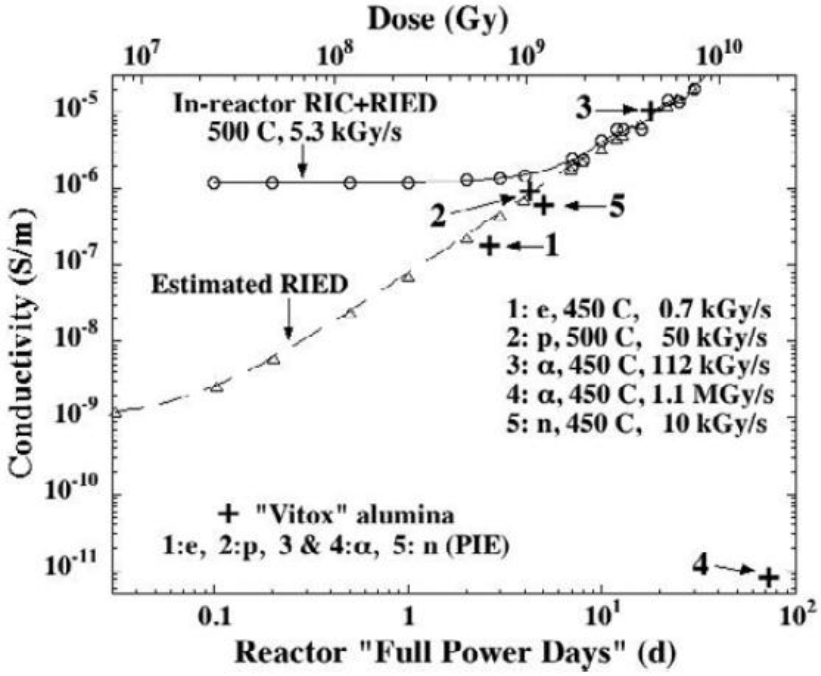

Fig. 2. JMTR in-reactor electrical conductivity measurement at 500°C, 5.3 kGy/s, and estimated RIED degradation plotted as a function of reactor full power days and total ionizing dose, together with data for electron (1: 450°C, 700 Gy/s), proton (2: 500°C, 50 kGy/s), alpha (3: 450°C, 110 kGy/s), alpha (4: 450°C, 1.1 MGy/s), and PIE neutron (5: 450°C, 10 kGy/s) irradiations plotted as a function of the total ionizing dose (Refs. 25 through 29 and 32).

Finally, although it is outside the scope of this summary, it has to be mentioned that at higher stopping powers (electronic dE/dx > 5–50 keV/nm, depending on the material), additional dpa`s can also be created via inelastic collision processes in the vicinity of the ion track (normally produced by swift-heavy-ions). This is also beyond the NRT dpa concept of damage, mainly due to the extreme energy density deposited locally.

Reference

1. M.T. Robinson, Journal of Nuclear Material **216** (1994) 1.
2. J. Lindhard, M. Scharff, H.E. Schiøtt, Mat. Fys. Medd. Dan. Vid. Selk. **33**, 14 (1963) 1.
3. J.C. Bourgoin, Radiat. Eff. Def. Solids **111&112** (1989) 29.
4. S.J. Zinkle, J. Nucl. Mater. **219** (1995) 113.
5. J.C. Bourgoin, Radiat. Eff. Def. Solids **111&112** (1989) 29.
6. T. Shikama, Materials Trans. JIM, **36**, (1995) 997.
7. E.R. Hodgson, Fusion Science and Technology **62** (2012) 89.

Technical Meeting on
"Primary Radiation Damage: from nuclear reaction to point defects"

1 - 4 October 2012, VIC, Room A2712, IAEA, Vienna, Austria

Meeting Agenda (*presentation's time includes questions***)**

Monday, 1 October 2012

09:15 - 09:30	**Arriving**
09:30 - 10:00	**Welcome, Opening Remarks, and Administrative Announcements** **Robin Forrest** (Section Head, Nuclear Data Section, NDS/IAEA) **Stanislav Simakov** (Meeting' Scientific Secretary, NDS/IAEA) **Victor Inozemtsev** (Meeting' Scientific Secretary, NEFW/IAEA) **Alexander Oechs** (Meeting' administrative arrangements, NDS/IAEA) Welcome Address (**Robin Forrest**) Administrative Announcements (**Alexander Oechs)** Self introductions of **Participants** Selection of **Chairperson & Rapporteur** Approval of Agenda
10:00 - 10:10	**Stanislav Simakov, IAEA** - Objectives of the Meeting
Presentations – General Overviews and Nuclear Data (calculation, evaluation and validation of PKA, KERMA and dpa cross sections)	
10:10 - 11:10	**Roger Stoller, ORNL** - "Dosimetry and Damage Correlation: Definitions and Distinctions"
11:10 - 11:30	*Coffee break*
11:30 - 12:30	**Kai Nordlund**, **University of Helsinki** - "Modified NRT equations for damage and mixing developed by the OECD NEA primary radiation damage group"
12:30 - 14:00	*Lunch break*
14:00 - 15:00	**Alexander Konobeev, KIT** - "What we can improve in the calculation of displacement cross-sections"
15:00 - 16:00	**Tokio Fukahori, JAEA** - "A calculation method of PKA, KERMA and DPA from evaluated nuclear data for medium and heavy elements by using an effective single-particle emission approximation (ESPEA) relating to the preparation of JENDL PKA/KERMA File"
16:00 - 16:20	*Coffee break*
16:20 - 17:20	**Junhyun Kwon, KAERI –** "Calculation of gamma displacement cross section. Generation of recoil spectra from ENDF/B"

Tuesday, 02 October 2012

09:00 - 10:00	**Patrick Griffin, SNL** - "Neutron Damage Metrics and Quantification of the Associated Uncertainty"
10:00 - 11:00	**Skip Kahler, LANL -** "NJOY/HEATR – What it Calculates Now, What Should it Calculate?"
11:00 - 11:20	*Coffee break*
11:20 - 12:00	**Alfred Hogenbirk, NRG -** *excused*
12:30-14:00	*Lunch break*

Presentations – Primary Radiation Damage Defects (calculation, validation and practical application …)	
14:00 - 15:00	**Sergei Dudarev, UKAEA** - "Direct observation of radiation defects: experiment and interpretation"
15:00 - 16:00	**Valerii Pechenkin, IPPE –** "Primary damage characteristics in metals under irradiation in the cores of thermal and fast reactors"
16:00 - 16:20	*Coffee break*
16:20 - 17:20	**Fernando Mota, CIEMAT** - "Primary displacement damage calculation induced by neutron and ion using binary collision approximation techniques (MARLOWE code)"

Wednesday, 03 October 2012

09:00 - 10:00	**Alexander Ryazanov, KIAE – "**Development of theoretical modeling of point radiation defects, cascades and sub-cascades formation in diatomic materials (Al_2O_3) irradiated by fast charged particles on accelerators and by fast neutrons in nuclear reactors"
10:00 - 11:00	**David Simeone, CEA Saclay –** "The interest of dpa to handle the microstructure of irradiated materials"
11:00 - 11:20	*Coffee break*
11:20 - 12:20	**Jean-Paul Crocombette, CEA Saclay – "**Primary damage in ceramics: complexity and inapplicability of the NRT dpa"
12:20 - 14:00	*Lunch break*
Discussions and drafting of Conclusions & Recommendations	
14:00 - 15:40	
15:40 - 16:00	*Coffee break*
16:00 - 17:30	
19:00 -	**Social event: Visit to Puerstner Gaststube (http://www.puerstner.com/)**

Thursday, 04 October 2012

Discussion and finalization of Conclusions & Recommendations	
09:00 - 10:40	
10:40 - 11:00	*Coffee break*
11:00 - 12:30	
12:30 - 14:00	*Lunch break*
14:00 - 15:00	***Final Remarks and End of the Meeting***

IAEA
International Atomic Energy Agency
Atoms for Peace

Technical Meeting on

"Primary Radiation Damage: from Nuclear Reaction to Point Defects"

1 to 4 October 2012
Vienna, Austria

LIST OF PARTICIPANTS

FINLAND

Mr Kai **Nordlund**
Department of Physics
University of Helsinki
P.O. Box 43
Pietari Kalmin Katu 2
HELSINKI 00014
Tel.: +358-9-19150007
Fax: +
E-mail: kai.nordlund@helsinki.fi

FRANCE

Mr Jean-Paul **Crocombette**
CEA Saclay
DEN/DANS/DMN/SRMP
Bat 520 - Pce 201
GIF-sur-YVETTE Cedex 91191
Tel.: +33-169-089285
Fax: +
E-mail: jpcrocombette@cea.fr

FRANCE

Mr David **Simeone**
CEA Saclay
DEN/DANS/DMN/SRMA/LA2M
Bat 453 - Pce 27B
GIF-sur-YVETTE Cedex 91191
Tel.: +33 1 69 08 29 20
Fax: +
E-mail: david.simeone@cea.fr

GERMANY

Mr Alexander **Konobeev**
Institute for Neutron Physics
and Reactor Technology
Karlsruhe Institute of Technology (KIT)
Hermann von Heimholtz Platz 1
EGGENSTEIN-LEOPOLDSHAFEN 76344
Tel.: + 49 721 608 23768
Fax: + 49 721 608 23718
E-mail: alexander.konobeev@kit.edu

JAPAN

Mr Tokio **Fukahori**
Nuclear Science and Engineering Directorate
Japan Atomic Energy Agency
Shirakata-Shirane 2-4,Tokai-mura, Naka-gun
IBARAKI-KEN 319-1195
Tel.: +81 29-282-6369
Fax: +81 29-282-6122
E-mail: fukahori.tokio@jaea.go.jp

Republic of KOREA

Mr Junhyun **Kwon**
Korea Atomic Energy Research Institute
(KAERI)
1045 Daedeok-daero
Yuseong-gu
DAEJEON 305-353
Tel.: +82 42 868 8588
Fax: +82 42 868 8549
E-mail: jhkwon@kaeri.re.kr

RUSSIAN FEDERATION

Mr Valerii A. **Pechenkin**
Institute of Physics and Power Engineering
Bondarenko Sq 1
Kaluga Region
OBNINSK 249033
Tel.: +7 48439 98019
Fax: +7 48439 98582
E-mail: vap@ippe.ru

RUSSIAN FEDERATION

Mr Alexander **Ryazanov**
National Russian Research Centre
"Kurchatov Institute"
Kurchatov Sq 1
MOSCOW 123182
Tel.: +7 499 196 91 77
Fax: +7 495 421 45 98
E-mail: Alexander.Ryazanov@cern.ch
E-mail: ryazanoff@comail.ru

SPAIN

Mr Fernando **Mota**
Laboratorio National de Fusion (CIEMAT)
Proyecto IFMIF-EVEDA España
Avenida Complutense 40
MADRID 28040
Tel.: +34 91 346 6578
Fax: +
E-mail: fernando.mota@ciemat.es

SPAIN

Mr Rafael **Vila**
Laboratorio National de Fusion (CIEMAT)
Head, Fusion Materials Unit
Avenida Complutense 40
MADRID 28040
Tel.: +34 91 3466580
Fax: +
E-mail: rafael.vila@ciemat.es

UK

Mr Sergei **Dudarev**
UK Atomic Energy Authority
Culham Centre for Fusion Energy
Abingdon
OXFORDSHIRE UK OX14 3DB
Tel.: +44 1235 466513
Fax: +44 1235 466435
E-mail: sergei.dudarev@ccfe.ac.uk

UK

Mr Jean-Christophe **Sublet**
UK Atomic Energy Authority
Culham Centre for Fusion Energy
Abingdon
OXFORDSHIRE UK OX14 3DB
Tel.: +44 1235 466400
Fax: +
E-mail: jean-christophe.sublet@ccfe.ac.uk

USA

Mr Patrick J. **Griffin**
Sandia National Laboratories
Org. 1384, MS 1146
P.O. Box 5800
87185-1146 ALBUQUERQUE NM
Tel.: +1 505 845 9121
Fax: +1 505 284 3651
E-mail: pjgriff@sandia.gov

USA

Mr Albert C. (Skip) **Kahler III**
Los Alamos National Laboratory
Theoretical Division
T-2, Nuclear & Particle Physics,
Astrophysics & Cosmology Group Build. 200
P.O. Box 1663, MS B214
87545 LOS ALAMOS NM
Tel.: +1 505 606 2042
(LANL cell) +1 505 500 6633
Fax: +1 505 667 1931
E-mail: akahler@lanl.gov

USA

Mr Roger E. **Stoller**
Oak Ridge National Laboratory
Materials Science and Technology Division
P.O. Box 2008
37831-6114 OAK RIDGE, TN
Tel.: +1 865 576 7886
Fax: +1 865 241 3650
E-mail: stollerre@ornl.gov
E-mail: rkn@ornl.gov

GERMANY (Observer)

Mr Thorsten **Stahl**
Gesellschaft fuer
Anlagen- und Reaktorsicherheit (GRS)mbH
Radiation and Environmental Protection Division
Schwertnergasse 1
COLOGNE 50667
Tel.: +49 221 2068-857
Fax: +49 221 2068 10857
E-mail: thorsten.stahl@grs.de

IAEA (Observer)

Mr Zhi Xiong **Chong**
Intern
Safety Assessment Section
Department of Nuclear Safety and Security
Tel.: +43 1 2600 22664
Fax: +43 1 2600 7 22664
E-mail: z.x.chong@iaea.org

IAEA

Mr Robin A. **Forrest**
Head
Nuclear Data Section
Division of Physical and Chemical Sciences
Tel.: +43 1 2600 21709
Fax: +43 1 2600 7 21709
E-mail: r.forrest@iaea.org

IAEA

Mr Stanislav P. **Simakov**
Head of Nuclear Data Service Unit
Nuclear Data Section
Division of Physical and Chemical Sciences
Tel.: +43 1 2600 21717
Fax: +43 1 2600 7 21717
E-mail: s.simakov@iaea.org

IAEA

Mr Victor **Inozemtsev**
Team Leader
Nuclear Fuel Cycle and Materials Section
Division of Nuclear Fuel Cycle
and Waste Technology
Tel.: +43 1 2600 22760
Fax: +43 1 2600 7 22760
E-mail: v.inozemtsev@iaea.org

IAEA

Mr Naohiko **Otsuka**
Nuclear Data Section
Division of Physical and Chemical Sciences
Tel.: +43 1 2600 21715
Fax: +43 1 2600 7 21715
E-mail: n.otsuka@iaea.org

IAEA

Ms Valentina **Semkova**
Nuclear Data Section
Division of Physical and Chemical Sciences
Tel.: +43 1 2600 21727
Fax: +43 1 2600 7 21727
E-mail: v.semkova@iaea.org

IAEA

Mr Roberto **Capote Noy**
Nuclear Data Section
Division of Physical and Chemical Sciences
Tel.: +43 1 2600 21713
Fax: +43 1 2600 7 21717
E-mail: v.zerkin@iaea.org

Nuclear Data Section
International Atomic Energy Agency
P.O. Box 100
A-1400 Vienna
Austria

e-mail: services@iaeand.iaea.org
fax: (43-1) 26007
telephone: (43-1) 2600-21710
Web: http://www-nds.iaea.org